The role of grain angle, knots, tension wood, compression wood, and other anomalies on the mechanical properties of wood

Hoffmeyer, Preben

Publication date:
1987

Document Version
Publisher's PDF, also known as Version of record

TECHNICAL REPORT 183/87

THE ROLE OF GRAIN ANGLE, KNOTS, TENSION WOOD, COMPRESSION WOOD, AND OTHER ANOMALIES ON THE MECHANICAL PROPERTIES OF WOOD

Preben Hoffmeyer

Building Materials Laboratory
Technical University of Denmark
Building 118
DK-2800 Lyngby, Denmark

THE TECHNICAL UNIVERSITY OF DENMARK
DEPARTMENT OF CIVIL ENGINEERING
BUILDING MATERIALS LABORATORY

THE ROLE OF GRAIN ANGLE , KNOTS , TENSION WOOD , COMPRESSION WOOD, AND OTHER ANOMALIES ON THE MECHANICAL PROPERTIES OF WOOD

PREBEN HOFFMEYER

MAY 1987

TABLE OF CONTENTS

.... But in seeking correlations between performance and structure it is tempting to describe the latter in terms of smaller and smaller structural units, but a cautionary note must be recorded, for it is all too easy to overlook the significance of the gross features. This is particularly so where large sections of timber are being used under practical conditions; in these situations gross features such as knots and grain angle are highly significant factors.

J.M.Dinwoodie

INTRODUCTION

The role of anomalies on the mechanical properties of wood has been recognized ever since Buffon (1740) cautioned that small clear specimens alone can give no reliable information on the behavior of structural wood elements.

However, it is predominantly the research of the last only thirty years which has contributed to today's knowledge. This period has experienced a marked industrialization of the wood construction sector, resulting in the development of new wood based materials and components, and even in totally new construction concepts. In such a situation the traditional "trial and error" philosophy of past centuries has had to yield to much more rational analytical and experimental approaches.

At the same time the timber design codes have gradually been transformed from simple, general rules into complex and sophisticated codes, which now allow incorporation of detailed knowledge of the influence of specific materials parameters, load parameters, environmental parameters etc. Thus, it has been both necessary and feasable to study the engineering properties of wood.

Examples of new knowledge obtained are plentiful. The belief, for instance, that tensile strength along the grain is the prime strength even of structural lumber has only slowly yielded to the facts established through full-scale tests on such lumber; during the thirty-year period the tensile strength has gradually dropped to approximately one-third of its original value.

More knowledge of the role of anomalies is collected currently, often as a result of large and costly programs (e.g. North American In-Grade Test Program).

The present report attempts to review and comment the current knowledge of the influence of the most important growth related anomalies such as reaction wood, grain angle, knots, compression failures, and microbiological degradation. Anomalies caused by processing of the wood such as checks or collapse due to drying are not considered.

First, Thales thought that water was the principle of all things. Heraclitus of Ephesus fire. But the school of the Pythagoreans added air and the earthy to water and fire.

Since therefore from these, being in correspondence, all things seem to come together and be born, I thought I ought first to deal with the varieties and differences of the use of them and what qualities they show in buildings.

Vitruvius, 1 century B.C.

1. REACTION WOOD

1.1 Introduction

When a cross section of a growing tree is subjected to uneven stress distributions, the tree may react by producing abnormal wood tissue. Such wood is called reaction wood. The action to which the tree reacts may be caused by a lean, a bend, the weight of a fallen neighboring tree, a predominant wind direction, etc.

In conifers reaction wood forms in the areas predominantly subjected to compression stresses and is therefore termed compression wood. Conversely, in hardwoods reaction wood forms in the areas predominantly subjected to tensile stresses, and it is therefore termed tension wood.

Reaction wood behaves quite differently from normal wood with respect both to mechanical and physical properties. Extensive occurrence of reaction wood therefore excludes such wood for constructional purposes.

Table 1.1 (Côté and Day, 1964) lists the abnormal characteristics of reaction wood. These features are further detailed in the following chapters. As conifers are more important than hardwoods with respect to wood construction, the compression wood will receive most attention in the following.

1.2 Formation

By bending young stems into complete loops it has been demonstrated (Ewart and Mason-Jones, 1906; Jaccard, 1938) that reaction wood forms at the top and bottoms of the loops. However, compression wood always forms in the lower part of a cross section. Consequently, in the lower part of the loop compression wood is formed in the tension side. The opposite is true for tension wood.

In a related experiment (Burns, 1920) young stems were bent horizontally, and reaction wood was formed in the lower side subjected to varying levels of both compression and tension stresses.

The conclusion was that gravity rather than stress governs formation of reaction wood.

Table 1.1 Comparison of Tension Wood and Compression Wood Characteristics (Côté and Day, 1964)

	Tension Wood	Compression Wood
Gross and physical characteristics; mechanical properties	Eccentricity of stem cross section: "upper side" Dry, dressed lumber: silvery sheen of tension wood zones in many species; darker than normal in certain tropical and Australian species Green sawn boards woolly on surface Longitudinal shrinkage up to 1% Particularly high tensile strength in dry tension wood; lower than normal in green condition	Eccentricity of stem cross section: "lower side" Non-lustrous, "dead" appearance Darker colored ("Rotholz") than normal wood Longitudinal shrinkage up to 6-7% Modulus of elasticity, impact strength, tensile strength: low for its density
Anatomical characteristics	Gelatinous (tension wood) fibers present though they may be lacking in some species Vessels reduced in size and number in tension wood zones Ray and vertical parenchyma apparently unmodified	Rounded tracheids Inter-cellular spaces Transition pattern, spring-wood-summerwood, altered: more gradual than in normal wood
Micro-structure	G-layer present; convoluted or not Slip planes and compression failures in tension wood fiber walls G-layer in secondary wall of gelatinous fibers in 3 types of arrangement: $S_1 + S_2 + S_3 + G$ or S_G $S_1 + S_2 + G$ or S_G $S_1 + G$ or S_G	Helical checks or cavities in S_2 Slip planes and compression failures generally absent
Ultra-structure	Primary wall appears normal S_1 may be thinner than normal Microfibrillar orientation of G-layer nearly parallels fiber axis; high parallelism within G-layer	S_3 layer absent S_1 may be thicker than normal S_2 microfibrillar orientation approaches 45^o Ribs of cellulose parallel to direction of microfibril orientation; cellulose lamellae parallel with wall surface
Chemical composition	Lignification of tension wood fibers variable; G-layer only slightly lignified Abnormally high cellulose content Abnormally low lignin content More galactan than normal Less xylan than normal	"Extra" lignin deposited as a layer between S_1 and S_2 Abnormally low cellulose content Abnormally high lignin content More galactan than normal Less galactoglucomannan than normal

The formation of reaction wood is thought to be triggered by the production of auxins (Haygreen and Bowyer, 1982; Nix and Brown, 1987). Already Wershing and Bailey (1942) and later Wardrop and Davies (1964) showed that injection of indole acetic acid causes production of compression wood.

Whether gravity force and the subsequent production of auxins are the only factors responsible for reaction wood production remains to be proved. There are indications that reaction wood forms even in stems that are not permanently displaced (Haygreen and Bowyer, 1982).

Own observations of breast-height cross sections of 20-40-year old straight grown *Picea abies* plantation stands suggest that formation of some reaction wood in the stems is normal.

1.3 Gross Characteristics

Reaction wood in conifers is often seen in a cross section as dark, dense annual rings and on planed surfaces as dark, reddish streaks (Figure 1.1).

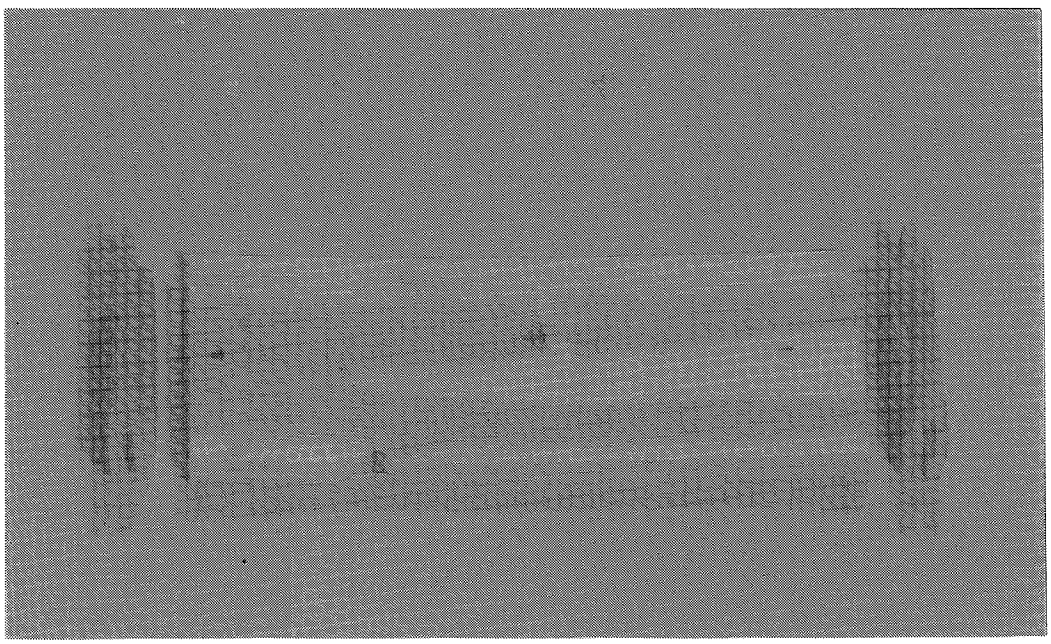

Figure 1.1. Compression wood in a patterned board of *Picea abies* (Hoffmeyer, 1987).

In logs and especially in branches reaction wood is recognizable through the presence of eccentric growth rings. In compression wood the pith will be displaced towards the tension side (Figure 1.2) and opposite for tension wood.

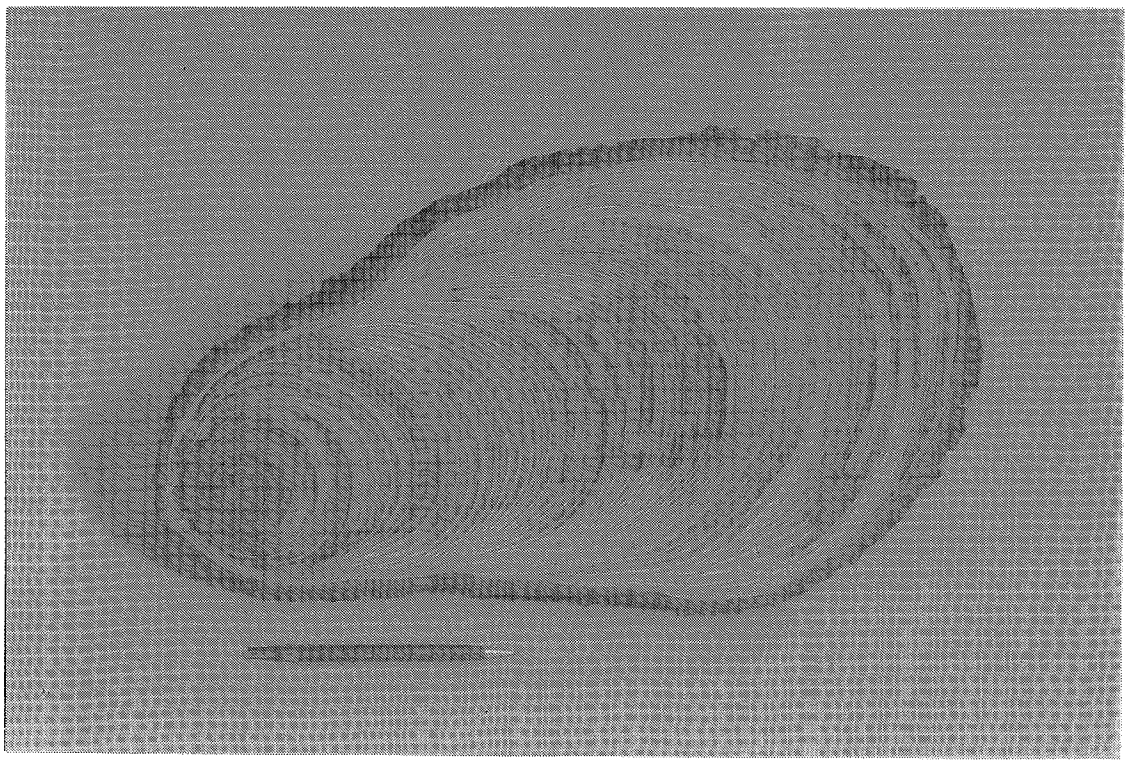

Figure 1.2

Eccentric growth and compression wood formation in a branch of *Abies alba*. (Hoffmeyer 1987a; sample by courtesy of Ths.Thomassen).

Tension wood stands out in dressed lumber because it is more reflective than normal wood. When processed green, tension wood tends to produce a fuzzy surface.

1.4 Anatomical Characteristics

A consistent feature in compression wood anatomy is the rounded rather than square shape of the tracheids as seen in a cross section (Côté and Day, 1964). This shape results in the formation of inter-cellular spaces at the junction of three or four tracheids.

Radial checks through S_2 to S_1 are seen as helical openings in the cell wall, thus revealing the extraordinarily low fibril angle of the compression wood S_2-layer (Figure 1.3). The S_3-layer is absent in compression wood.

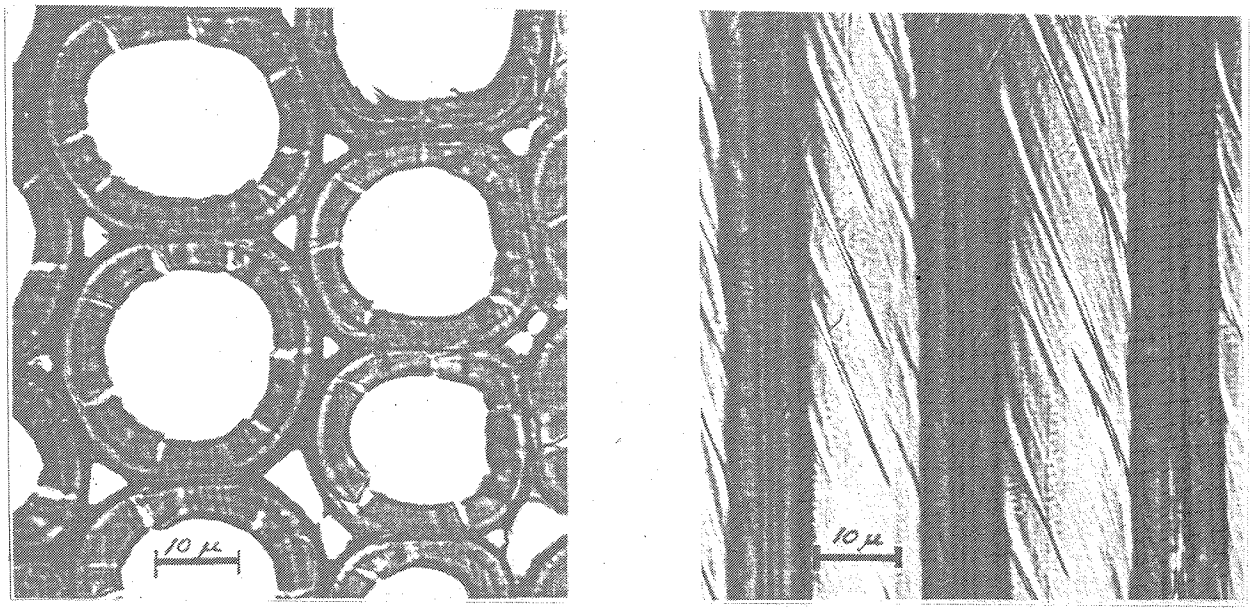

Figure 1.3. Compression wood tracheids in redwood, *Sequoia sempervirens*. a: cross section, b: longitudinal section (Côté and Day, 1964).

The tracheids of compression wood are significantly shorter than normal wood tracheids (Ollinmaa, 1959). The tips of compression wood tracheids are reported to be somewhat distorted (Wardrop, 1964b) with less than normal lengthwise overlap between tracheids. This characteristic may partially account for the glassy, short fibered failure typical of compression wood.

The helical angle of the order 45^{o} (Côté and Day, 1964; Fengel and Wegener, 1984) is not only responsible for the abnormal shrinkage and swelling behavior, but may also account for most of the abnormal mechanical properties.

A typical, but not consistent feature in tension wood anatomy is the presence of a gelatinous layer termed the G-layer. This layer may either replace the S_2-layer or the S_3-layer, or the G-layer may be added to the three normal secondary wall layers (Dadswell, Wardrop, and Watson, 1958).

The G-layer consists of concentric layers of highly crystalline cellulose fibrils aligned in the direction of the fiber axis, and the tension wood fiber is therefore particularly well suited to sustain tension stresses. However, such fibers will be less suited to sustain compression stresses, and slip planes and minute compression failures are actually reported to be occurring frequently in the G-layer (Wardrop and Dadswell, 1947; Isebrands and Parham, 1974).

1.5 Chemistry and Topochemistry

Normal softwoods and hardwoods both usually contain 42 ± 2% of cellulose. The lignin content of softwoods varies between 25 and 35%, while in hardwoods the range is 18 to 25%. The softwood hemicelluloses occur as galactoglucomannan (appr. 20%) and xylan (appr. 10%), while in hardwoods xylan accounts for 20 to 35%, and glucomannan occurs in only small amounts.

The chemical composition of compression wood differs significantly from normal wood as is seen in Table 1.2 (Timell, 1982). Compression wood contains 20-25% less cellulose and 30-40% more lignin than normal conifer wood. Compression wood cellulose is less crystalline, and the lignin is more condensed and contains more carbon-carbon bonds (Timell, 1982).

Table 1.2. Average chemical composition of normal and compression woods of conifers. All values in percent of extractive-free wood (Timell, 1982).

Constituent	Normal Wood	Compression Wood
Lignin	30	39
Cellulose	42	30
1,3-Glucan (laricinan)	Trace	2
Galactan	Trace	10
Galactoglucomannan	18	9
Xylan	8	8
Other polysaccharides	2	2

The microdistribution across the cell wall of the polysaccharides in compression wood is illustrated in Figure 1.4 (Côté et al., 1968).

The distribution of lignin in compression wood is different from that of normal wood. A larger proportion of the lignin is located within the secondary wall in compression wood than in normal wood tracheids. Over 90% of the total lignin is located within the secondary wall with a concentration of up to 50-60% in the S_2-layer.

The high lignification of the entire secondary wall together with the large microfibril angle is probably responsible for the high compressive strength of compression wood.

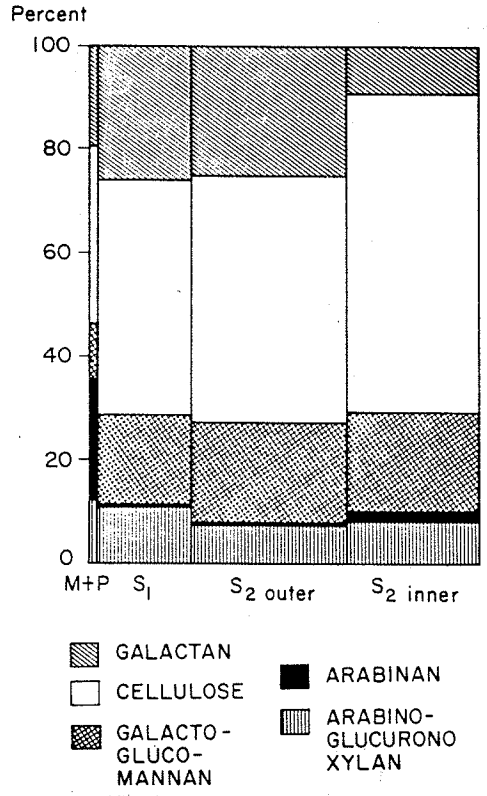

Figure 1.4. Graphical representation of the distribution of polysaccharides in compression wood tracheids of *Abies balsamea* (Côté et al., 1968).

There is less lignin holding the tracheids together in compression wood than in normal wood. This characteristic could also be part of the reason for the reported low tensile and impact strength values for compression wood.

The chemical composition of tension wood is illustrated in Table 1.3 (Schwerin, 1958 (here after Kollmann and Côté, 1984)).

Table 1.3 Composition of normal and tension wood from *Eucalyptus goniocalyx* (Schwerin, 1958 (here after Kollmann and Côté, 1984)). (All values in percent of extractive-free wood).

	Cellulose	Lignin	Pentosan	Acetyl	Galactose Residue
Normal Wood	44.0	29.5	15.1	3.0	2.5
Tension Wood	57.3	13.8	11.0	1.9	7.4

The composition reflects the relative importance of the cellulose-rich G-layer. The scarcity or absence of lignin in this layer makes it soft or gelatin-like, rather than stiff like other wall layers.

1.6 Physical Properties

Compression wood has a considerably higher density than normal wood. Data for carefully selected normal and severe compression woods of nine conifers (Timell, 1982) suggest a density ratio of approximately 1:2. Most often, however, the density contrast is much less pronounced (Pillow, 1937; Trendelenburg, 1958; Knigge, 1958; Perem, 1958; Ollinmaa, 1959; Cockrell and Knudson, 1973; Jensen, 1980).

Tension wood also exhibits a density difference compared to normal wood (von Pechmann, 1953; Trendelenburg, 1955; Knigge, 1958; Ollinmaa, 1959), but less pronounced than that of compression wood.

Compression wood generally shrinks more longitudinally and less transversely than normal wood (Trendelenburg, 1932; Pillow and Luxford, 1937; Ollinmaa, 1959; Panshin and de Zeeuw, 1970). This characteristic is related to the large fibril angle of the S_2-layer which is known to cause abnormal longitudinal shrinkage properties (Meylan, 1968).

Table 1.4 summarizes shrinkage values for a number of species. The calculated volumetric shrinkage shows that the total shrinkage of compression wood for some species is only 70-80% of that of normal wood. This may be accounted for by the high lignin content of compression wood as lignin holds less water (Stamm, 1964) and therefore shrinks less than holocelluloses.

The longitudinal shrinkage for tension wood is larger than for normal wood though the difference is not as large as for compression wood. The increased longitudinal shrinkage for tension wood cannot be explained by any large fibril angle as the fibrils of the G-layer are almost perfectly aligned with the fiber axis. However, as the G-layer is not always intimately connected to the rest of the cell wall, the shrinkage of layers as the S_1 may play a more dominant role than usual (Haygreen and Bowyer, 1982).

The abnormally large longitudinal shrinkage of reaction wood gives rise to very substantial internal stresses which may result in excessive deformations (Figure 1.5) or even the release of stresses through checks and fractures (Figure 1.6).

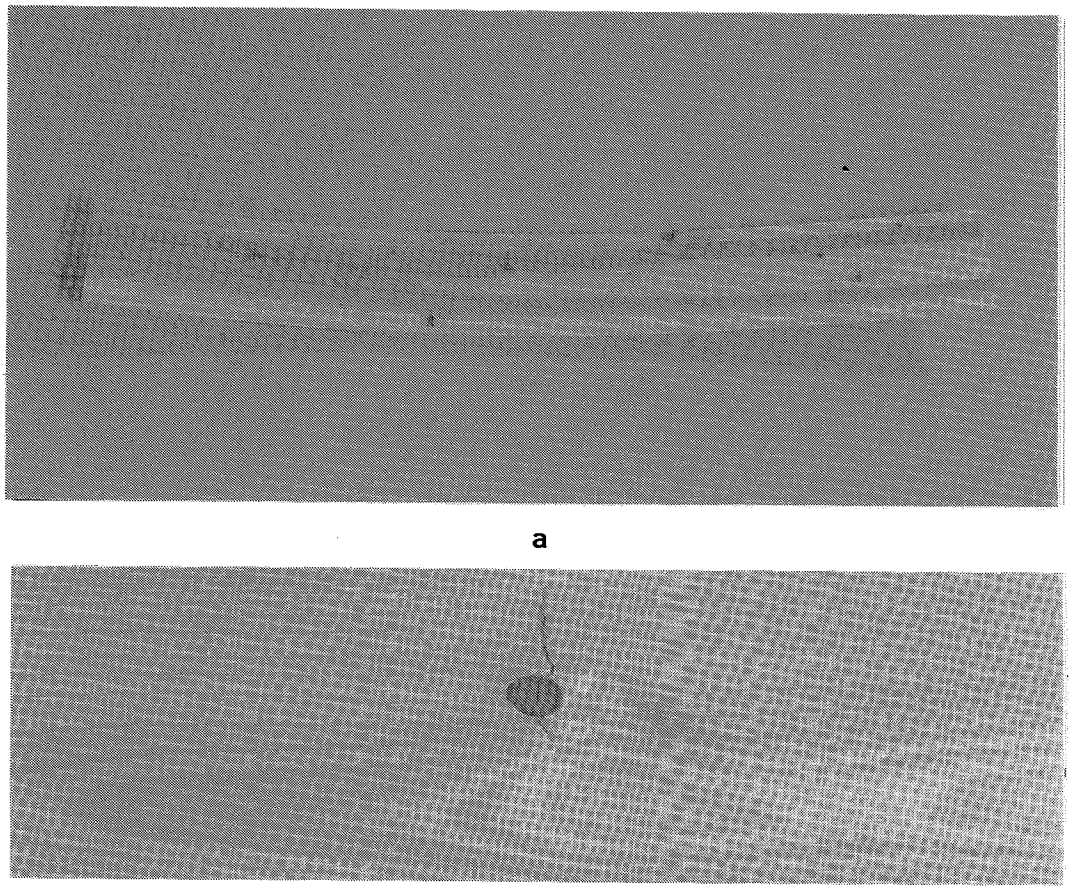

a

b

Figure 1.5 a: Deformation of spruce board containing compression wood. b: Enlargement of area around knot showing tensile failure along the grain due to internal stresses. (Hoffmeyer, 1987a).

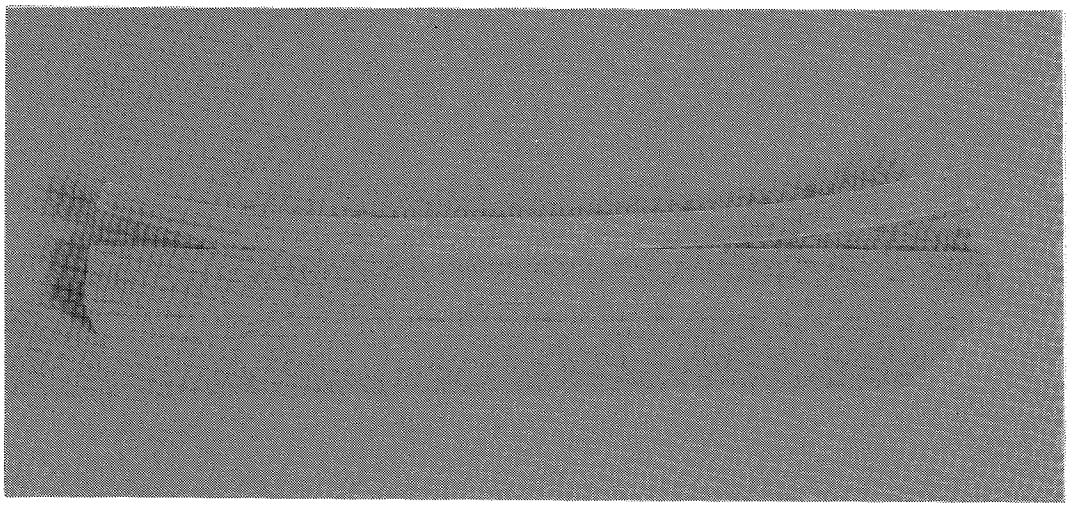

Figure 1.6 Differential longitudinal shrinkage in *Fagus silvatica* caused by the presence of tension wood. (Hoffmeyer, 1987a).

Table 1.4. Shrinkage (%) from green to oven-dry condition for normal wood (NW), compression wood (CW), and tension wood (TW).

Species	Type of Wood	Shrinkage (%) from green to oven-dry condition			
		Longitud.	Radial	Tangential	Volumetric
COMPRESSION WOOD					
Pinus ponderosa[1]	NW	0.4	4.6	6.2	11.3
	CW	2.5	2.2	2.6	7.3
Pinus ponderosa[2]	NW	0.2	3.1	6.4	9.7
	CW	0.8	2.2	5.1	8.1
Pseudotsuga menziezii[2]	NW	0.2	3.4	5.9	9.5
	CW	0.7	2.5	4.2	7.4
Sequoia sempervirens[2]	NW	0.1	1.5	3.5	5.1
	CW	1.2	1.4	2.4	5.0
Picea abies[3]	NW	0.2	4.8	6.5	11.5
	CW	3.6	2.1	3.2	8.9
TENSION WOOD					
Betula spp.[4]	NW	0.3	4.3	6.3	11.9
	TW	0.6	4.5	6.8	11.9
Acer saccharum[2]	NW	0.2	6.2	10.7	17.1
	TW	0.5	6.8	7.7	15.0

1) Trendelenburg, 1932
2) Pillow and Luxford, 1937
3) Ollinmaa, 1959
4) Ollinmaa, 1955
5) Marra, 1942 (here after Panshin and de Zeeuw, 1970)

1.7 Mechanical Properties

The mechanical properties of compression wood have been assessed by Pillow and Luxford (1937), Perem (1958), Ollinmaa (1959), Bernhardt (1966), Furono (1969), Kucera (1970,1973), Cockrell and Knudson (1973), Jensen (1980). Table 1.5 lists ratios between mechanical properties of reaction wood and normal wood as found by these authors.

In order to compare the mechanical properties of the compression wood tissue itself it is necessary to take into account the often very big difference between densities of compression wood and normal wood. Table 1.6 lists average ratios between mechanical strength of compression wood and normal wood for those values from Table 1.5 where density values have been available. In addition, specific ratios are given, referencing all strength values to the same

Table 1.5. Ratios between mechanical properties of reaction wood and normal wood based on actual density. The specific strength ratios taking into account the difference in density between reaction wood and normal wood are obtained by multiplying the ratios in Columns 3-7 by the ratios in Column 8.

(1)	(2)	(3)		(4)		(5)		(6)		(7)		(8)
Tree Species	Source	Compression strength		Tensile strength		Toughness		MOR		MOE		Ratio between density of normal wood and reaction wood
		green	dry	green	dry	green	dry	green	dry	green	dry	
COMPRESSION WOOD												
Douglas fir	Pillow & Luxford, 1937	1.27	0.99	0.79	0.97	0.98	0.44	1.18	0.97	0.74	0.71	0.87
White fir	Pillow & Luxford, 1937	1.29	1.13			1.09	0.98	1.25	1.21	0.83	0.83	0.74
Loblolly pine	Pillow & Luxford, 1937	1.16	0.84			0.78	0.63	1.04	0.88	0.51	0.49	-
Ponderosa pine	Pillow & Luxford, 1937	1.41	1.14	0.82		1.72	1.27	1.32	1.19	0.78	0.76	0.75
Old-growth redwood	Pillow & Luxford, 1937	1.17	1.01	0.58	0.85	0.84	1.00	1.02	0.87	0.62	0.63	-
Second-growth redwood	Pillow & Luxford, 1937	1.34	1.20			1.17	0.84	1.32	1.14	0.92	0.92	0.75
White spruce	Perem, 1958	1.21	1.05			1.30	0.65	1.15	1.04			0.85
Red pine	Perem, 1958	1.12	1.04			1.10	0.87	1.11	0.98			0.89
Picea abies	Ollinmaa, 1959	1.89										0.58
Pinus sylvestris	Ollinmaa, 1959		1.07									-
Picea abies	Bernhardt, 1966		0.94		0.81		0.75		0.94		0.90	1.00
Picea abies	Kucera, 1973								1.08			-
Giant sequoia	Cockrell & Knudson, 1973	1.44	1.30	1.14	1.81	1.39	2.33	1.65	1.42	0.99	0.92	0.63
Picea abies	Jensen, 1980		0.92		0.68							0.97
Picea jezoensis	Furono et al., 1969 1)			0.38	0.34							-
TENSION WOOD												
Betula spp.	Olinmaa, 1955 2)	0.90										-
Populus sp.	Rünger et al., 1953 2)	0.76			1.65							-
Populus tremuloides	Hale et al., 1961 2)	0.97	0.95			1.62	1.43	0.98	0.95			-
Populus sp.	Klauditz et al., 1955			0.85	1.66							0.87
Populus deltoides	Lassen, 1956 2)		0.93				2.24					-
Fagus silvatica	von Peckmann, 1958				1.15							-

1) here after Bodig and Jayne, 1982
2) here after Kärkkäinen and Raivonen, 1977

Table 1.6 Average ratios between mechanical strength of compression wood and normal wood based on those values from Table 1.5 for which density values are available (Giant Sequoia not included). Italic numbers indicate specific ratios referencing all strength values to the same density.

Compression strength		Tensile strength		Toughness		MOR		MOE		Average ratio between density of normal wood and compression wood
green	dry	green	dry	green	dry	green	dry	green	dry	
1.36	1.05	0.81	0.82	1.23	0.83	1.22	1.07	0.82	0.82	
1.05	*0.89*	*0.68*	*0.67*	*0.99*	*0.67*	*0.99*	*0.86*	*0.50*	*0.50*	0.80

density. The ratios listed in Table 1.6 are meant to indicate only general trends, and they should not be used as typical values for all conifers.

Compression wood in green condition shows significantly higher values of compression strength, toughness, and bending strength than does normal wood. Tensile strength is reduced by almost 10%, and modulus of elasticity is reduced by 15%. The relatively higher compression strength and lower tensile strength of compression wood would be expected to produce more brittle bending failures with no development of compression failures before ultimate failure as is seen in normal wood. This behavior has been noted by Cockrell and Knudson (1973).

The trends mentioned above would be expected considering the higher lignin content in the entire secondary wall, the lower lignin content of the middle lamella, and the approximately 45^{o} orientation of the fibrillar angle of the S_2-layer. However, when referring the mechanical values in green condition to the same density (specific ratios), there seems to be no improvements of any of the mechanical properties of compression wood tissue. From the point of view of mechanical properties it could therefore seem like wasted efforts of the living tree to change the whole structure and chemical composition of compression wood tissue rather than to just produce denser normal wood. As this of course must be an erroneous conclusion, one would have to look for other important properties or flaws in the interpretations. Two possible answers are suggested below.

1. Deflection at maximum load and thus the energy absorption capacity of non-failed wood would perhaps present an answer to the question. The data from Cockrell and Knudson (1973) actually shows that the energy absorption at maximum load for green *Sequoia gigantea* subjected to bending is four times

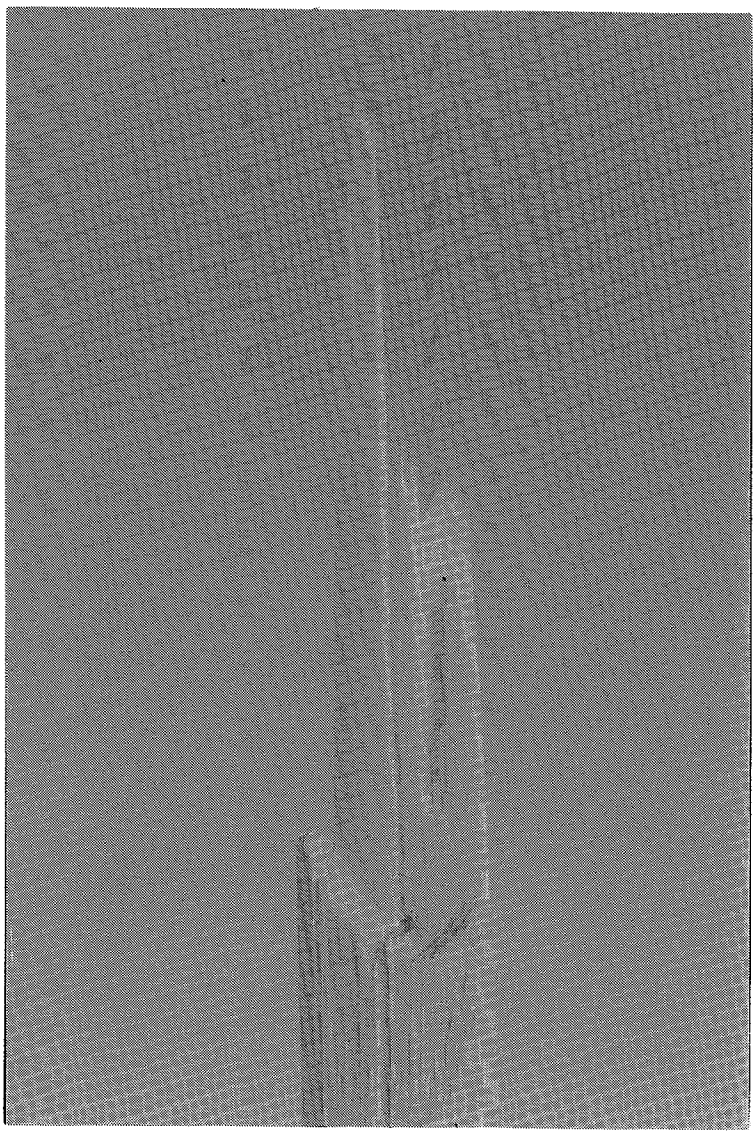

Figure 1.7

Tensile failure in *Picea abies*. The presence of compression wood (nearer, lower part) causes a short-fibered, brash fracture in contrast to the long-fibered fracture of normal wood (farther, upper part). (Hoffmeyer 1987a).

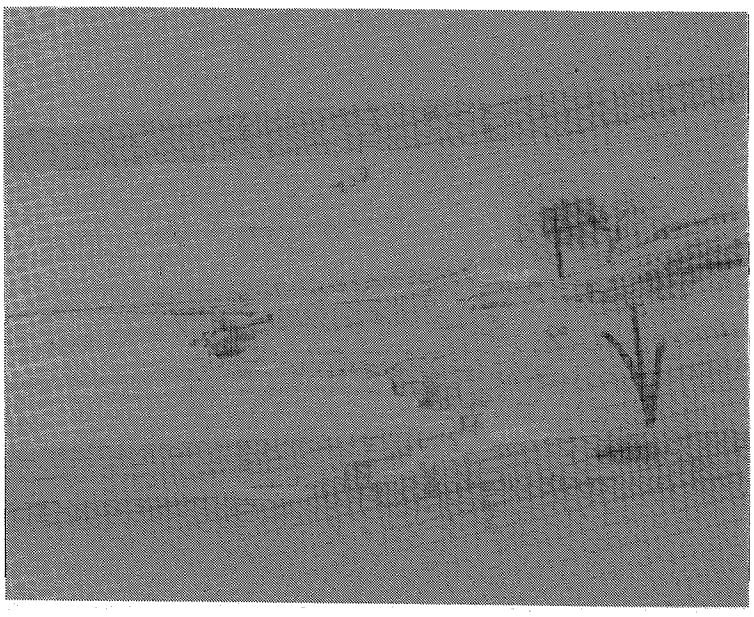

Figure 1.8

Bending failure in a 45x95mm board of *Picea abies*. The presence of compression wood causes a brash failure in the tension side in some distance from the knot. Creases in the compression side were produced after ultimate failure as a result of using a dead-load test rig (duration of load test). (Hoffmeyer 1987a).

greater for compression wood than for normal wood (Figure 1.9), whereas there is only a 2.1-time difference in total work to failure (toughness). In an ordinary toughness test (ASTM 143-52) on green wood Cockrell and Knudson demonstrated a 1.4-time difference.

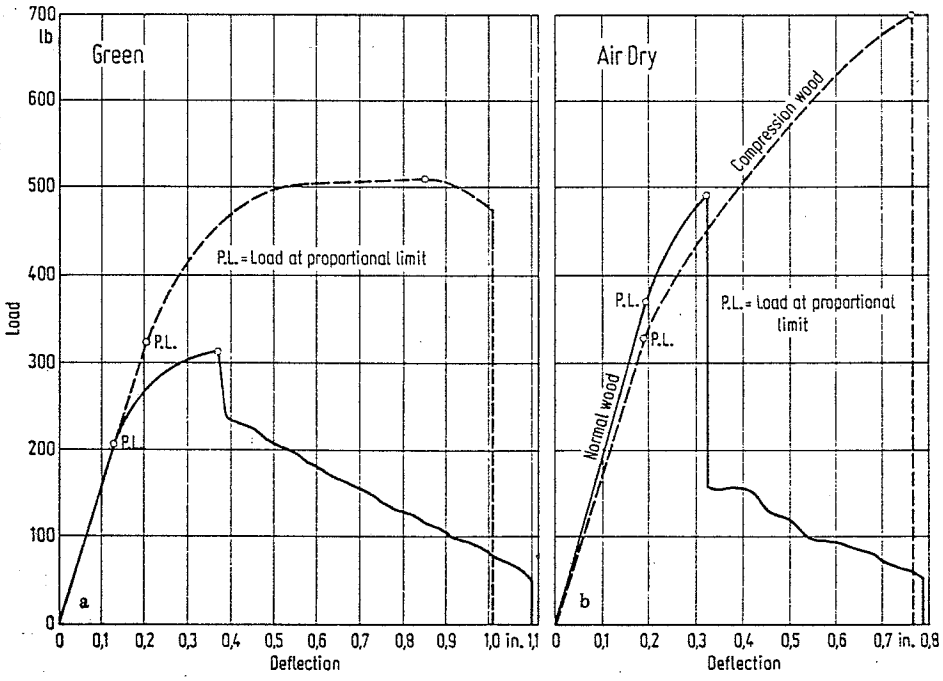

Figure 1.9. Comparison of static bending stress-strain curves of normal wood and compression wood tested a) green and b) dry (Cockrell and Knudson, 1973). Ratios between energy absorption of compression wood and normal wood are calculated 1) as energy at maximum load : ratio between areas left of point of maximum load and 2) as total energy (toughness): ratio between total stress/deflection areas.

The specific ratios (same density) would be 2.5 and 1.32 for work to maximum load and work to total failure, respectively. Clearly, for a living tree, work to maximum load would be more important than the total work to failure (toughness) which includes deflections that would be fatal for the living tree anyway.

2. Normal clear wood subjected to bending in green condition will always fail in the compression side long before the ultimate failure in the tension side is reached. A "plastic flow" (compression creases) will develop, and the neutral axis will be shifted towards the tension side while the tensile stresses continue to grow until they reach their ultimate value. Long before, however, the sap transportation in the tracheids of the compression side of a living tree would have ceased to function.

Thus, the bending strength (MOR) as assessed in an ordinary test often far exceeds that highest strength which a living tree can tolerate. To compare ordinary MOR values in order to understand the function of compression wood is therefore meaningless. What should be compared are the highest nominal bending stresses where compression failure has not yet been produced.

Compression wood has a much higher strain at maximum load and therefore allows the ultimate tensile stresses to develop without introducing fiber failures in the compression side.

Except for tensile strength and modulus of elasticity, drying of compression wood results in less increase of mechanical properties than is usual for normal wood. As seen in Table 1.6, there are only small differences between strength properties of dry compression wood and dry normal wood. The strength of dry compression wood tissue (specific ratios) is 10-15% lower than that of normal wood.

The properties of tension wood of hardwoods differ from those of compression wood. When green, both compression strength and tensile strength values are lower than those of normal wood (Table 1.5), whereas toughness seems to be higher. When dried, the tensile strength value seems to increase quite dramatically (Figure 1.10).

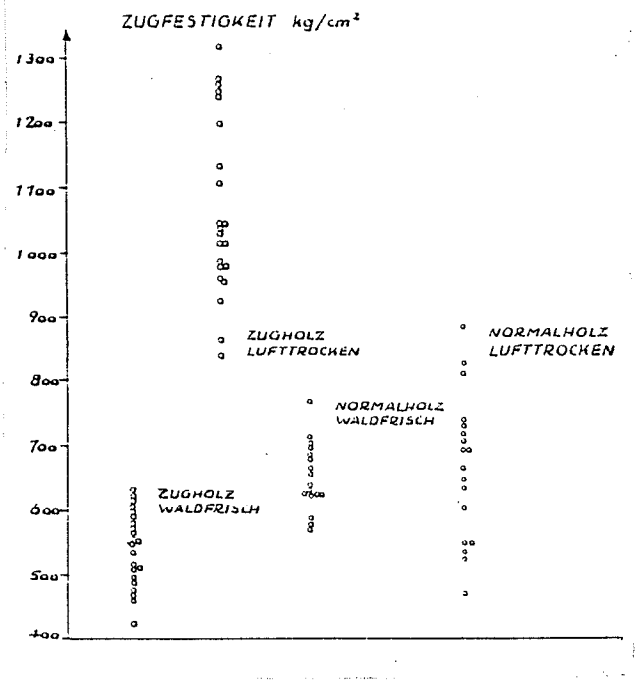

Figure 1.10. Tension strength of tension wood and normal wood of *Populus regen.* in green and dry condition (Klauditz and Stolley, 1955).

.... And first, the fir has most air and fire and least moisture and earth. Being thus furnished with the lighter powers of nature, it is not weighed down. It is held together by a natural stiffness, and is not quickly bent by a load, but remains straight in the flooring.

Vitruvius , 1 century B.C.

2. GRAIN ANGLE

2.1 Introduction

When the alignment of fibers in a piece of wood does not coincide with the longitudinal axis of the piece, the wood is said to be cross-grained.

Due to the highly anisotropic nature of wood, a small misalignment or grain angle may cause significant alterations of the mechanical properties. Cross grain is therefore considered a major defect when grading wood for strength and elasticity.

Cross grain in a piece of wood is characterized by the angle between fiber direction and an edge. Such slope of grain can result either from the way the lumber is cut from the log or from a natural spiraling of the grain in the living tree (Figure 2.1).

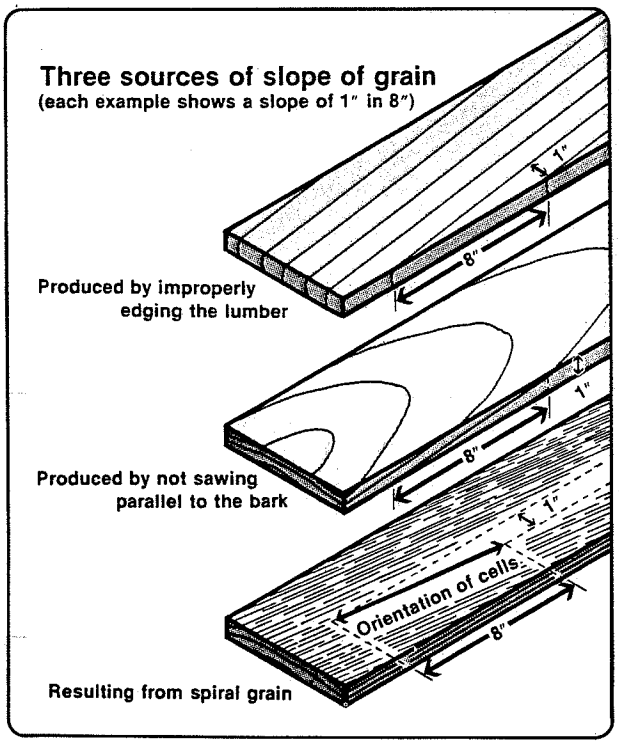

Figure 2.1. Cross grain in lumber can result from processing or from a natural spiraling of the fibers (Haygreen and Bowyer, 1982).

Grain angle problems may occur also in straight grown and correctly sawn lumber as a result of engineering design. Grain angle problems are present for instance in pitched or tapered beams and in practically all types of connections.

Grain angle problems are even the main reason why knots are considered to be the most serious strength reducing defect of all. The fiber disturbance around a knot rather than the knot itself is most often the cause of failure. Knots, however, will be dealt with in Chapter 3.

2.2 Types of Cross Grain

Spiral grain is a term used for the natural helical orientation of fibers in a tree stem (Figure 2.2). When such wood is processed into planks, cross grain appears.

The magnitude of spiraling varies widely in individual trees from pith to bark. Likewise the spiral grain pattern changes depending on the height in the trunk of the tree.

The tendency to spiral grain differs from species to species and even from tree to tree of the same species.

Young stems of conifers tend to develop left spiraling (Figure 2.2) followed by a gradual change to neutral and later to a right spiraling. Such a pattern for instance is typical of *Picea abies*. However, it is also possible to find *Picea abies* with no spiraling and even a few examples of a spiraling which is opposite to normal.

From own observations on *Picea abies* it seems that the left helix spirality is often confined to the juvenile wood. Therefore, fast grown timber having relatively more juvenile wood than slow grown timber of the same dimensions tends to cause significantly more twisting.

Mature wood has less tendency to warp due to the counterbalancing by the right helix.

When stock is sawn so that the grain of the wood intersects the surface at an angle, the piece has *diagonal grain* (Figure 2.2.b). This defect can be eliminated in straight logs by taper sawing.

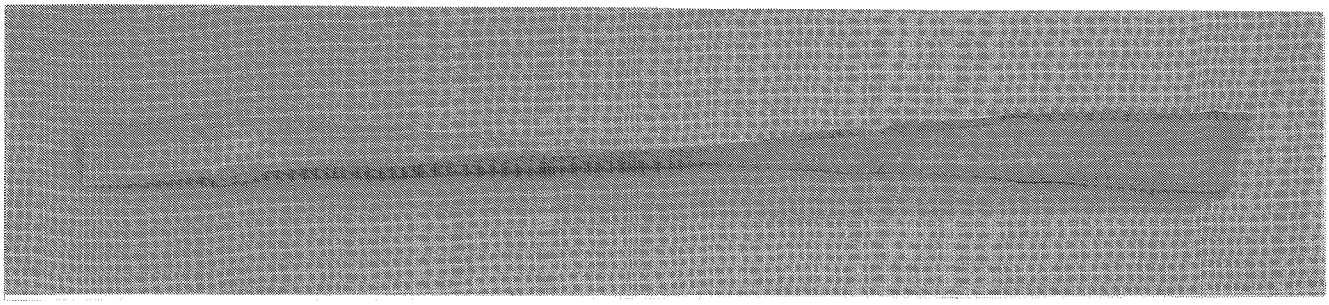

Figure 2.2.a. Left helix spiral grain in a young spruce stem. Wood material has been carefully removed, following the inclined grain, in order to reveal the characteristics better. (Hoffmeyer 1987a; sample by courtesy of Ths.Thomassen).

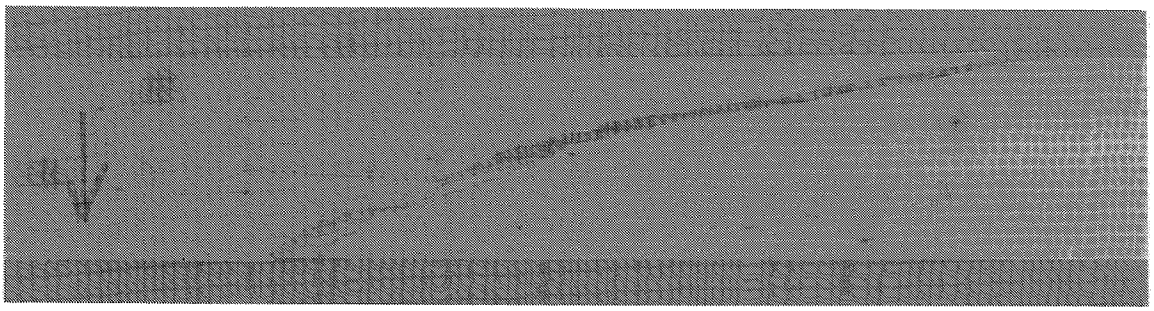

Figure 2.2.b. Bending failure in *Picea abies*. Failure is caused by diagonal grain. (Hoffmeyer 1987a).

2.3 Grain Angle and Elasticity

When wood is subjected to a load of an orientation different from the orientation of the principal axes, x,y,z, the elastic response changes.

The classical theory of linear elasticity can be very successfully applied to establish the relationship between the elastic parameters and the stress strain behavior in a rotated coordinate system. A brief description of the basics of theory of elasticity is given in Appendix A.

For rotation in one of the principal planes rather simple equations emerge (Appendix A, Section A.4). As an example, let us consider a rotation of the axes in the y,z plane (Figure 2.3.a). Furthermore, let us assess the variation of the important Young's modulus in this plane.

Equation A21 in Appendix A states that

$$S'_{22} = S_{22} \cos^4\theta + (2S_{23} + S_{44}) \sin^2\theta \cos^2\theta + S_{33} \sin^4\theta = 1/E_{y'} \qquad (2.1)$$

Similarly, a rotation as shown in Figures 2.3.b and 2.3.c produces the reciprocal Young's moduli:

$$S'_{11} = S_{11} \cos^4\psi + (2S_{12} + S_{66}) \sin^2\psi \cos^2\psi + S_{22} \sin^4\psi = 1/E_{x'} \qquad (2.2)$$

$$S'_{33} = S_{33} \cos^4\phi + (2S_{31} + S_{55}) \sin^2\phi \cos^2\phi + S_{11} \sin^4\phi = 1/E_{z'} \qquad (2.3)$$

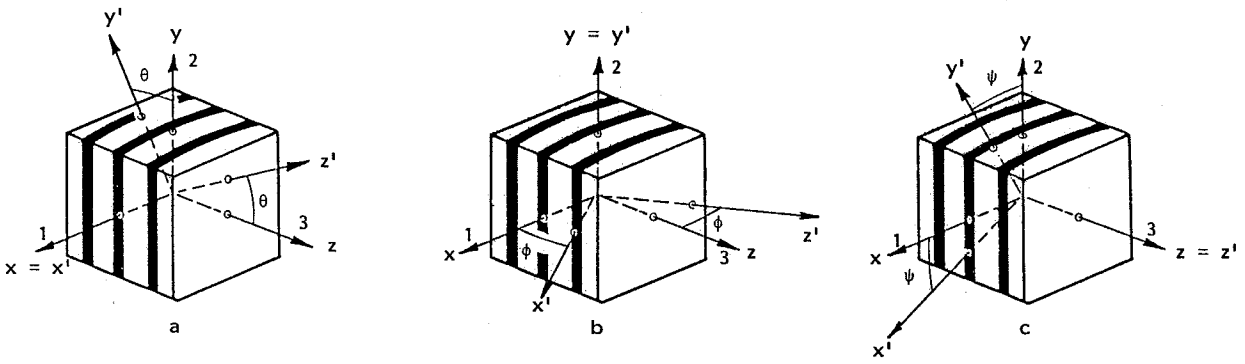

Figure 2.3. Rotation of coordinates in the principal planes.

Introduction of the compliance parameters from Table A.1 (Appendix A) gives values identical to those for pine (Kiefer) in Figure 2.4. Here, the anisotropy of Young's moduli becomes quite clear: In the x,y plane, Young's modulus varies from 0.6 to 17 GPa.

It is particularly interesting to note that the S'_{33} compliance parameter reaches a maximum value for a 45-degree angle to the annual rings due to the high S_{55} compliance parameter. Bodig and Jayne (1982) illustrate this behavior through tests on Sitka spruce (Figure 2.5). For the ring angle ϕ equal to 45 degrees, the reciprocal compliance parameter $1/S'_{33} = E_{z'}$ reaches a minimum value of 0.2 GPa.

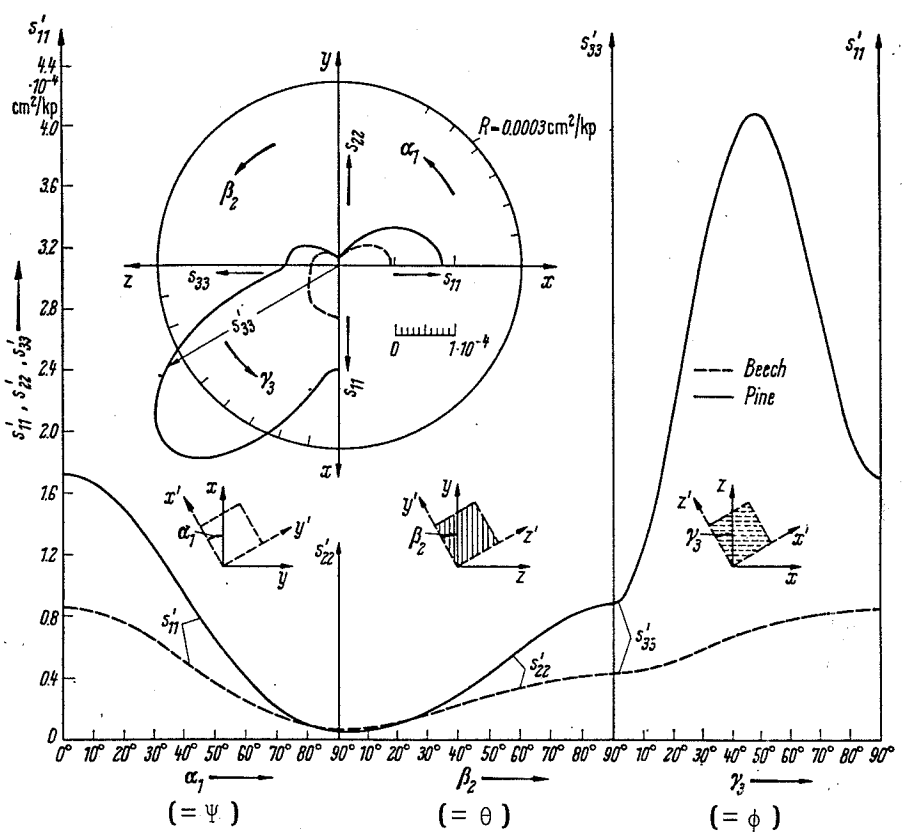

Figure 2.4. Sections through the deformation planes in *Fagus silvatica* (Buche) and *Pinus sylvestris* (Kiefer) (Keylwerth, 1951).

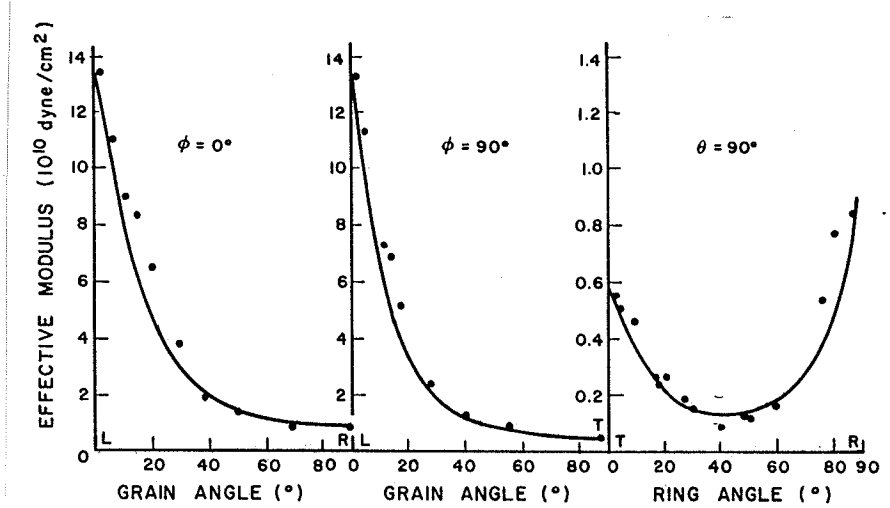

Figure 2.5. Effect of grain angle rotations on Young's modulus for Sitka spruce (Bodig and Jayne, 1982).

This peculiar elastic behavior of wood loaded perpendicular to grain was discussed already by Frey-Wyssling and Stüssi (1948). Small prisms of *Picea abies* were tested in compression, and stress-strain curves were obtained (Figure 2.6). The authors stated that a load applied in the radial or tangential

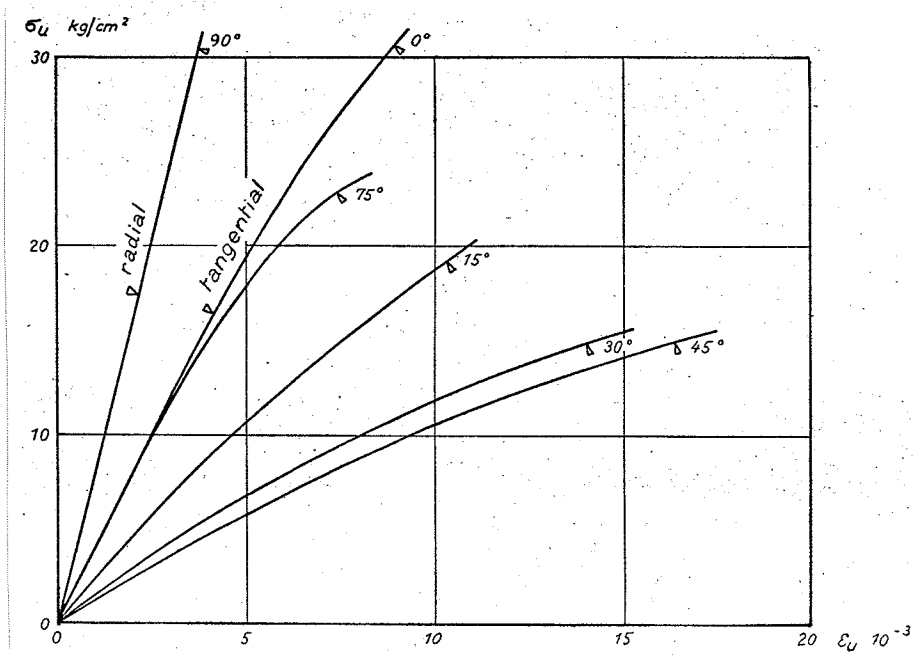

Figure 2.6. Stress-strain curves for *Picea abies* subjected to compression perpendicular to grain and with ring angle ϕ varying from 0 to 90 degrees (Frey-Wyssling and Stüssi, 1948).

direction resulted in an elastic response based only on the properties of the cell wall. Conversely, for $0^o < \phi < 45^o$ the elastic response is in addition a result of structural geometry. Here the cell geometry changes continuously as a function of load (Figure 2.7). The deformation therefore is a second-order function of load, and the stress-strain function is curved. Hoffmeyer (1971) puts forward the hypothesis that for tension perpendicular to grain an upward curved stress-strain function would have to show (Figure 2.7.3).

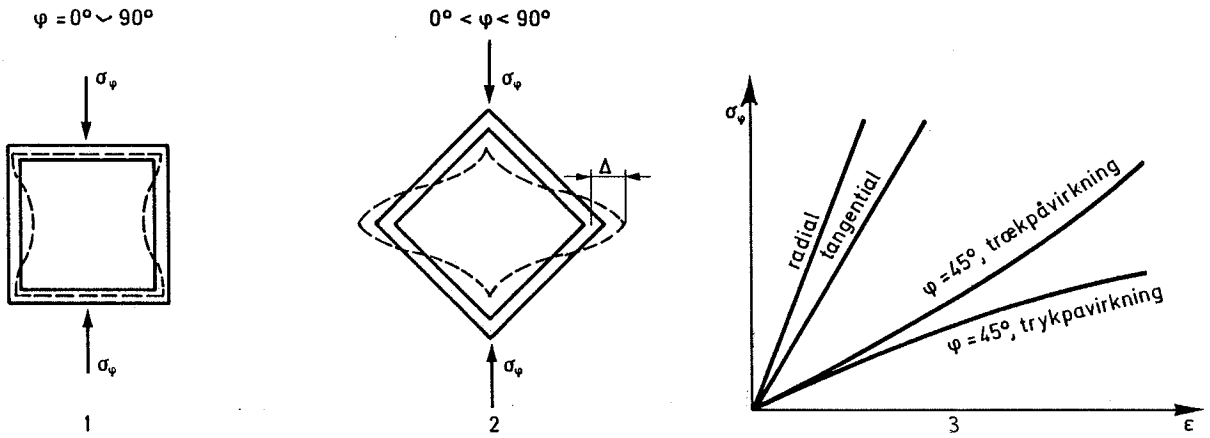

Figure 2.7. Single cell subjected to compression perpendicular to grain. (1) The cell sustains its original shape until final stability failure (linear stress-strain function). (2) The cell geometry changes continuously as a function of load. The deformation therefore is a second-order function of load (curved stress-strain function). (3) The stress-strain curve for tension perpendicular to grain at $\phi = 45^o$ consequently should be upward curved. (Hoffmeyer, 1970).

The calculation of the reciprocal Young's modulus may be simplified by introducing an experimentally determined compliance, S*, at 45^{o} grain angle. Keylwerth (1951) showed that Equation 2.1 can be transformed into

$$S'_{22} = (S_{22} \cos^2\theta - S_{33} \sin^2\theta) \cos 2\theta + S^*_{22} \sin^2 2\theta \qquad (2.4)$$

or written in engineering terms:

$$E_\theta = \frac{1}{\left(\frac{\cos^2\theta}{E_0} - \frac{\sin^2\theta}{E_{90}}\right) \cos 2\theta + \frac{\sin^2 2\theta}{E_{45}}} \qquad (2.5)$$

The equation has been experimentally proved to be very satisfactory (Keylwerth, 1951).

A pure "curve fitting equation" has been proposed for S'_{11} and S'_{22} (not to be used for S'_{33}) (Kollmann, 1934):

$$S'_{22} \approx S_{22} \cos^n\theta + S_{33} \sin^n\theta \qquad (2.6)$$

Based on experiments (Baumann, 1922), Kollmann suggested n = 3.

Long before, however, Hager (1842) (here after Gehri and Steurer, 1979) had carried out experiments on beams of pine and oak and had concluded:

> *«..... Wenn die Axe des Stabes einen gewissen Winkel (ϕ) mit der Holzfaser macht, so lässt sich der Elasticitäts-Modulus (e) aus demjenigen für die Längenrichtung der Faser (e') und demjenigen für die darauf senkrechte Richtung (e") herleiten, nämlich*
>
> $$e = \frac{e' \cdot e''}{e' \cdot \mathrm{Sin}\,\phi^3 + e'' \cdot \mathrm{Cos}\,\phi^3}$$
>
> *Mehrere Beobachtungen an Kiefern und Eichenholz bestätigen die Richtigkeit der Formel.»*

2.4 Grain Angle and Strength

Grain angle has a very marked influence on the strength of wood. The tensile strength in particular is very sensitive. Tensile strength along the grain is known to be the highest strength whereas the lowest is in tension perpendicular to grain. Compression strength is much less affected by grain angle. Dinwoodie (1981) reports on an anisotropy for Douglas fir in tension and compression of 48:1 and 7:1, respectively.

Anisotropy in strength is due in part to the cellular nature of timber and in part to the structure and orientation of the microfibrils in the wall layers. Bonding along the direction of the microfibrils is covalent, while bonding between microfibrils is by hydrogen bonds. Consequently, since the majority of the microfibrils are aligned at only a small angle to the longitudinal axis, it will be easier to rupture the cell wall if the load is applied perpendicular than if applied parallel to the fiber axis (Dinwoodie, 1981).

The grain angle/strength relationship for clear wood has early been the subject of numerous and very thorough investigations (e.g. Ayres, 1920; Robertson, 1920; Wilson, 1921; Baumann, 1922; Osgood, 1928; Winter, 1944; Stüssi, 1945; Kühne, 1955; Goodman and Bodig, 1971).

Much of this research was initiated as a result of the use of clear wood for highly stressed constructions like aircrafts.

As a typical example of these investigations, Figure 2.8 shows Baumann's (1922) results from compression tests.

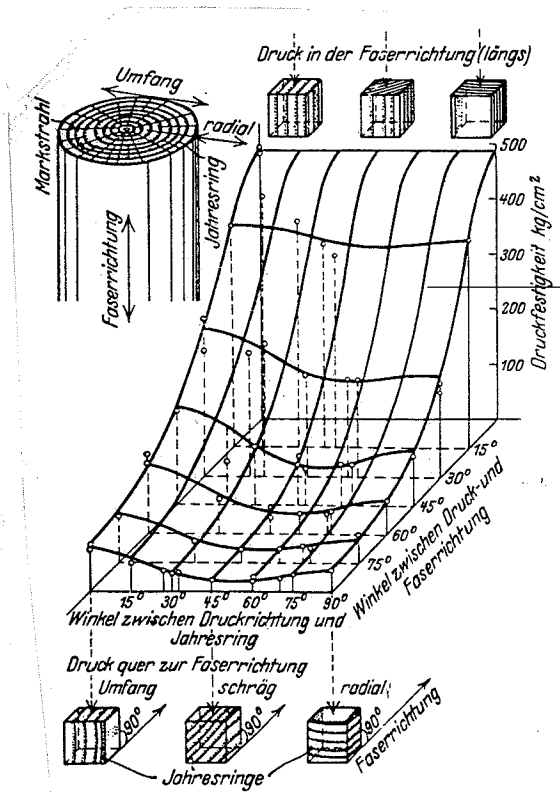

Figure 2.8. Relationship between fiber angle and load orientation (Baumann, 1922).

Note that at a 45-degree orientation to the annual rings, strength is at a minimum like the modulus of elasticity was shown to be (Section 2.3).

The modeling of strength as a function of grain angle is much less definitive than modeling of deformation. No general failure hypothesis for wood is yet available. Even quite simple static conditions are usually modeled by purely empirical expressions.

For the uniaxial condition, however, Robertson (1920) and later, independently, Stüssi (1946) used elementary theory of elasticity (Figure 2.9) to arrive at the hypothesis that ultimate stress f_θ is obtained for:

$$f_\theta = \min \begin{cases} f_0/\cos^2\theta \\ f_v/\sin\theta\ \cos\theta \\ f_{90}/\sin^2\theta \end{cases} \qquad (2.7)$$

where f_0 = strength parallel to grain

f_{90} = strength perpendicular to grain

f_v = shear strength

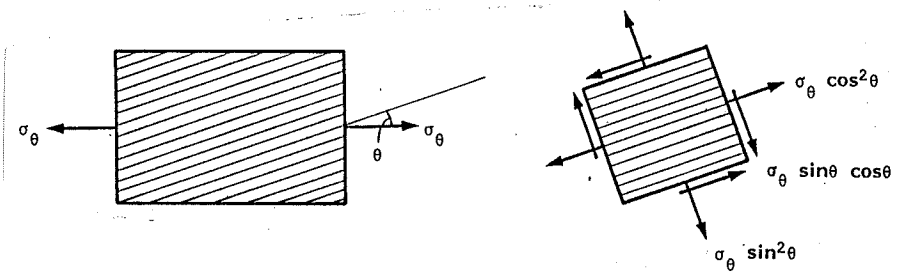

Figure 2.9. Uniaxially loaded wood prism.

Equation 2.7 was used by Stüssi (1946) to model Baumann's (1922) results (Figure 2.10) and has since been used successfully in several European countries. The three predicted failure modes are seen very clearly on specimens that have been subjected to compression failure (Figure 2.11). Note how different moisture content causes different grain angle intervals for the three failure modes. However, as three material properties are needed in Equation 2.7, simpler models (2.8) and (2.12) are used in timber codes. Note that

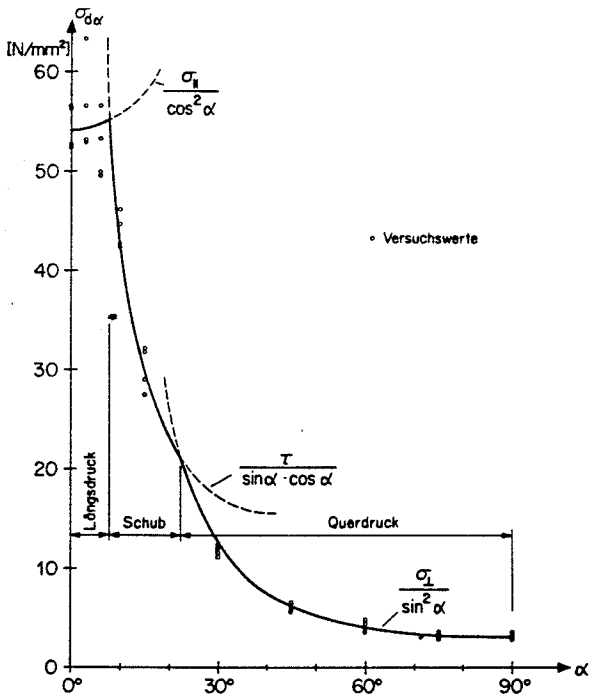

Figure 2.10. Compression strength as a function of grain angle modeled by Equation 2.7 (Stüssi, here after Gehri and Steurer, 1979).

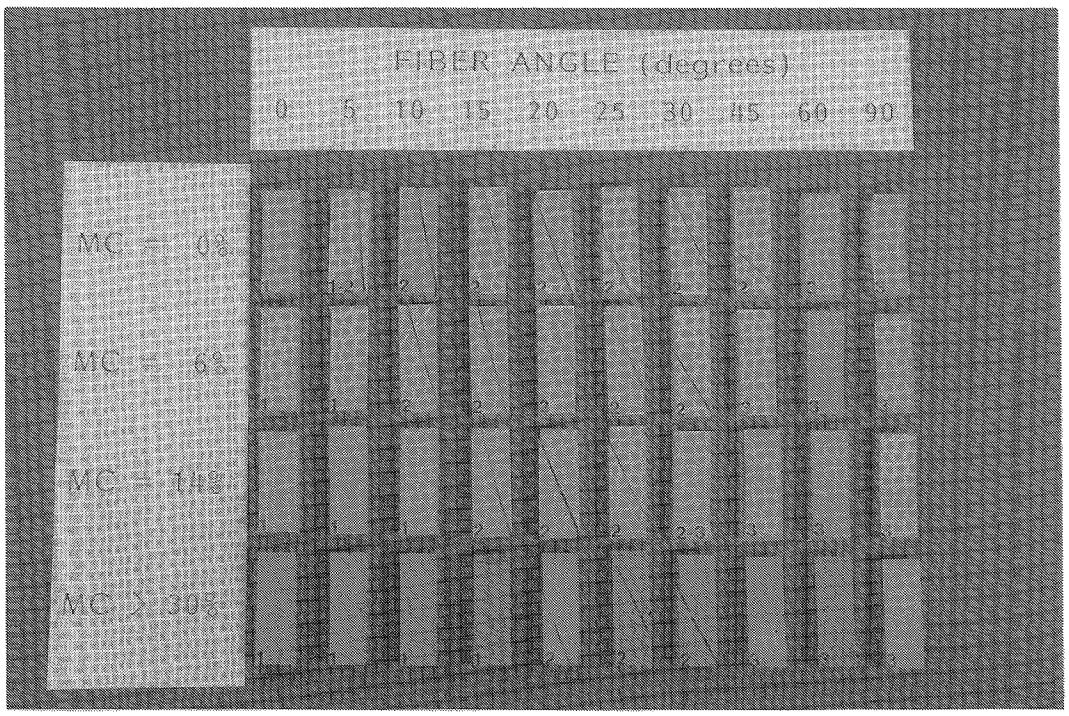

Figure 2.11. Compression tests using different angle θ between load and grain. The three different failure modes predicted by Equation 2.7 are clearly seen. (1) is compression failure parallel to grain, (2) is shear failure, and (3) is failure perpendicular to grain. Species is *Tsuga Heterophylla*, (Hoffmeyer, 1987a).

predicts a strength increase for increasing fiber angle as long as failure is caused by compression (or tension) parallel to grain.

A very useful empirical relation was suggested by Hankinson (1921):

$$f_\theta = \frac{f_0 \, f_{90}}{f_0 \sin^2\theta + f_{90} \cos^2\theta} \tag{2.8}$$

This equation needs only two materials properties and has now been generally recognized to produce sufficiently accurate predictions somewhat on the safe side. It is being used in timber design codes for instance in the U.S.A., Britain, and France.

Osgood (1928) improved Hankinson's equation by introducing a coefficient, a, that is supposed to be species dependent:

$$f_\theta = \frac{f_0 \, f_{90}}{f_{90} + (f_0 - f_{90})(\sin^2\theta + a \cos^2\theta) \sin^2\theta} \tag{2.9}$$

Kim (1986) tested a very limited number of specimens and concluded that the Osgood formula is superior to the Hankinson formula. This of course is hardly surprising as a three-parameter model should be expected to fit a single set of data better than a two-parameter model of the same type.

Kollmann (1934) probably independently suggested a relationship similar to Hankinson's

$$f_\theta = \frac{f_0 \, f_{90}}{f_0 \sin^n + f_{90} \cos^n} \tag{2.10}$$

and allowed n to have different values for tension, compression, etc.

Gehri and Steurer (1979) suggest an analogy to Equation 2.5 which seems to be based on a maximum strain to failure assumption:

$$\frac{1}{f_\theta} = \left[\frac{\cos^2\theta}{f_0} - \frac{\sin^2\theta}{f_{90}}\right] \cos 2\theta + \frac{\sin^2 2\theta}{f_{45}} \tag{2.11}$$

A very simple relationship, which is being used in a number of European timber codes, including the Scandinavian countries and West Germany, is

$$f_\theta = f_0 - (f_0 - f_{90}) \sin\theta \tag{2.12}$$

This equation, the origin of which is unknown to the author, is on the unsafe side for a large interval of grain angles.

Goodman and Bodig (1971) assumed the strength/fiber angle relationship in the x,z plane (T,R plane) to vary as a sinusoidal function, whereby they were able to expand the Hankinson equation (2.8) to three dimensions thus including both the angle θ and the ring angle ϕ (Figure 2.3):

$$f(\theta,\phi) = \frac{f_\theta}{\sin^2\phi + \frac{f_\theta}{f_L}\cos^2\phi} \qquad (2.13)$$

where

$$f_\theta = \left(\frac{f_R - f_T}{90}\right)\theta + f_T - K \cdot \sin 2\theta \left(\frac{f_T + f_R}{2}\right) \qquad (2.14)$$

The constant K in Equation 2.14 is approximately 0.4 for softwoods and 0.2 for hardwoods.

Figure 2.12 shows results from tests on oak (Goodman and Bodig, 1971).

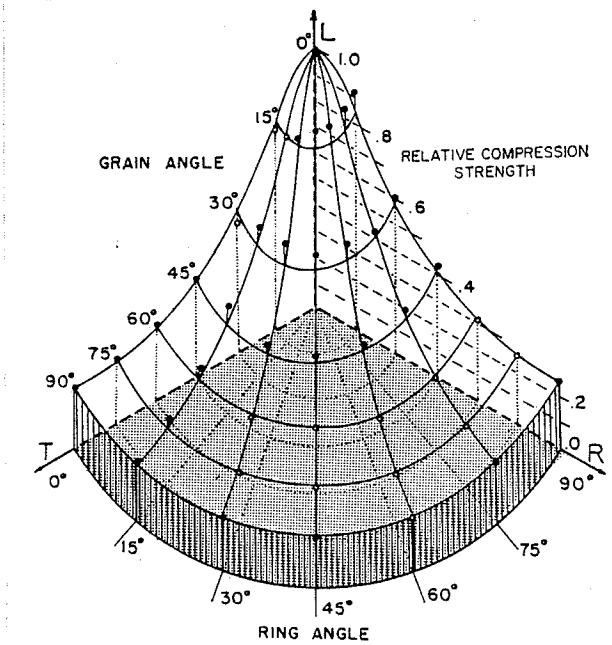

Figure 2.12. Comparison of experimental data and surface predicted by the three-dimensional Hankinson formula for oak (Equation 2.13) (Goodman and Bodig, 1971).

For multiaxial load, Norris (1939) suggested the interaction failure criterion

$$\left[\left(\frac{\sigma_0}{f_0}\right)^2 + \left(\frac{\sigma_{90}}{f_{90}}\right)^2 + \left(\frac{\tau}{f_v}\right)\right]^2 = 1 \qquad (2.15)$$

where σ_0, σ_{90}, and τ are stresses in the principal directions.

Norris' failure criterion is today widely used in timber design codes all over the world, for instance to design tapered beams (e.g. Maki and Kuenzi, 1965; Gehri and Steurer, 1979; Larsen and Riberholt, 1983; ISO, 1986).

2.5 Grain Angle as a Stress Grading Parameter

For design purposes the influence of defects is often quantified by using so-called strength ratios. The strength ratio is the ratio of the strength of a structural member which contains the defect to the strength of a defect-free member of the same dimensions.

Bodig and Jayne (1982) present a relationship between general slope of grain and different properties (Table 2.1).

Table 2.1. Strength ratio as a function of slope of grain (Bodig and Jayne, 1982). 1) Note that "parallel to grain" should read "parallel to edge of board".

	Strength Ratio, %	
Slope of Grain	Bending or Tension Parallel to Grain	Compression Parallel to Grain
1 in 6	40	56
1 in 8	53	66
1 in 10	61	74
1 in 12	69	82
1 in 14	74	87
1 in 15	76	100
1 in 16	80	–
1 in 18	85	–
1 in 20	100	–

Limits on the general slope of grain parameter along with limits on a dozen other parameters like knots, wane, fissures, etc. form the basis of stress grading rules. Such rules most often divide the lumber into three or more strength classes. An example of typical values for the slope of grain limits is shown in Table 2.2. Both North American rules and a set of European rules (EEC) are included. Numbers for typical 5-percentile values of bending strength have been extracted from Fewell (1984) and Hoffmeyer (1981).

Table 2.2. Slope of grain limits for North American and European (EEC) stress grading rules.

	ALS and CLS			European EEC		
	SS	No. 1	No. 2	S10	S8	S6
Slope of grain	1:12	1:10	1:8	1:10	1:10	1:6
Typical 5-percentile values of bending strength (MPa)*	26	18	18	27	22	17

* ALS and CLS values based on a mix of SPF, Hem-Fir, and Douglas-Fir. EEC values based mainly on *Picea abies* and *Pinus sylvestris*.

Bodig and Jayne (1982) state that for dimension lumber slope of grain "is usually the most critical of all (defects)". This is contradicted by other findings. Littleford (1978) showed that invariable of stress grade, general slope of grain even including "grain distortion" accounts for less than 10% of failures for NLGA grades of dimension lumber (Table 2.3). In a series of bending tests including 520 low-quality boards of *Picea abies*, Hoffmeyer (1984) confirmed Littlewood's findings, and he also found a very modest 0.20 coefficient of correlation between bending strength and slope of grain (Table 2.4).

Vinopal (1980) conducted strength tests on more than 800 boards of a pine species and concluded that there seemed to be no correlation between strength and slope of grain.

Foslie and Moen (1972) had up to 30% grain angle caused failures in tests on spruce lumber. However, many of these failures were triggered by the presence of a knot causing a steep, but local inclination of grain.

Table 2.3. Percentage of failures associated with various strength reducing characteristics for NLGA grades of dimension lumber (Littleford, 1978).

CAUSE OF FAILURE	GRADE				
	Sel. Str.	No. 1	No. 2	No. 3	All Grades
Knots					
Edge	44	61	44	40	48
Non-Edge	23	27	25	20	24
Slope of grain	4	2	5	4	4
Grain distortion	2	2	4	6	3
Splits, checks, shakes	0	0	2	8	2
Unsound wood	0	0	0	4	1
Wane	0	0	0	0	0
Other factors	27	8	20	18	18
TOTALS	100	100	100	100	100

Table 2.4. Correlation coefficients for bending strength as dependent on various stress grading parameters (Hoffmeyer, 1984).

Stress grading parameter	Coefficient of correlation, R
Knots	0.45
Grain angle	0.20
Annual ring width	0.52
Density	0.55
Modulus of elasticity (MOE)	0.73
Knots and annual ring width	0.65
Knots and MOE	0.76
Knots, density, and MOE	0.78

It may be concluded then that although the presence of knots is the single most important strength reducing parameter, the general slope of grain ranks high among the secondary causes of failure. However, if local slope of grain around knots is also considered, grain angle will probably be the single most important parameter.

.... The oak, on the other hand, abounds in earthy saturations of the elements, and has little moisture and fire and air. When it is buried in foundations, it has unlimited duration.

Vitruvius , 1 century B.C.

3. KNOTS

3.1 Introduction

Knots are the parts of limbs that are embedded in the main stem of the tree. As the tree grows, branching is initiated by lateral bud development from the twig (Figure 3.1).

The lateral branch thus was originally connected to the pith of the main stem. Each successive growth ring or layer forms continuously over the stem and branches, although the growth ring is thicker on the stem than on the branches, and the branch diameter increases more slowly than the trunk. As the girth of the trunk increases, a cone of branch wood - the intergrown knot - develops within the trunk (Figure 3.2). Such knots are also termed tight knots because they are intergrown with surrounding wood, or red knots, especially in conifers where they often have a distinct reddish tinge. At some point the limb may die, perhaps as a result of overshadowing by limbs higher up. The limb dies back to approximately the trunk surface, its dead cambium unable to add further girth. So subsequent growth rings added to the main stem simply surround the dead limb stub, which may begin to rot. A number of years of growth may be added to the main stem, surrounding the branch stub. The dead part of the stub becomes an encased knot. It is not intergrown and therefore is called a loose knot, often with bark entrapped. Knotholes result when an encased or loose knot falls out of a board. Enclosed knots also are called black knots because they commonly are discolored by stain and decay. In time the stub may become weakened by decay and fall or be broken off, or it may be pruned back flush with the trunk. Further growth layers will enclose the stub, and eventually the cambium will form a continuous layer. From this point on, solid layers of wood and bark will be formed beyond the overgrown knot.

Knots may be classified by how they are cut from the tree. If they are split by radial sawing and extend across the face of the board, they are termed spike knots. On flat-sawn boards they usually appear round or oval and are called round knots. Knots smaller than 1/4 inch in diameter are called pin knots (Hoadley, 1981).

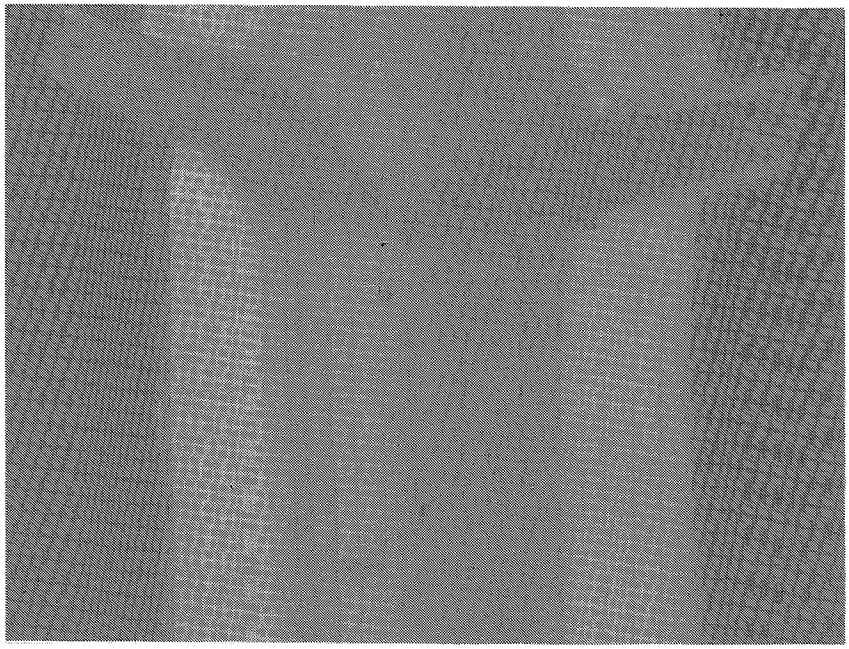

Figure 3.1.a. The lateral branch is connected to the pith of the main stem. Each successive growth ring or layer forms continuously over the stem and branches, although the growth ring is thicker on the stem than on the branches. (Hoffmeyer 1987a).

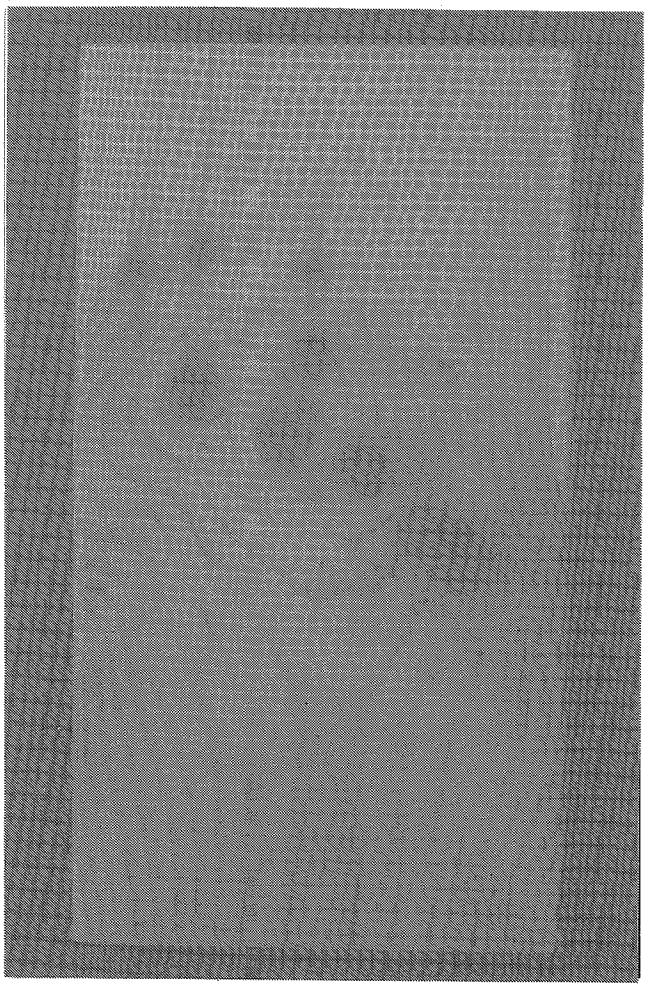

Figure 3.1.b.

Coniferous trees are characterized by having a dominant stem from which whorls of lateral branching occur at regular intervals or nodes.

A softwood board therefore shows knots in clusters separated by the often clear wood of the internodes. (Hoffmeyer, 1987a).

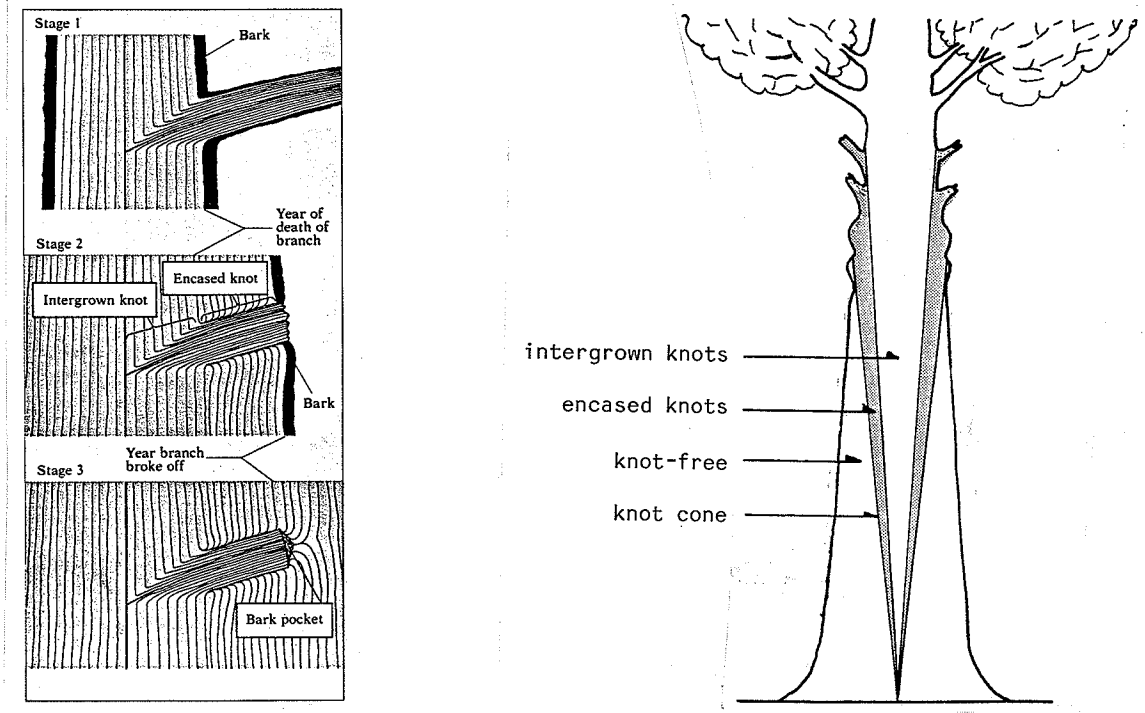

Figure 3.2. (a): Stages of "formation of knots" (Hoadley, 1981). (b): Location of knots in the stem of a tree (Hoffmeyer, 1969).

Coniferous trees are characterized by having a dominant stem from which whorls of lateral branching occur at regular intervals or nodes. A softwood board therefore shows knots in clusters separated by the often clear wood of the internodes.

3.2 Knots and Mechanical Properties

Knots are by far the single most important defect in connection with mechanical properties. At the same time it is the most difficult defect to model.

The strength and stiffness reducing effects of knots are related to the form, size, number, and position of knots and also to the kind of load to which the member is subjected. Even moisture and duration of the load affects the influence of knots.

The strength and stiffness reducing effect is a result both of the geometrical reduction of the cross section caused by the weak knot, but also of the fiber disturbance caused by the knot (Figure 3.3). Add to this the general anisotropy of the wood, and the result is an extremely complicated, three-dimensional stress distribution.

Appendix C presents pictures of failure initiating knots including some explanatory notes.

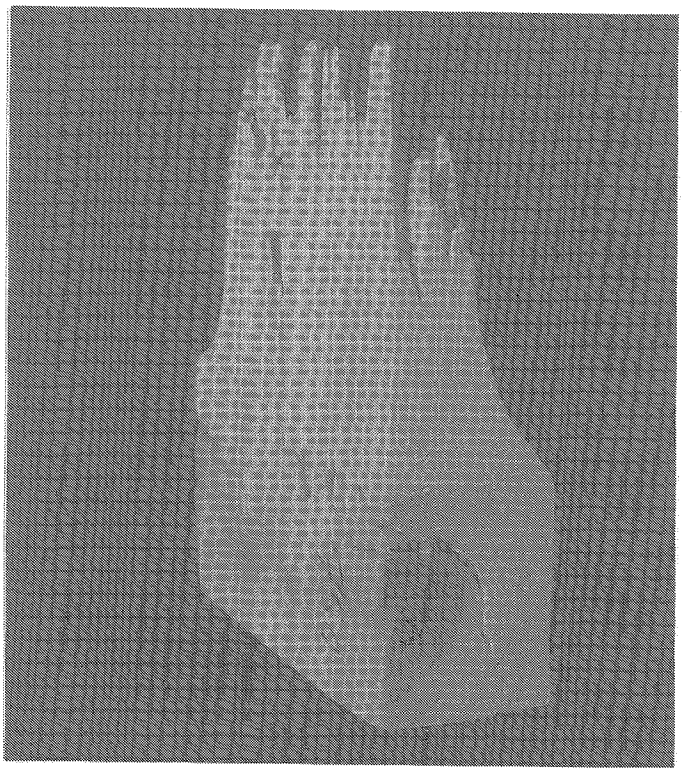

Figure 3.3.

The strength and stiffness reducing effect of knots is a result both of the geometrical reduction of the cross section caused by the knot, but also of the fiber disturbance caused by the knot. The figure shows a *Picea abies* board failed in tension. (Hoffmeyer 1987a).

Tensile strength is particularly sensitive to the presence of knots. Dawe (1964) demonstrated a reduction of tensile strength greater than what should be expected from the mere geometrical reduction of the cross section (Figure 3.4). This suggests that either the knot causes stress peaks to occur or the fiber disturbance adds to the strength reduction.

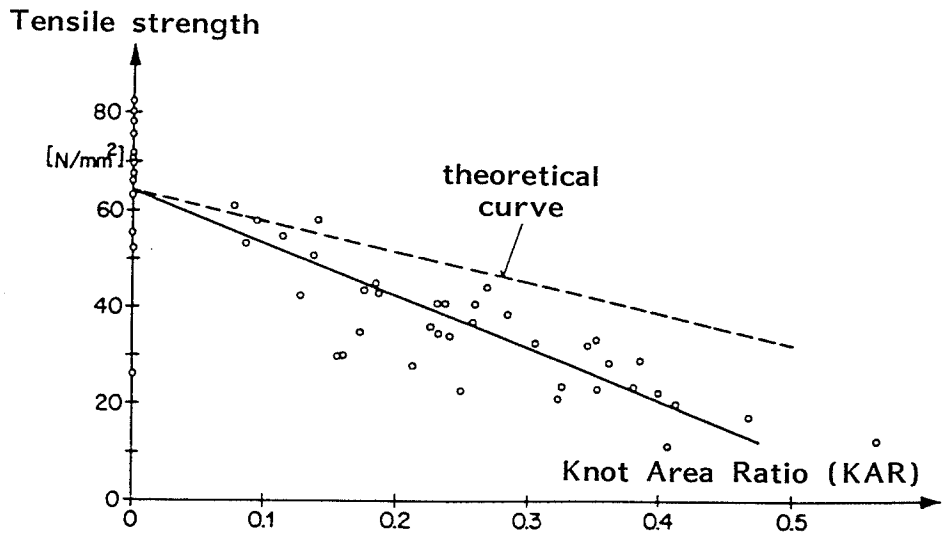

Figure 3.4. Tensile strength as a function of knot area ratio for Pinus sylvestris (Dawe, 1964).

While Dawe (1964) used boards with knots in the central portion of the cross section, Kunesh and Johnson (1972) introduced two knot positions, center and edge knots. A significantly lower strength of edge-knot boards was demonstrated (Figure 3.5). The difference in strength is explained by the eccentric loading caused by the edge knot and also by the lack of "embedment" of the cross grain at the edge.

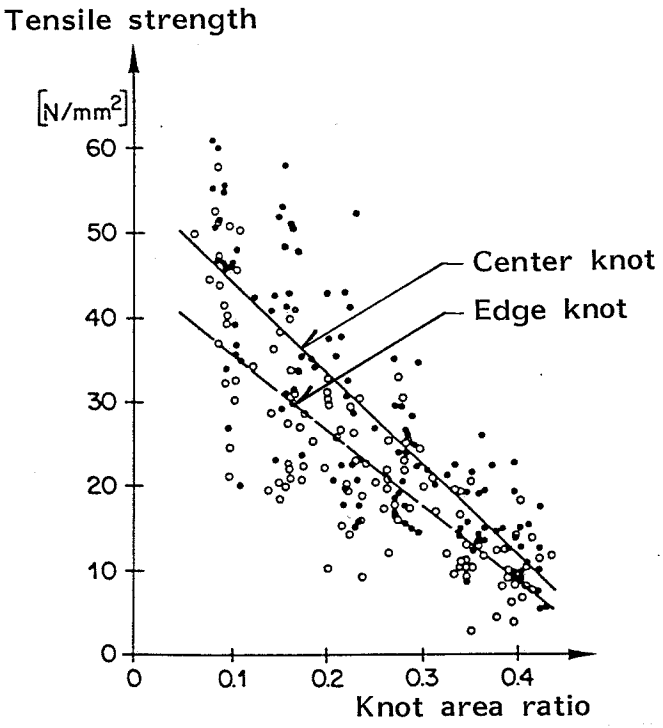

Figure 3.5. Tensile strength as dependent on knot area ratio and position of knot (Kunesh and Johnson, 1972). Here in an adapted version after Gehri and Steurer (1979).

Compression strength is influenced by knots, but much less so than tensile strength (Figure 3.6). Consequently, bending strength should be expected

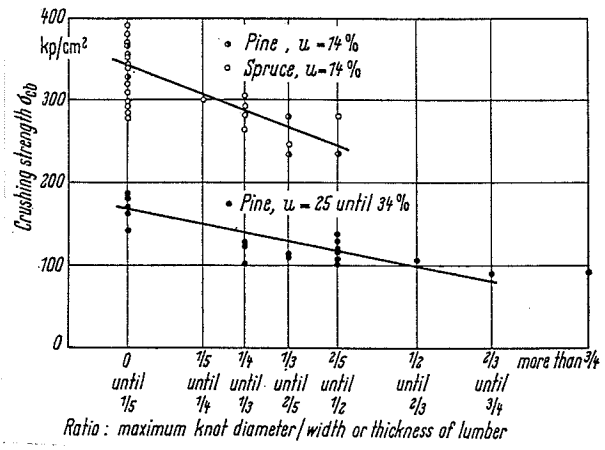

Figure 3.6. Effect of knot size on the compression strength (Graf, 1938, in: Kollmann and Côté, 1984).

to be very sensitive especially to the position of knots. Littlewood (1978) showed this by orienting the boards at random in the testing machine and then noting whether the weakest edge was actually in tension or compression (Figure 3.7).

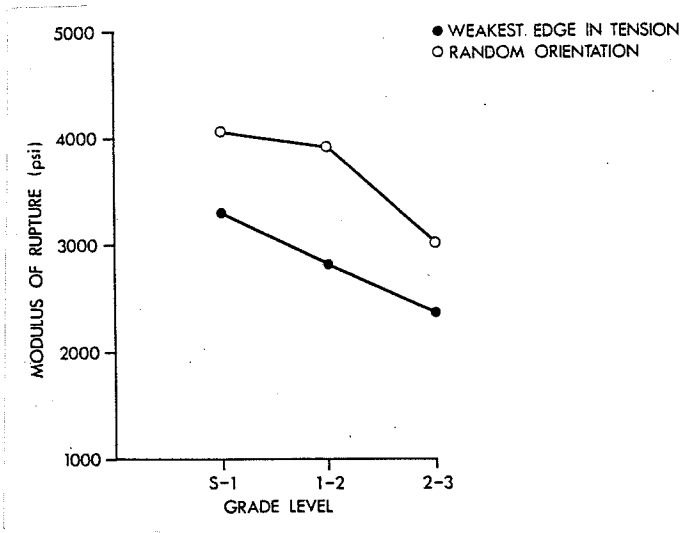

Figure 3.7. Effect of orientation of test piece on modulus of rupture (Littlewood, 1978).

If the weakest edge is placed at random, and if furthermore failure causing defects other than knots are present, a rather poor correlation between modulus of rupture and knots results (Hoffmeyer, 1984) (Figure 3.8). This is

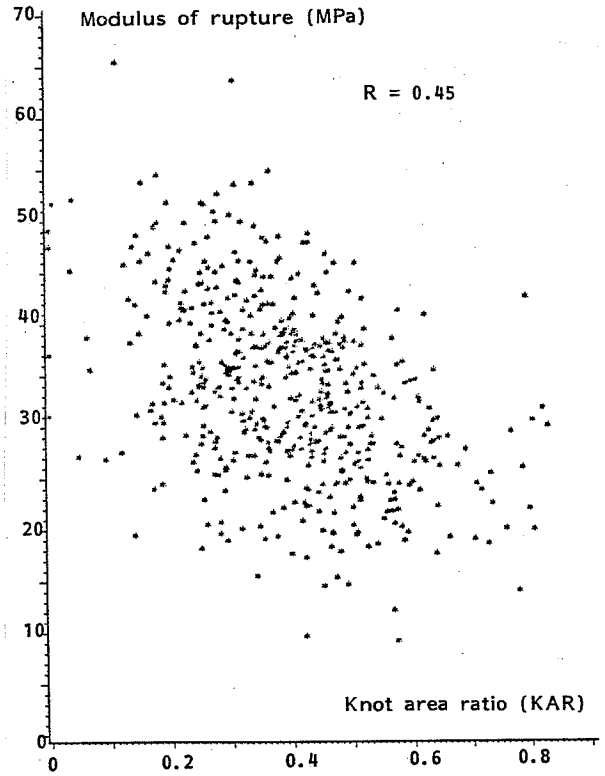

Figure 3.8.

Relation between modulus of rupture and knot area ratio (KAR) for 520 boards of *Picea abies*. The weakest edge oriented at random. (Hoffmeyer, 1984).

the normal situation when lumber is used in construction work. The figure demonstrates that additional strength dependent parameters must be added in order to produce efficient visual stress grading rules.

3.3 Modeling the Influence of Knots

To be able to model the influence of knots on the mechanical properties is a prerequisite of an efficient use of timber in load bearing constructions.

Knot models may be crude, easy to use rules for stress grading or they may be highly sophisticated mathematical models used for instance to assess the stress peaks around knots of well defined location, geometry, and properties.

Both the simple and the sophisticated models are necessary in order to promote further the use of wood.

The simple models must embrace a wide variety of knot characteristics and be able to assess the mechanical properties with modest accuracy. Such models exist today. However, they can easily be improved. A good example is the North American stress-grading rules (ALS and CLS), which are at present unable to distinguish between the two grades, No. 1 and No. 2 (Table 2.2). This shortcoming is, in part, due to inefficient knot modeling (Littleford, 1978; Fewell, 1984).

The sophisticated models, on the other hand, are necessary in order to improve our understanding of failure mechanisms. An example would be the understanding of the combined shear and tension perpendicular to grain failure caused by local grain deviation around knots. How, for instance, are stress peaks and the interrelationship between shear and tension perpendicular influenced by mositure or the duration of stresses?

Although modeling of the influence of knots has been a research area for a long period, recent years have experienced a growing interest for both simple and sophisticated models. Some of this research is still only reported as M.Sc. theses (e.g. SUNY, Syracuse; Colorado State University) and has not been available to this study.

3.3.1 Knot Ratio (KR) and Knot Area Ratio (KAR)

All stress grading rules characterize knots either by their appearance on the surface of a board (knot ratio (KR)) or by an assessment of the ratio between the (imagined) knot area in a cross section and the area of the total cross section (knot area ratio (KAR)) (Figure 3.9).

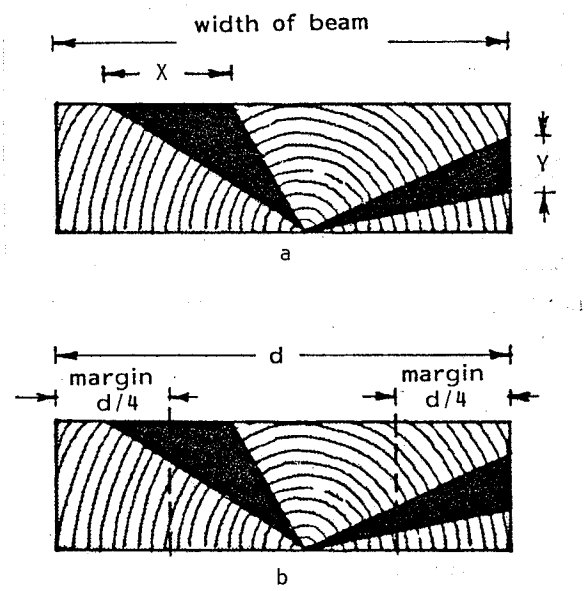

Figure 3.9

The influence of knots may be assessed either by
(a) knot ratio (KR) which involves measurement of dimensions on the surface of the boards (X,Y), or by
(b) knot area ratio (KAR) based on an assessment of the ratio between the (imagined) knot area in the cross section and the area of the whole cross section. Often there is a distinction between total KAR (TKAR) and margin KAR (MKAR), which is the KAR of the worst margin, (Hoffmeyer, 1981).

The knot ratio depends not only on the size of the knot, but also on its position within the board; a piece of timber with an edge knot, for example, will have a higher knot ratio than one where the same knot is a central one. Knot ratio is usually defined as shown in Figure 3.10 (Vinopal, 1980), but often more detailed modeling is introduced taking into account the different importance of "pith-side" and "bark-side" knots.

The knot area ratio approach usually makes such a differentiation by placing more emphasis on knots in the outer margin areas.

Both the KR and KAR models have proved very useful in the non-destructive assessment of timber (e.g. Curry and Fewell, 1977; Vinopal, 1980; Echenique-Manrique, 1980; Madsen, 1980; Hoffmeyer, 1984).

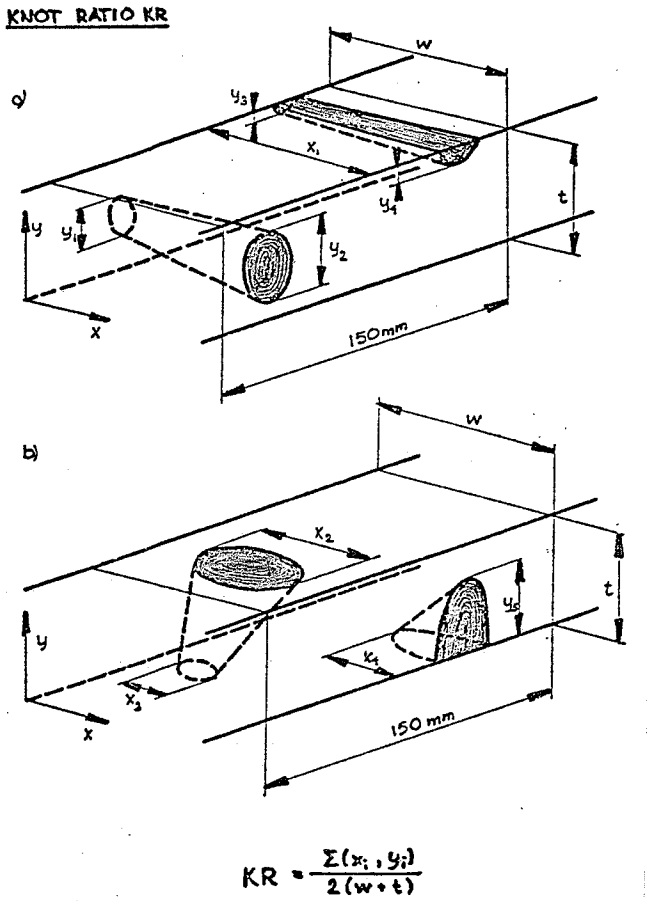

Figure 3.10.

Definition of knot ratio (KR). (Vinopal, 1980)

3.3.2 Fracture Mechanics

Fracture mechanics has long been recognized as a valuable tool to characterize the mechanical properties of wood (Porter, 1964; DeBaise, Porter, and Pentoney, 1966; Schniewind and Pozniak, 1971; Schniewind and Lyon, 1973; Schniewind and Centeno, 1973; Walsh, 1974; Pearson, 1974; Williams and Birch, 1975; Jeronimidis, 1976; Foschi and Barrett, 1976; Schniewind, Bartels, and Gammon, 1978; Chow and Wood, 1978; Buskov and Krenk, 1978; Murphy, 1979; Boatright and Garrett, 1979; Triboulot et al., 1984; Fonselius, 1986). The technique has been used to predict tensile strength perpendicular to grain, failure of notched beams, shear strength and size effect of checked laminated beams, the effect of butt joints in laminated beams, etc. As most of these topics are outside the scope of this paper, there will be made no attempt to give a thorough treatise of fracture mechanics and wood in general.

However, a brief summary of linear elastic fracture mechanics is presented in Appendix B. Also included in the appendix is a brief introduction to the idea of using viscoelastic fracture mechanics to predict time to failure for wood under load.

The significance of fracture mechanics lies in the fact that it permits prediction of the strength of individual structural members of a given geometry and loading given a knowledge of fracture toughness, critical flaw size, and fracture location. Simple problems can be solved readily, but more complex anisotropic problems are usually solved using a numeric scheme such as the finite-element method.

Pearson (1974) described the behavior of knots in terms of the critical stress intensity factor K_{Ic} (Appendix B, Equation B11):

$$K_{Ic} = \sigma_c \sqrt{\pi a}\, C \qquad (3.1)$$

where

σ_c = critical (ultimate) stress
a = half crack length
C = geometry parameter = $f(\ell/w)$
ℓ = length
w = width

The critical stress intensity factor, a material property, can be found by determining the ultimate stress, σ_c, for an initial crack length of 2a. Equation 3.1 must be adjusted to the actual, finite dimensions by including the correct value of $C = f(\ell/w)$. Such values are found in handbooks.

For a specimen of a known K_{Ic} value, Equation 3.1 defines the *equivalent crack length*, $2a = L_e$.

Pearson (1974) showed that for central knots and edge knots (Figure 3.11) there was a good correlation between L_e and knot size L_k (Figure 3.12). Pearson also showed that using $L_e \equiv L_k$ produces an R^2-value for the relationship between predicted strength and actual strength of 0.76 and 0.92 for central knots and edge knots, respectively (Figure 3.13).

The estimated fracture stresses were on the average the same as the test values for equivalent crack lengths of 78% and 91% of the knot diameter for central knots and edge knots, respectively. This suggests that edge knots reduce strength more than central knots and that an edge knot reduces strength almost as much as a slot of the same dimension.

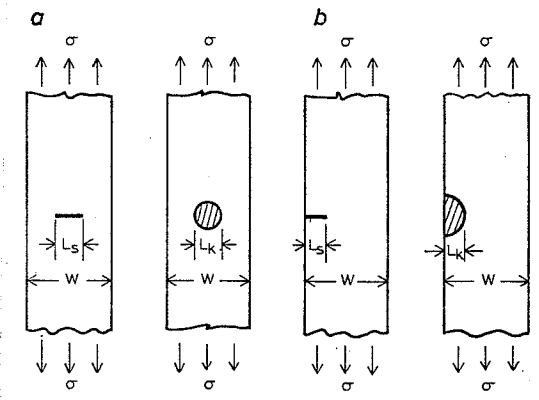

Figure 3.11

Matched pairs of specimens with slots and knots (a. central; b. edge) (Pearson, 1974).

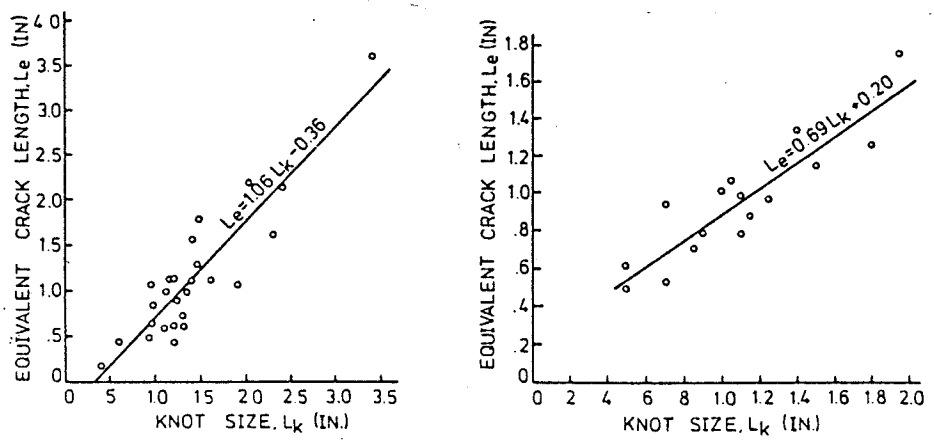

Figure 3.12. Relationship between equivalent crack length and knot size for specimens with a. central defects and b. edge defects (Pearson, 1974).

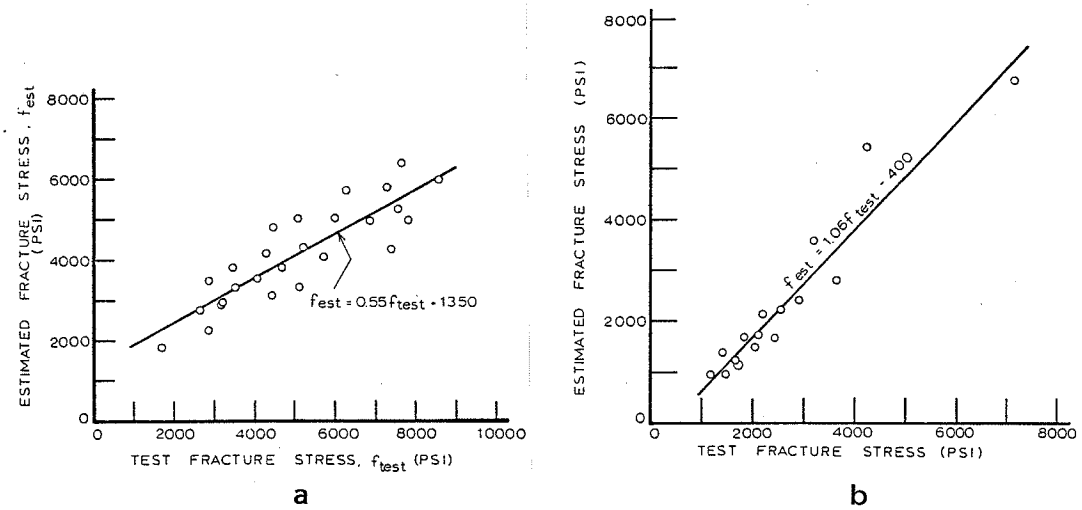

Figure 3.13. Relationship between estimated fracture stress based on length equal to knot size and test value for a. central knot ($R^2 = 0.76$) and b. edge knot ($R^2 = 0.92$) (Pearson, 1974).

It must be stressed that Pearson's specimens contained very little grain disturbance around the knot.

Boatright and Garrett (1979) investigated the effect of extended cross grain on the equivalent crack length for specimens tested in bending. The results, shown in Figure 3.14, do suggest a trend for lower values of L_e for a given L_k. Extended slope of grain, therefore, appears to strengthen the knot.

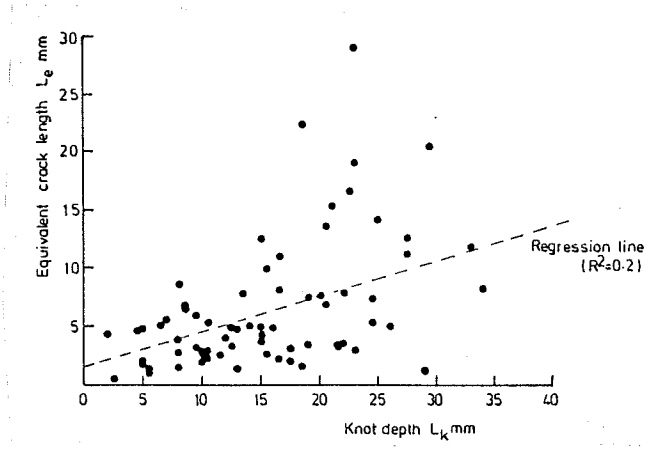

Figure 3.14. Equivalent crack length as a function of knot depth L_k for margin knots in bending with extensive sloping grain (Boatright and Garrett, 1979).

Schniewind et al. (1978) tested 12x25x125 mm white fir specimens in bending. Some specimens contained a knot in the tension side and others a 45-degree notch. They found the K_{Ic} factors for pieces containing a knot to be on the average 60% higher than for pieces containing a notch, thus confirming Boatright and Garrett's findings. Schniewind et al. also found equal K_{Ic} factors for pieces with knots and pieces with only knot holes; this is not quite to be expected according to numerical calculations (e.g. Tang, 1984).

3.3.3 Stress Concentrations around a Knot

Calculations of anisotropic stress concentration factors to determine the failure load were first carried out by Green and Taylor (1939, 1940) (here after Boatright and Garrett, 1979). Their results are shown in Figure 3.15. (a) shows the tensile stress distribution around the hole. It can be seen that the stress concentration factors at the side of the hole, i.e. at $\theta = 90^o$, are 3 for the isotropic case and about 6.4 for wood (spruce). (b) shows the corresponding distribution of shear stresses. In the case of loading parallel to the grain the shear stress in the isotropic material reaches a peak of approximately 0.9 of the distant, applied tensile stress, whereas spruce shows a peak of roughly

0.7. The position of maximum shear stress for spruce occurs around $\theta = 80^{o}$. For the isotropic material the corresponding angle is around 65^{o}.

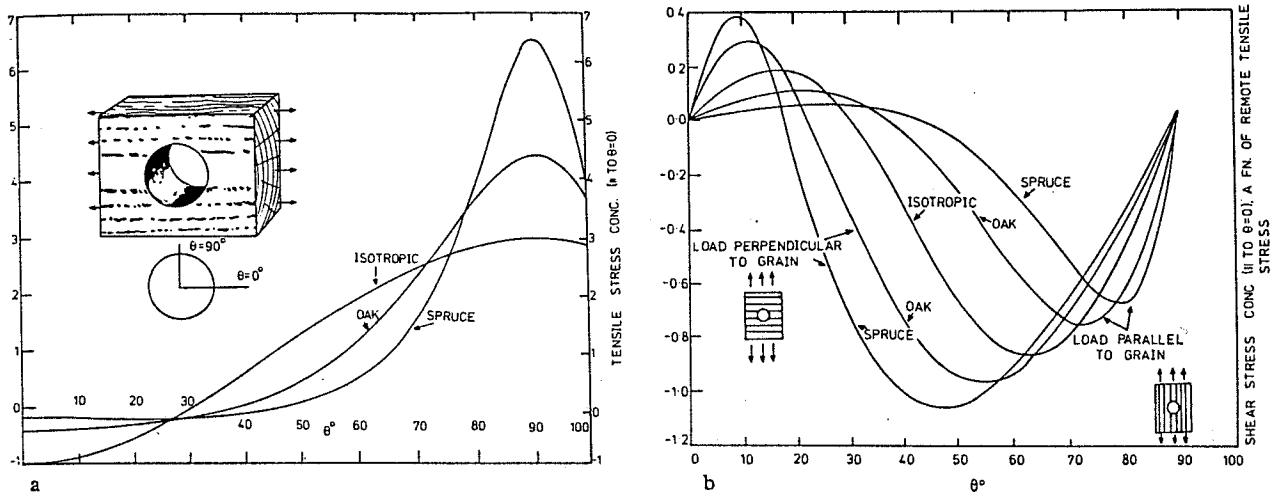

Figure 3.15. Calculated parallel-to-grain stress concentration around hole in timber as a function of θ. (a) tensile stress, (b) shear stress (Green and Taylor, 1939, 1940, in: Boatright and Garrett, 1979).

Tang (1984) also developed a mathematical model to predict elastic stress concentrations around knots. His model gave solutions for stresses around a sound knot, decayed knot, a knothole, and a wooden plug in a two-lamination simply supported beam. Grain deviations were neglected, and only stresses on the perimeter of the knot-wood interface were computed.

According to Tang's calculations, decay or missing knot material will significantly increase the stress concentration. However, if the knot is replaced by a wooden plug, stress concentrations will be significantly reduced. Small knots were found to produce considerably less stress concentrations than large knots, and the orientation of elliptic knots was found to influence stress concentration.

As a result of the work of Dabholkar (1980), a concept now known as the "Flow Grain Analogy" was introduced (Goodman and Bodig, 1978, 1980; Cramer and Goodman, 1983, 1986; Cramer, 1981; Cramer, Goodman, Bodig, and Smith, 1984; Phillips, Bodig, and Goodman, 1981).

The Flow Grain Analogy relates grain lines in the vicinity of a knot to streamlines of laminar fluid flow around an elliptical (or cylindrical) object (Figure 3.16a). The grain angles predicted by the analogy were compared to actual

measured values and the agreement found to be satisfactory (Phillips et al., 1981).

A finite element mesh is fitted to the predicted grain pattern so that it simulates the grain deviation around a knot in the two-dimensiona, longitudinal (L) tangential (T) plane of the wood.

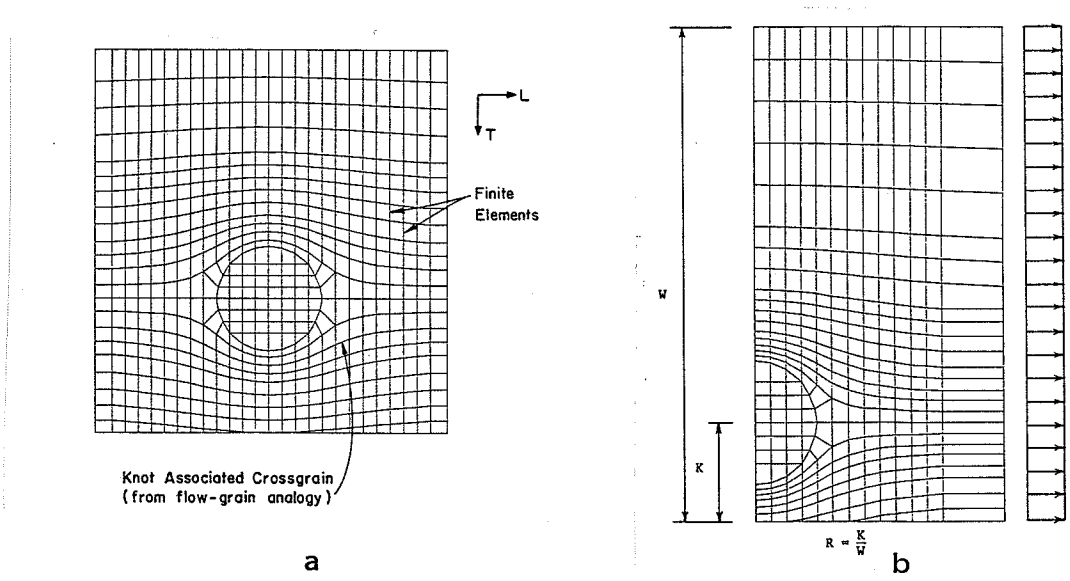

Figure 3.16. (a) simulated grain pattern resulting from the Flow Grain Analogy. (b) example of finite element mesh for knot location study and definition of the knot location ratio R = K/W (Cramer and Goodman, 1983).

The analytical model can handle knots that are located anywhere totally within the cross section, as well as knots that intersect the edge. However, at least half of the knot cross section must be within the member. The model also handles cross grain and even approximates existing cracks by placing a series of their elements with near-zero properties at the crack location.

Cramer and Goodman (1983) illustrate the stress and strain analysis by calculating stress concentration factors as dependent on the position of a round knot the size of which is 1/4 of the width of the board subjected to tension (Figures 3.16b and 3.17).

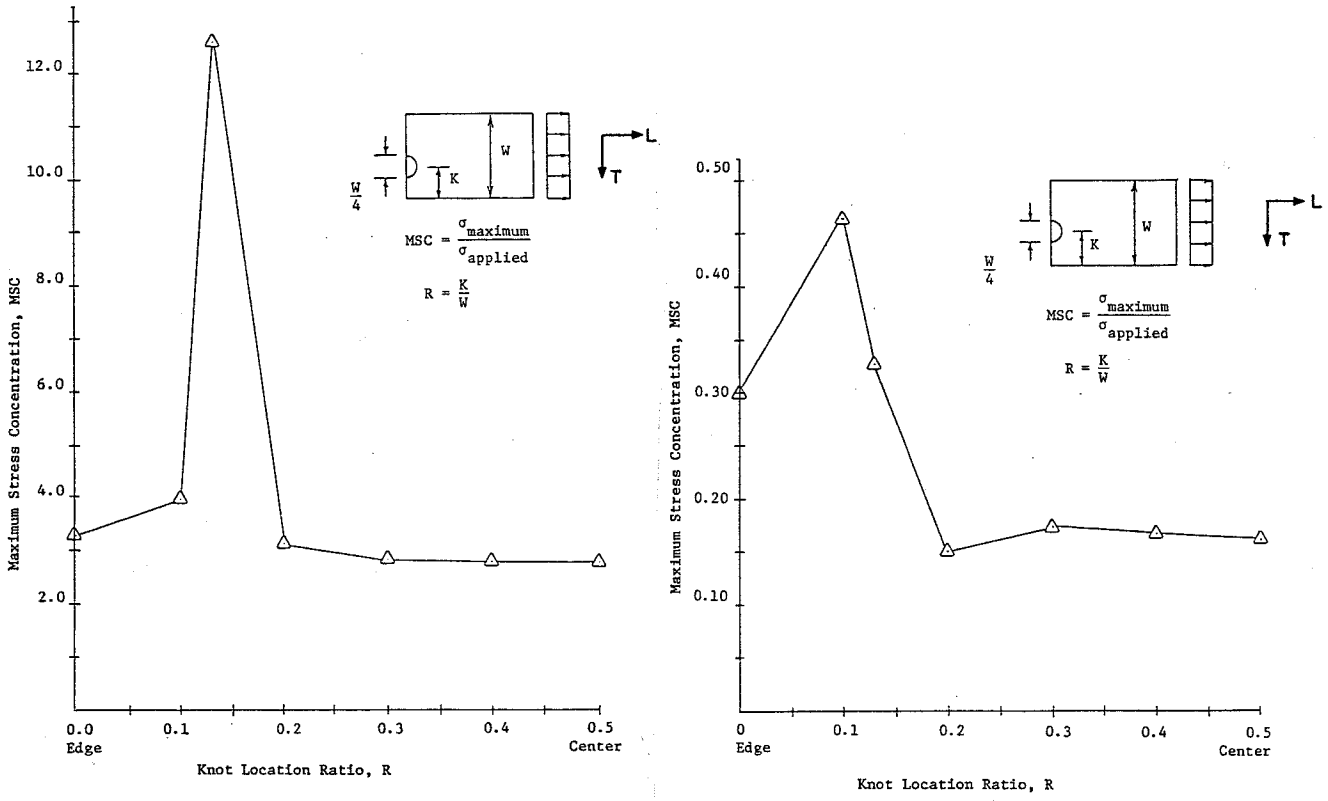

Figure 3.17. (a) longitudinal stress concentration factors for varying knot location. (b) transverse stress concentration factors for varying knot location (Cramer and Goodman, 1983).

As seen from Figure 3.17a, the longitudinal stress concentration factor attains a maximum of more than 12 when there is but a small fraction of wood left between the knot and the edge. The maximum transverse stress concentration is seen when the knot has already crossed the edge. The analysis shows that the stress concentration factor for a center knot is less than that predicted by Green and Taylor (1939, 1940), thus confirming that grain deviations around knots strengthen the knot compared to a similar sized hole.

The Flow Grain Analogy seems to form a valuable tool for the detailed analysis of failure mechanisms around knots. However, the limitations of the model are still too severe to warrant use for general engineering purposes.

Boatright and Garrett (1979) carried out an evaluation of the methods presented here as 1) the knot ratio (and knot area ratio) methods, 2) the fracture mechanics methods, and 3) the analytical/finite element methods. They concluded that "the knot ratio approach appears to be the most universally applicable method for assessing the overall strength-reducing effects of knots, subject only to significant statistical distributions".

3.3.4 Frequency of Knot Occurrence

In ordinary timber design practice the maximum design load is supposed never to exceed the maximum strength of any wood member. In other words, in the design situation the highest load is supposed to coincide with the weakest member's weakest cross section.

The introduction of probabilistic or "semi-probabalistic" design, however, makes it easier to specify such characteristic strength values for structures or structural components which are linked to specific load situations.

This makes it possible to take into account the fact that both load and strength are stochastic variables and that it is therefore very unlikely that maximum load coincides with minimum strength.

The strength distribution along the length of a board therefore appears to become an important materials property. The occurrence of knots is probably the single most important parameter in this respect.

Figure 3.18 illustrates how the ultimate strength may vary along the length of a board. The general strength levels of the boards are results mainly of density, general slope of grain and reaction wood, whereas local drops in strength are due to finger joints, knots, ingrown bark, etc.

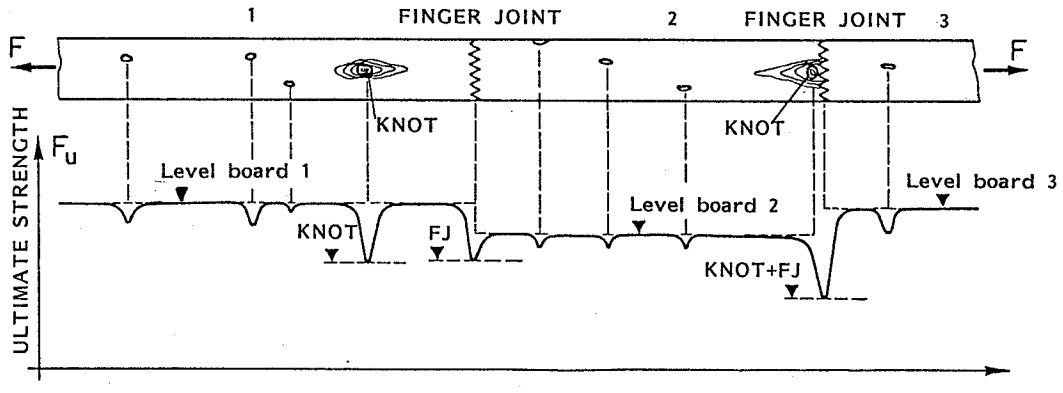

Figure 3.18. Example of lengthwise variation of ultimate strength, F_u (Gehri and Steurer, 1981).

The lengthwise distribution of knots is governed by the growth characteristics of the tree. This materials property is therefore dependent not only on species, but also to a high degree on the growth rate of the individual trees.

The lengthwise strength distribution was assessed on the basis of machine stress grading readings by Riberholt and Madsen (1979), Källsner and Norén (1978), and Kline et al. (1986).

A related topic, the "length effect" was investigated by Madsen and Buchanan (1985) and Jonasson et al. (1984). These treatments were aimed at assessing the "size effect". As would be expected, increasing the length of a board increases the possibility of including a particularly weak cross section and thus to introduce a particularly low strength.

.... But the elm and the ash have an excess of moisture, very little air and fire, and are provided moderately with a mixture of the earthy. When they are wrought for buildings, they are pliant and, owing to the weight of moisture, they are without stiffness and quickly bend.

Vitruvius , 1 century B.C.

4. COMPRESSION FAILURES

4.1 Causes

The stem of a normal grown tree adopts a geometrical shape which results in constant strains along the stem when bent by the wind (Ylinen, 1953). Heavy wind loads may cause stresses in the compression side of the bent stem to reach the ultimate value thus causing compression failures. A further increased wind load will cause the compression failure to progress inward until the tensile stresses at the opposite side of the stem reach their ultimate value thus causing final failure of the stem (Figures 4.2 and 4.3). Only very "knotty" stems may fail in tension before compression failures have shown.

Both the fallen trees and many of the trees left to continue growth may now abound in compression failures. A living tree will overgrow the wound (Figure 4.1) which often appears as ripples in the bark.

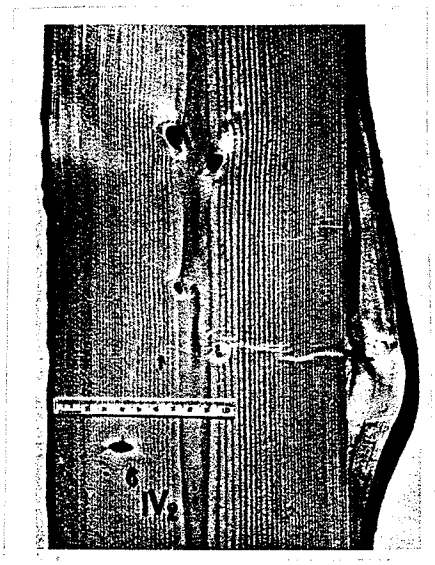

Figure 4.1

Longitudinal section through overgrown compression failure in a stem of pine sp. (Trendelenburg, 1955).

Ripples of that appearance are often seen on the lee side of such *Fagus silvatica* stems which are particularly exposed to high wind loads. The ripples are equidistantly spaced, often along the entire length of the stem. If proved that the ripples are actually induced by compression failure, their existence would confirm the "mechanical stem shape theory" first put forward by Schwendener (1874) (in: Trendelenburg et al., 1955).

Compression failures may occur at varying frequencies in trees of all species. *Picea abies*, for instance, is reported to show compression failures more often than for instance *Pinus sylvestris* (Trendelenburg et al., 1955).

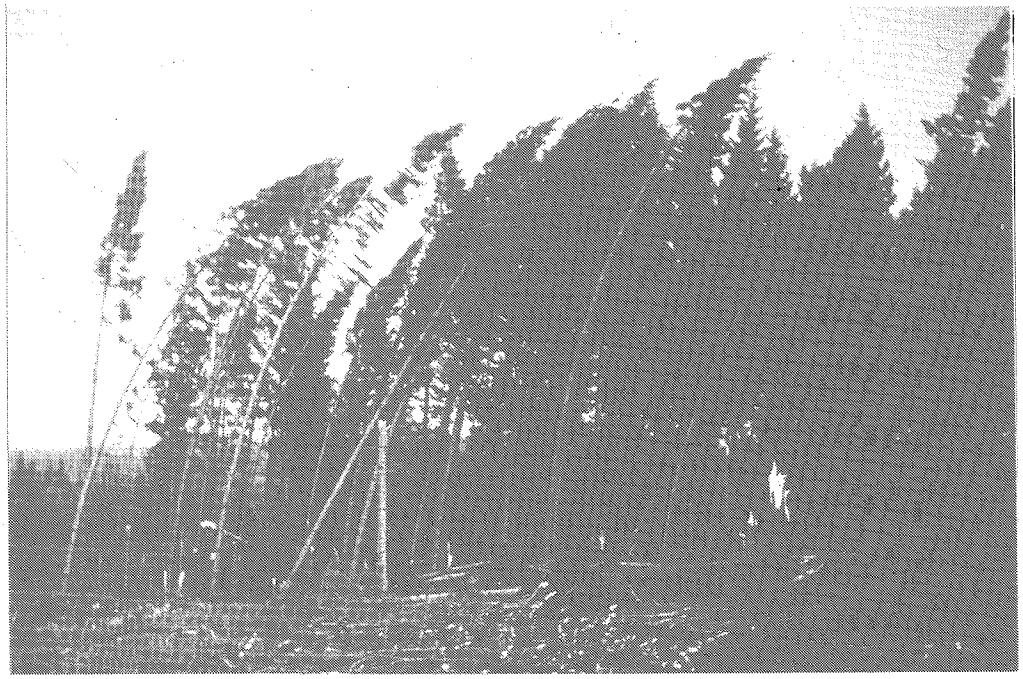

Figure 4.2 *Picea abies* subjected to heavy wind loads. (By courtesy of P. Moltesen).

Figure 4.3 The fallen trees and many of the trees left to continue growth may abound in compression failures. (By courtesy of P. Moltesen).

"Brittle heart" is a type of compression failure of the inner heartwood found for instance in *Eucalyptus* spp. and *Shorea* spp. This type of compression failure is ascribed to the presence of large internal growth stresses, and it shows as slip planes in the cell wall particularly in the lower parts of a stem (Chafe, 1977).

Both types of compression failure have a marked influence on strength, especially the tensile, bending, and impact strengths. The fracture is brittle and the fracture surfaces very "short-fibered". The strength reduction causes most stress grading standards to exclude timber containing compression failures from being used for load bearing purposes. At the same time, however, compression failures are very difficult to detect on rough planks.

Below is presented a brief description of the microscopic and macroscopic characteristics of compression failure as induced by wind loads. These characteristics differ in no important manner from the characteristics typical of compression failure of an overloaded structural member.

This latter area is clearly outside the scope of the present presentation, and there will be made no attempt to give an exhaustive treatment of "compression failure" as such, nor will the list of references pretend to be complete.

4.2 Gross Characteristics

Compression failure occurs on boards of newly sawn logs as light-colored, irregular bands. When dry, the bands stand out clearly, but less distinct than in wet wood (Figure 4.4).

In a tangential plane the compression creases run perpendicular to the longitudinal axis, whereas in a radial plane the creases are inclined at 50-65^{o} to the longitudinal axis. This behavior is caused by the earlywood-latewood composite structure. The latewood will develop compression creases at an inclined angle, whereas the often very thin-walled earlywood cells will be subjected to stability failure (Figure 4.6). In a radial face, compression creases run entirely within the single latewood layer. In a radial face, on the other hand, the latewood creases are interrupted by the earlywood stability failure, and although the creases of the individual latewood layers are inclined, the resultant orientation of the creases is perpendicular to the longitudinal axis.

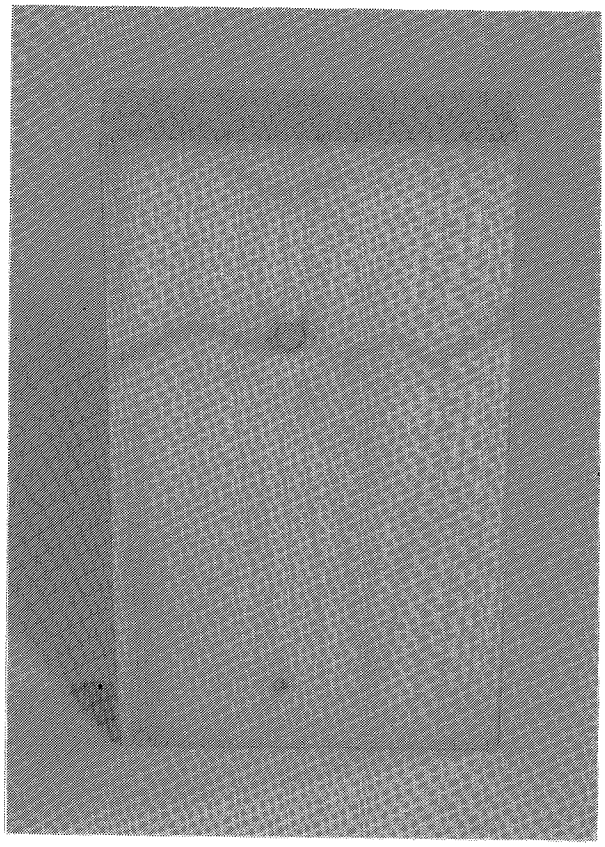

Figure 4.4

Compression creases as they appear in a moist board of *Picea abies* (Hoffmeyer 1987a).

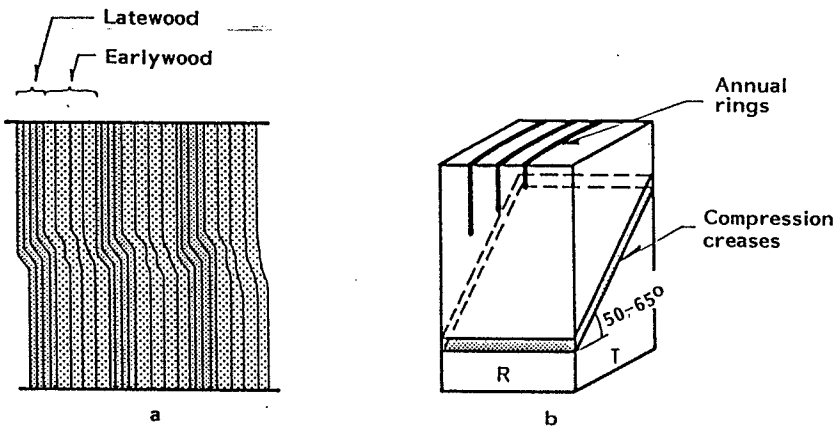

Figure 4.5. (a) Compression creases in a radial face develops as a combination of a shear-like failure in latewood and stability failure in earlywood. (b) In a tangential face the creases are inclined at approximately 50-65° to the longitudinal axis.

4.3 Microscopic Characteristics

Compression deformation assumes the form of a small kink in the microfibrillar structure (Figure 4.7). Because of the presence of crystalline regions in the cell wall, it is possible to observe the change of fibrillar orientation associated with the kinds using polarization microscopy (Figure 4.6).

The first detailed observations on the appearance of microscopic deformations in wood cell walls associated with longitudinal compressive stress were recorded by Robinson (1920). He termed the deformation "slip planes". Numerous other terms for the same phenomenon have since been used. Recently, Wilkins (1986) reviewed the nomenclature of cell wall deformations. He suggested to use Robinson's term, which will be done throughout this paper.

Important work on the anatomical characteristics of compression failure have been contributed by Kisser and Steininger (1952), Bienfait (1926), Green (1962), Keith and Côté (1968), Chafe (1977), Côté and Hanna (1983), Keith (1970,1972), Bariska and Kucera (1985), Kucera and Bariska (1982), Delorme and Verhoff (1975), Hansen (1967), Hartler (1969), Hartler and LéMon (1969), Frey-Wyssling (1953), and Dinwoodie (1968,1974).

The prevailing opinion on slip plane formation now seems to be that the irreversible deformations originate in the tracheid or fiber wall at that point where the longitudinal cell is displaced vertically to accommodate the horizontally running ray (Figure 4.6.). As stress and strain increase, these slip planes become more prominent and increase numerically, generally in a preferred lateral direction as shown in Figure 4.5.

Dinwoodie (1974) showed that the angle at which the slip plane traverses the cell wall varies systematically between earlywood and latewood between different species and with temperature. Wilson, McEvoy, Jr., and Perkins (1978) used the anisotropic plate to model the cell wall. They presented an analytical model which was able to predict slip plane angle and the load at slip plane creation for a model material of fiber reinforced epoxy. A slip plane angle dependency of degree of reinforcement was demonstrated.

The number and distribution of slip planes depend on moisture content. In a standing tree slip plane formation is more evenly distributed and is initiated at lower strains than in its dry "counterpart" - the sawn timber, subjected to design (over-) loads. In dry wood the formation of creases, the continuous bands of slip planes, appears to be associated with strains of 0.33% (Keith, 1972).

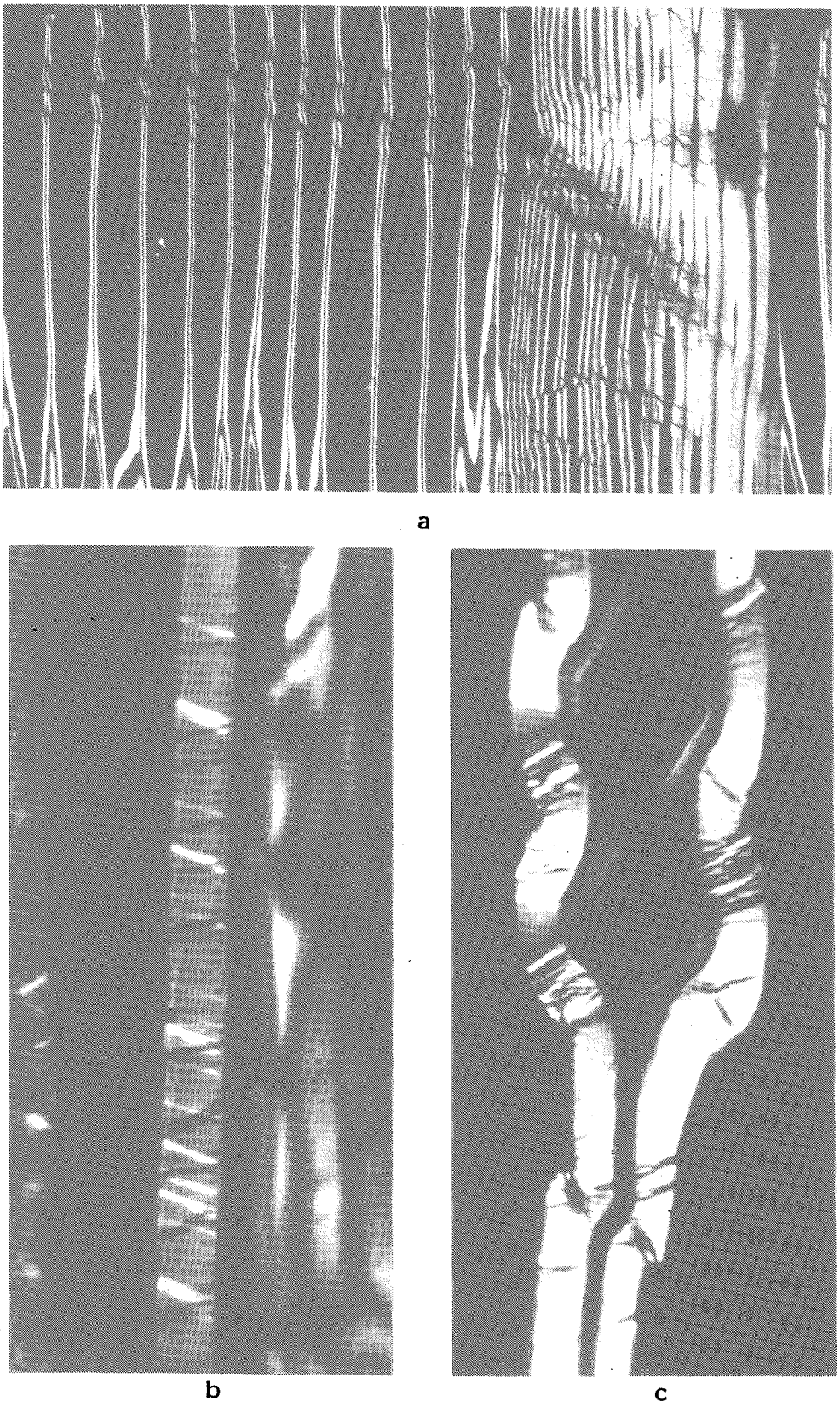

Figure 4.6.

Compression failure in *Picea abies* as revealed by polarization microscopy of thin-sections. (a) Stability failure in earlywood and 'shear failure' in latewood tracheids. C2-creases have been formed. 100X. (b) Slip planes in tracheid showing a distinct slip plane angle. 2800X. (c) Slip planes predominantly originate where tracheids are displaced vertically to accommodate the rays. 1000X. (Specimen preparation and photo by Hoffmeyer).

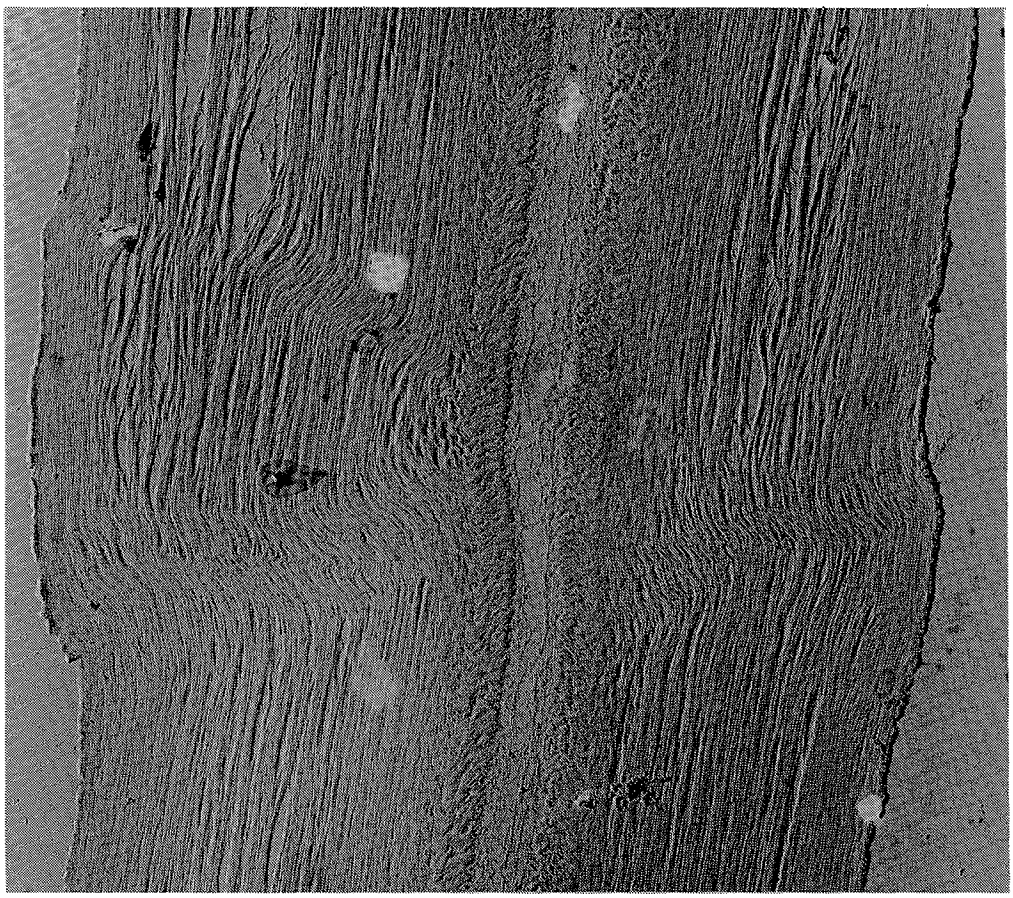

Figure 4.7

Compression failure in L-T plane of *Picea abies* tracheid. Transmission electron microscopy of ultra thin section (9000X). Lignin has been removed to better expose the microfibrillar structure of the cell wall. Note the (missing) middle lamella and the difference of microfibrillar orientation of S1 and S2. (Specimen preparation and photo by Hoffmeyer).

There seems to be a difference of opinion concerning the levels of stress at which slip planes occur. Dinwoodie (1968) observed slip planes already at a stress less than 25% of the ultimate failing stress. Keith (1970) and Kisser and Steininger (1952) consider that these early stages do not develop until about 50-60% of the ultimate. The present author has observed the first slip planes around rays to occur at stresses around 50% of the ultimate.

An example of the slip plane initiating stress level is contained in an experiment carried out by the author and briefly described below. Although the experiment was carried out on a small beam of dry wood, it may even suggest why compression creases in a standing tree would tend to form equidistantly.

Development of compression failure in a beam subjected to bending :

A small beam (20 x 20 x 300 mm) of *Picea abies* was subjected to a constant 4-point load corresponding to 80% of the short-term load. Moisture content was 15%, and the time to failure approximately 2 days. The annual rings of the beam cross section were vertically oriented.

In order to analyze the slip plane formation, a part of the failed beam was microscopically examined. 5 x 5 x 5 mm cubes were cut, methacrylate embedded, and sectioned (4 x 5 x 0.0004 mm) (Figure 4.8). The thin sections were analyzed using polarized microscopy.

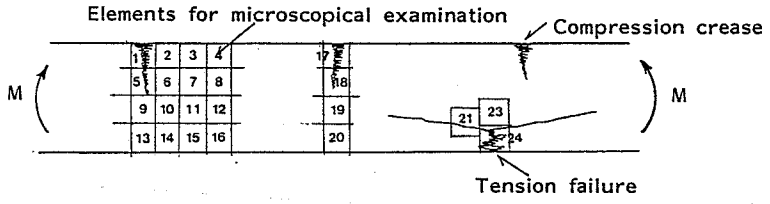

Figure 4.8. Elements (5 x 5 x 5 mm) from the middle section of a failed 4-point loaded *Picea abies* beam (20 x 20 x 300 mm) were examined microscopically to assess the extent of slip plane formation.

The characterization of slip plane formation was carried out in accordance with the classification of Dinwoodie (1968), adding a class, G, which is the final step where geometrical changes or stability failures occur:

SP = Single slip plane
C1 = Fine microscopic crease. 2 or a few slip planes combine
C2 = Microscopic crease. Slip plane bands extending through entire annual ring
C3 = Gross microscopic creases. Several creases combine. Local stability failure
G = Gross stability failure. Visible to the naked eye

Based on this analysis it is possible to summarize the bending failure of dry, clear wood as follows (Figure 4.9):

A. Slip plane formation starts at a nominal bending stress af approximately 50% of the ultimate compression strength. The first slip planes are initiated predominantly in tracheids around ray cells. At the same stress level slip planes also combine to form continuous bands (C1-creases).

B. At 70-80 percent of the ultimate bending strength C2-creases are developing, thus resulting in a distinctly non-linear stress-strain curve.

C. In a particular cross section, local stability failure now develops (C3-creases), and the strength of that wood tissue drops. The neutral axis is shifted towards the tension side, and the location of maximum compression stress is gradually moving inwards. The formation of C3-creases causes the compression stresses of the outermost fibers in neighboring cross sections to drop, and they will now never be subjected to failure stresses.

D. The second C3-crease develops in a certain minimum distance from the first formed. The minimum distance is dependent on the beam height and the elastic parameters of the wood. The final stage is the merging of local C3-creases to develop into yhe ultimate stability failure, which provoke tensile failure in the same cross section.

Due to the above mechanisms, compression creases tend to form equidistantly.

Figure 4.9. Model of slip plane and compression crease formation in wood subjected to bending. →

A

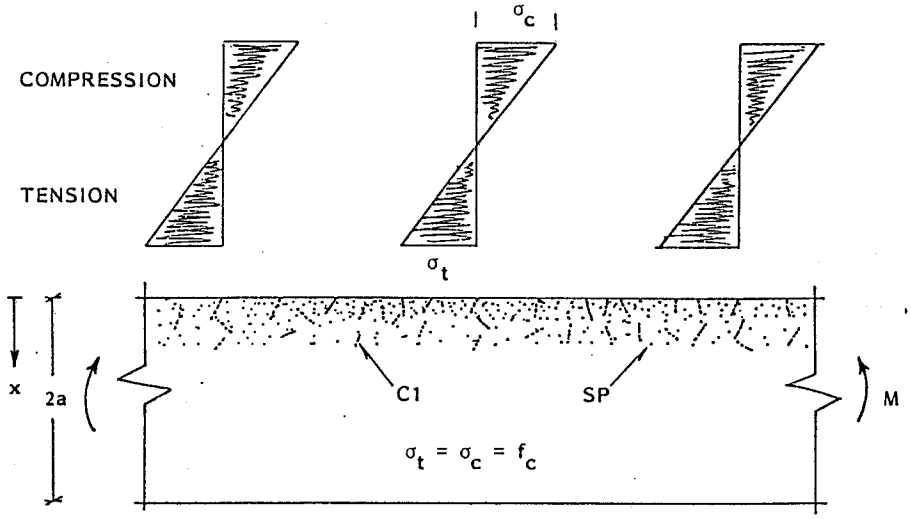

SLIP PLANES FOR $x \leq 0.5\ a$
C1-CREASES FOR $x \leq 0.5\ a$

B

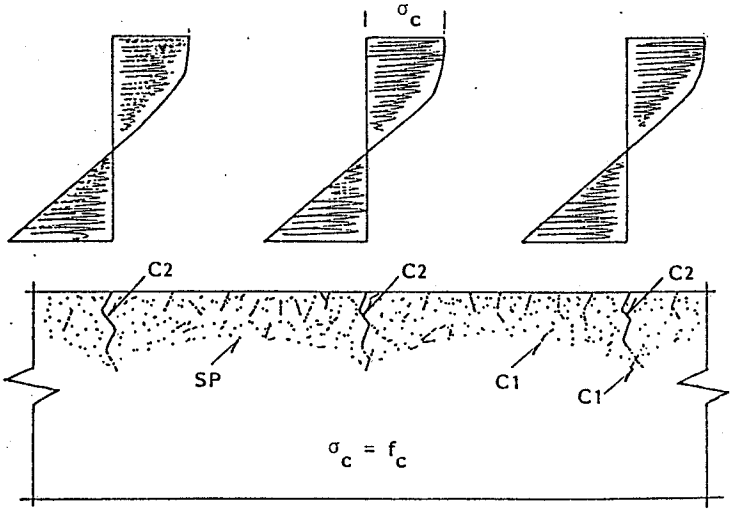

SLIP PLANES FOR $x \leq 0.75\ a$
C1-CREASES FOR $x \leq 0.75\ a$
C2-CREASES FOR $x \leq 0.60\ a$

C

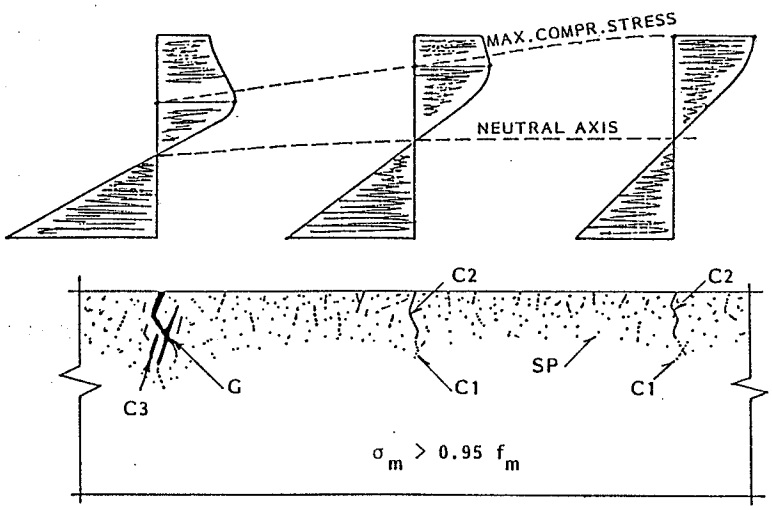

SLIP PLANES FOR $x \leq 0.9\ a$
C1-CREASES FOR $x \leq 0.75\ a$
C2-CREASES FOR $x \leq 0.75\ a$
C3-CREASES FOR $x \leq 0.70\ a$
G-CREASES FOR $x \leq 0.65\ a$

D

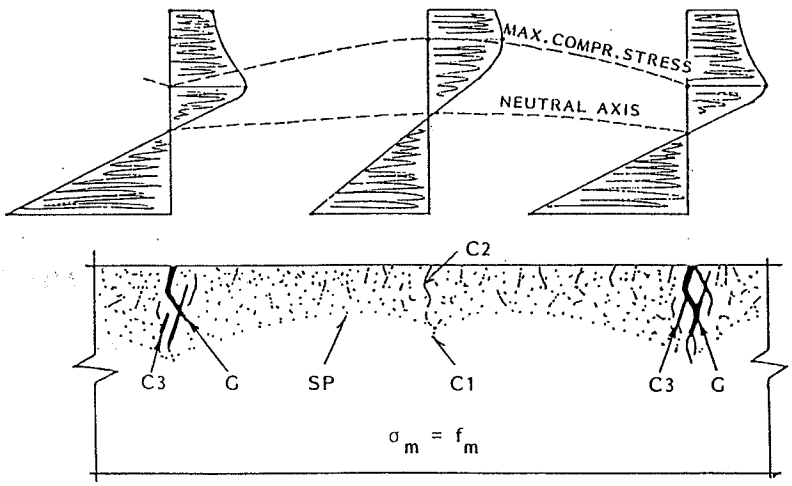

SLIP PLANES FOR $x \leq 0.90\ a$
C1-CREASES FOR $x \leq 0.75\ a$
C2-CREASES FOR $x \leq 0.75\ a$
C3-CREASES FOR $x \leq 0.70\ a$
G-CREASES FOR $x \leq 0.65\ a$

4.4 Modeling

Most models developed to relate mechanical behavior to microscopical structure have been confined to considerations of tensile stresses, often in a single cell (Cowdrey and Preston, 1966; Cave, 1968; Schniewind and Barrett, 1969; Tang, 1970). A particularly extensive and successful treatment has been given by Mark (1967).

Attempts to treat the stability problem of compression failure are few (Stupnicki, 1968, 1970; Grossman and Wold, 1971; Pincus, 1967; Wilson, McEvoy and Perkins, 1978 (commented p. 53)).

Pincus (1967) adopted the Newlin-Trayer fiber-support concept and considered compression failure to be initiated by the Euler-stability failure of the outermost fibers. He assumed stability failure to start at the proportional limit and demonstrated good agreement between experiments and a theoretical expression based on modulus of elasticity, tension perpendicular to grain strength, and two parameters pertaining to the cell properties.

Stupnicki (1968, 1970) developed an analytical model to predict the symmetrical and asymmetrical buckling behavior of earlywood and latewood, respectively. He also demonstrated very close predictions of compression strength. However, Stupnicki's assumptions concerning cell wall properties seem quite fictitious. He assumes, for instance, the middle lamella to be highly anisotropic and responsible for more than 95% of the strength in the longitudinal direction!

Grossman and Wold also explain the compression strength on the basis of column failure. They propose the thesis that the importance of the slip plane formation is not so much in weakening the fibers, but loosening the bond between them so that once a sufficiently long portion of a fiber becomes virtually separated from its neighbor, it becomes an unstable column. Grossman and Wold predict compression strength values and compression crease angles with no great precision. Particularly the lighter species had predicted strength values several times higher than test values. Grossman and Wold concluded that for thin-walled wood samples failure is rather a result of buckling of the cell wall.

Considering the lack of satisfactory models and the importance of compression failure, also for structural timber (e.g. creep behavior), it seems that the development of better models is still a feasible area of research.

Wood is a structure of very conveniently aligned holes surrounded by food.

A. Hypha

5. MICROBIOLOGICAL DEGRADATION

When man uses wood, he removes for a span of years the wood from the cycle in Nature. Sooner or later, however, Nature calls in the loan and transforms the complicated organic compounds of wood into their origins, carbondioxyde, water, and energy.

The microorganisms responsible for this degradation are fungi and bacteria. They use enzymes as tools for degradation. A variety of enzymes are combined with a variety of ways of applying these, and therefore a multiplicity of degradation mechanisms results.

Bacteria may produce pectinase and feed only from the membranes of the pits (Figure 5.2.b) or they may produce lignin-degrading enzymes and feed from the middle lamellae. The former types of bacteria may cause no strength reduction whereas the latter may cause the entire cell structure to fall apart. Some bacteria known as "erosion bacteria" confine themselves to the surfaces of lumen, whereas others penetrate the cell wall and become "tunneling bacteria" or "cavity bacteria".

Likewise, the fungi employ a variety of techniques. In brown rot, only the carbohydrate fraction of the wood is removed to a significant degree, while in white rot both the carbohydrate and lignin fractions of the wood are eventually removed. Mould, stain, and soft rot fungi may use the wood only as a habitat drawing food from stored material in the rays causing no strength reduction (e.g. blue stain) (Figure 5.1.a), or they may feed from the carbohydrates of the S2 layer, eventually removing the whole layer (Figure 5.2.c-f).

White-rot fungi are producing a progressive thinning of the secondary wall, beginning at the lumen and progressing outwards towards the middle lamella. No such progressive thinning has been observed in brown rot. These differences occur despite the fact that proportionate amounts of cell-wall material are being removed in both types of decay, as indicated by an increasing loss in weight as decay progresses. This observation leads to the concept

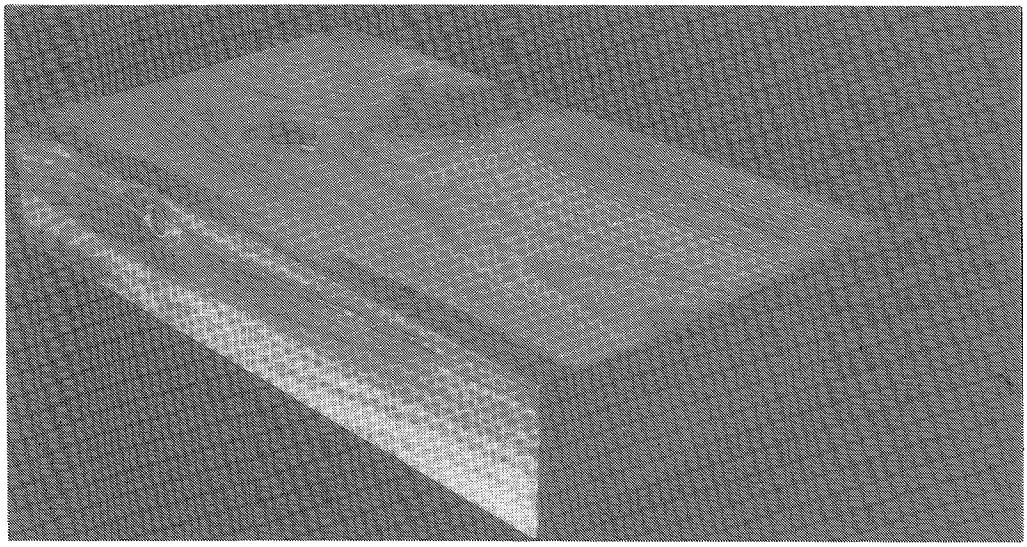

a

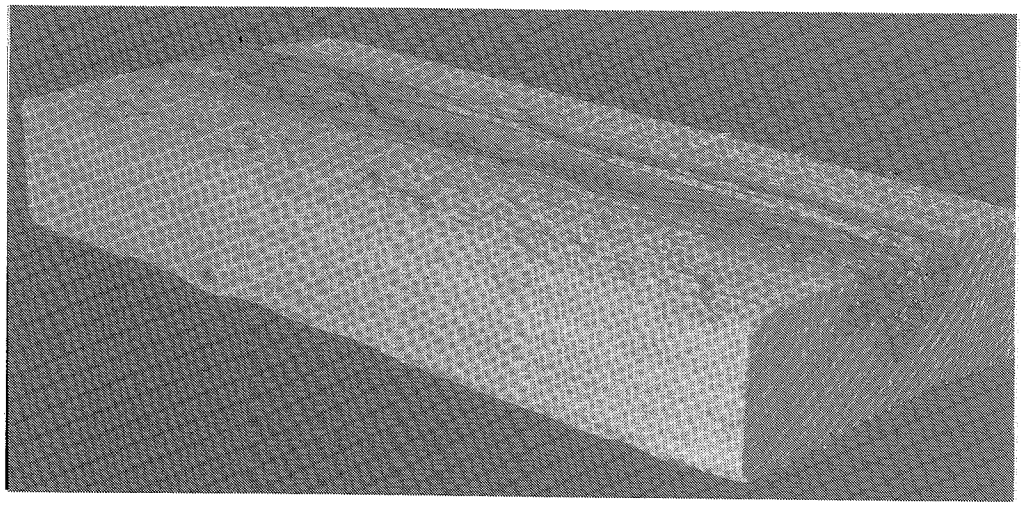

b

Figure 5.1. (a) Blue stain in *Pinus sylvestris*. Stain fungi may use the wood only as habitat drawing food from stored material in the rays. Stain fungi therefore normally cause no strength reduction.
(b) Brown rot in *Picea abies* feeding from the carbohydrates in the S2 layer thus causing strength reduction.

that decomposition in white rot takes place on exposed cell-wall surfaces and is relatively complete before moving on to new surfaces, while decomposition in brown rot is generally spread throughout the cell wall and is incomplete at any particular location (Wilcox, 1973).

It is hardly surprising that removal of the middle lamella or the decomposition of cellulose into low molecular weight sugars causes the strength of wood to drop dramatically. Already Ifju (1964) demonstrated the effect of a depolymerization of cellulose on strength. It is more surprising to realize that very

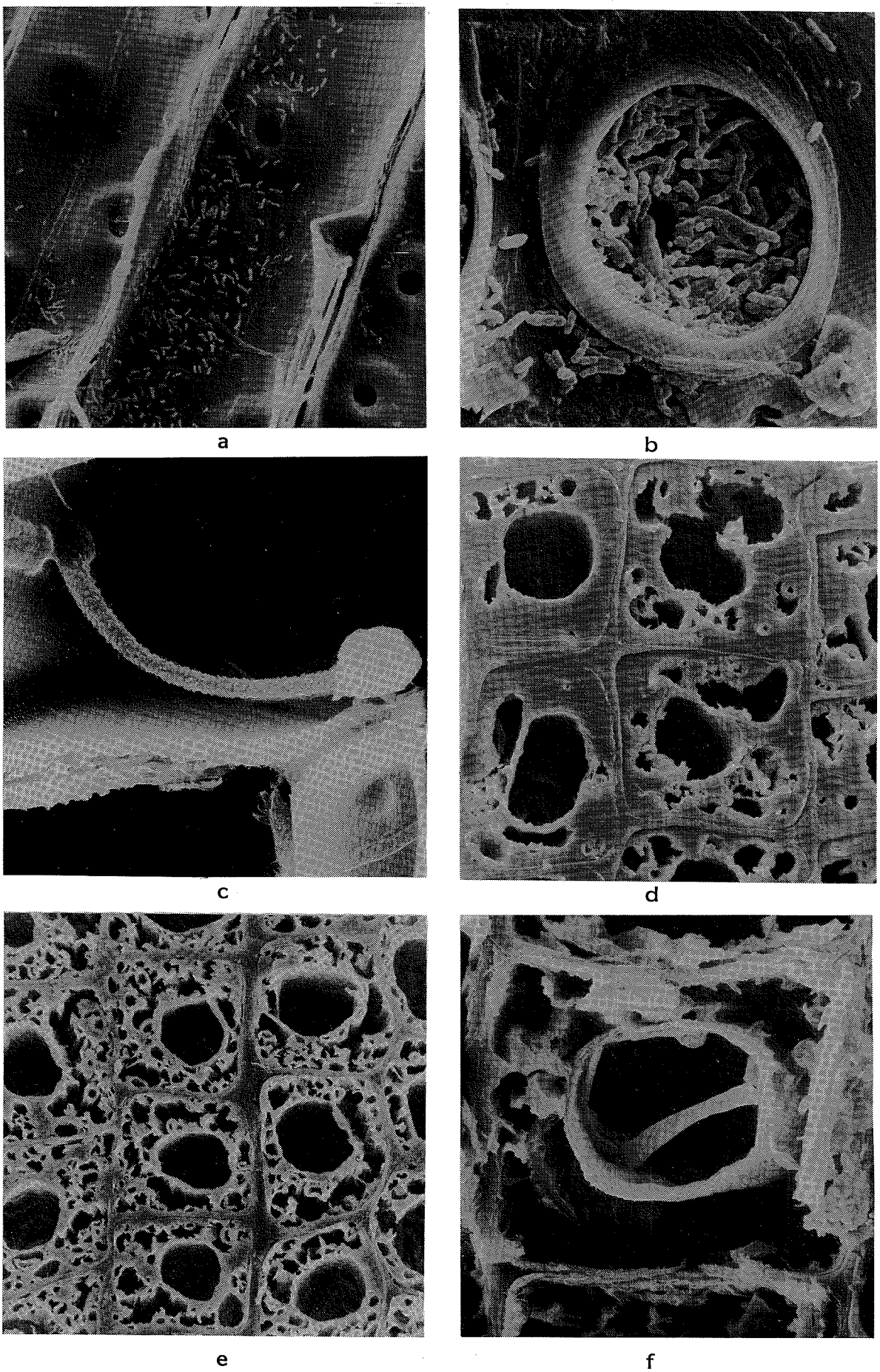

Figure 5.2 (a) and (b): Bacteria in ponded *Picea abies* in tracheid lumen and concentrated in a bordered pit.
(c): Soft rot spore in lumen of an earlywood cell of a pine utility pole. The spore has germinated and penetrated into S2
(d) - (e): Progressive stages of soft rot degradation of latewood cells in a pine utility pole.
(Hoffmeyer, 1976).

few researchers have yet addressed themselves to the important problem of quantifying the change of mechanical properties in terms of useful non-destructive parameters.

Microbiologists have used mechanical properties as destructive parameters to assess the progressive degrees of decay. The designer, on the other hand, needs the reverse information.

von Peckmann and Schaile (1950) (in: Bavendamm (1974)) demonstrated that strength loss in residual brown-rotted wood far exceeds the visible effects on the wall, while in white-rotted wood strength losses closely parallel the visible effects. This suggests that brown-rot enzymes are allowed to diffuse into the cell wall to a larger extent than are white-rot enzymes. This has been confirmed for instance by Henningsson (1967) who demonstrated a higher loss of impact strength for brown rot than for white rot in birch (Figure 5.3).

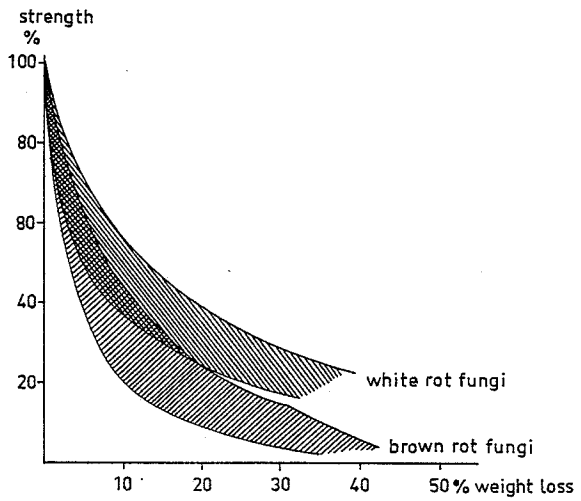

Figure 5.3. Relationship between impact strength and weight loss for birch decayed by white rot and brown rot (Henningsson, 1967).

A number of other researchers likewise demonstrated a strength loss due to fungal activity (e.g. Wang et al., 1980; Morrell and Zabel, 1985). Unfortunately however, strength loss was always related to weight loss, which is a very insensitive strength predictor (Figures 5.3 and 5.4).

True non-destructive parameters were introduced by Toole (1971) and Bariska et al. (1983). The former used dynamic E-modulus, while the latter used both G-modulus and internal damping. The results seem to suggest a correlation to strength. Unfortunately, again only weight loss was used as predicted parameter.

Hoffmeyer (1976) assessed the residual strength of soft-rot decayed utility poles. He, also, demonstrated a significant loss of tensile strength for very small weight losses (Figure 5.4) and concluded that soft rot enzymes penetrate the S2 cell wall much in the same way as brown rot enzymes. Note how well the tensile strength-weight loss relationship for soft rot (Figure 5.4) agrees with the impact strength-weight loss relationship for brown rot (Figure 5.3).

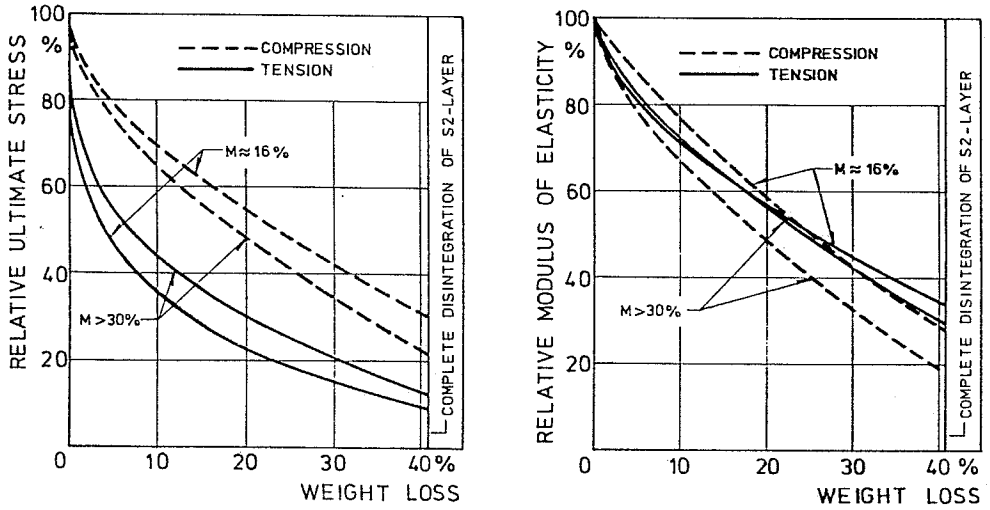

Figure 5.4. Relative ultimate stress and relative modulus of elasticity as functions of weight loss for soft rot decayed utility pine poles (Hoffmeyer, 1976).

Hoffmeyer related strength loss to a microscopical assessment of degree of soft rot decay using the scale shown in Table 5.1. The results shown in Figure 5.5 reveal an almost linear relationship between the important tensile strength and soft rot degree.

Table 5.1. Definition of soft rot degree (Hoffmeyer, 1976)

Degree of soft rot	Cavities, % of cross-section of secondary cell wall
1	1- 10
2	10- 40
3	40- 90
4	90-100

Increment cores were now taken from ground line cross sections of a large number of poles. A failure load was calculated based on the strength values of Figure 5.4; the concept of "transformed cross sections" was used. The

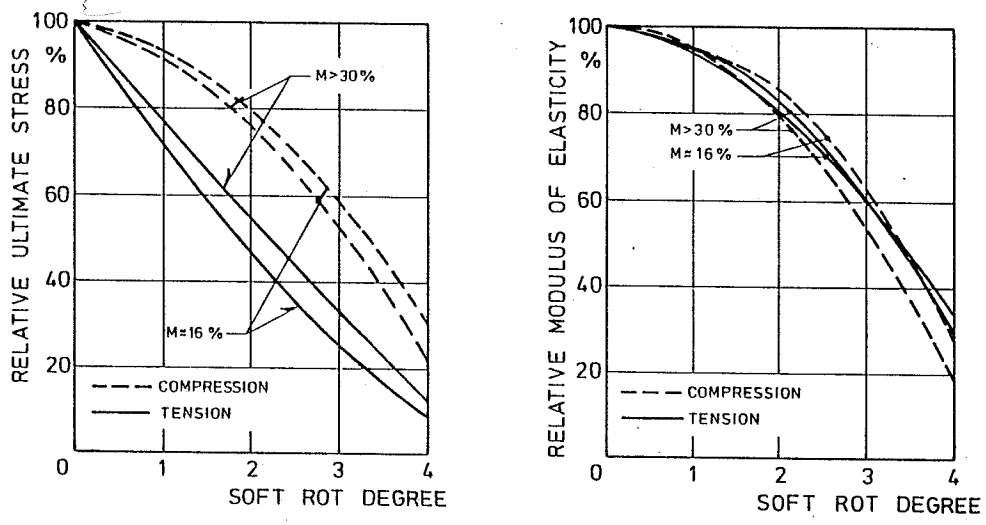

Figure 5.5. Relative ultimate strength and relative ultimate modulus of elasticity as functions of soft rot degree.

poles were then tested to destruction in the field (Smith and Jacobsson, 1976). A good correlation between predicted load and actual failure load was obtained (Figure 5.6).

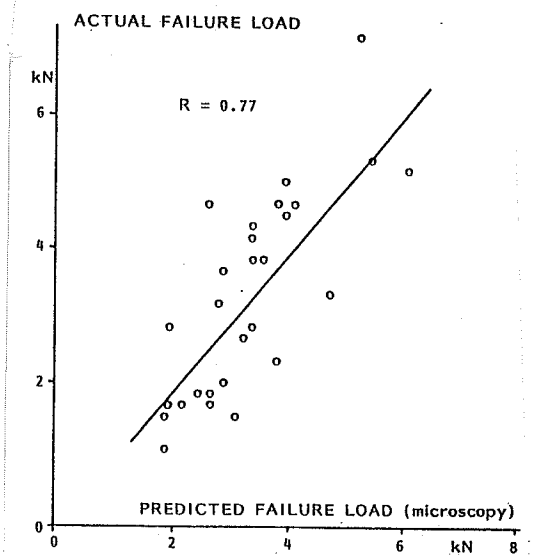

Figure 5.6. Full-scale field tests with soft rot decayed poles. Relationship between actual failure load and load as predicted by the soft rot degree-strength relationship in Figure 5.5 (Hoffmeyer, 1978).

.... Thus, if anyone can follow out the instructions laid down, he will be wiser and more able in his work to choose the use of the material.

Vitruvius, 1 century B.C.

REFERENCES

Albers, K., 1969: "Elasticität und Festigkeit von technischem Sperrholz". Holzzentralblatt. Nr. 141, Vol. 95, 24.

Alfrey, Turner (Jr.), 1948: "Mechanical Behavior of High Polymers". Interscience Publishers, New York.

Archer, R.R., 1987: "On the Origin of Growth Stress in Trees". Wood Science and Technology 21:139-154.

Ayres, Q.C., 1920: "Crushing Strength of Southern Pine at Angles to Grain". Eng. News Record 84(14):653-654.

Barenblatt, G.I., 1959a: "The Formation of Equilibrium Cracks during Brittle Fracture. Axially-Symmetric Cracks". J. Appl. Math. and Mechanics 23.

Barenblatt, G.I., 1959b: "Equilibrium Cracks Formed during Brittle Fracture. Rectilinear Cracks in Plane Plates". J. Appl. Math. and Mechanics 23.

Barenblatt, G.I., 1962: "The Mathematical Theory of Equilibrium Cracks in Brittle Fracture". Advances in Applied Mechanics 7:55-129.

Bariska, M., A. Osuskỳ, and H.H. Bosshard, 1983: "Anderungen der mechanischen Eigenschaften von Holz nach abbau durch Basidiomyceten". Holz als Roh- und Werkstoff 40:241-245.

Bariska, M., and L.J. Kučera, 1985: "On the Fracture Morphology in Wood". Wood Science and Technology 19:19-34.

Baumann, R., 1920: "Die bisherigen Ergebnisse der Holzprüfungen in der Materialprüfungsanstalt an der Tech. Hochschule Stuttgart". Forsch. Gebiete. Ingenieurw. H231, Berlin.

Bavendamm, W., 1974: "Die Holzschäden und ihre Verhütung". Wissenschaftliche Verlagsgesellschaft, Stuttgart.

Bernhardt, A., 1966: "Über die statische und dynamische Kurzzeitfestigkeit von Fichtenholz - absolut, rohdichtebezogen und unter Druckholzeinfluss". Forstwiss. Cbl. 85(9/10):275-295.

Bienfait, J.L., 1926: "Relation of the Manner of Failure to the Structure of Wood under Compression Parallel to the Grain". J. Agric. Res. 33:183-194.

Boatright, S.W.J., and G.G. Garrett, 1979: "The Effect of Knots on the Fracture Strength of Wood". Holzforschung 33:68-77.

Bodig, J., and B.A. Jayne, 1982: "Mechanics of Wood and Wood Composites". van Nostrand Reinhold Company.

Buffon, G.L.L., 1740, 1741: "Experiences sur la Force du Bois". Paris l'Academie Royale des Sciences. Histoire et Memoires Vol. 292/Vol. 453.

Burns, G.P., 1920: "Eccentric Growth and the Formation of Red Wood in the Main Stem of Conifers". Vt. Agric. Exp. Station Bull. 219.

Byskov, E., and S. Krenk, 1978: "The Fracture Strength of Wood" (in Danish). Bygningsstatistiske Meddelelser 49(4):93-111.

Cave, I.D., 1968: "The Anisotropic Elasticity of the Plant Cell Wall". Wood Sci. and Technology, 2:268-278.

Chafe, S.C., 1977: "Radial Dislocations in the Fibre Wall of *Eucalyptus regnans* Trees of High Growth Stress". Wood Sci. Technology 11:69-77.

Chow, C.L., and C.W. Woo, 1978: "Orthotropic and Mixed Mode Fracture of Wood". Proc. First International Conf. on Wood Fracture, Banff, Alberta.

Clouser, W.S., 1959: "Creep of Small Wooden Beams under Constant Bending Load". U.S.D.A. FPL Report No. 2150, Madison, Wisconsin.

Cockrell, R.A., and R.M. Knudson, 1973: "A Comparison of Static Bending, Compression, and Tension Parallel to Grain and Toughness Properties of Compression Wood of a Giant Sequoia". Wood Science and Technology 7(4):241-250.

Côté, W.A., and A.C. Day, 1964: "Anatomy and Ultrastructure of Reaction Wood". In: Cellular Ultrastructure of Woody Plants, Ed. W.A. Côté, Syracuse University Press.

Côté, W.A., N.P. Kutscha, B.W. Simson, T.E. Timell, 1968: "Studies on Compression Wood VI. Distribution of Polysaccharides in the Cell Wall of Tracheids from Compression Wood of Balsam Fir (*Abies balsamea*). Tappi 51:33-40.

Côté, W.A., and R.B. Hanna, 1983: "Ultrastructural Characteristics of Wood Fracture Surfaces". Wood and Fiber Sci. 15:135-163.

Cowdrey, D.R., and R.D. Preston, 1966: "Elasticity and Microfibrillar Angle in the Wood of Sitka Spruce". Proc. Roy. Soc. (London), 166B:245-272.

Cramer, S.M., 1981: "A Stress Analysis Model for Wood Structural Members". M.Sc. Thesis, Dept. of Civil Eng., Colorado State Univ., Fort Collins, Colorado.

Cramer, S.M., and J.R. Goodman, 1983: "Model for Stress Analysis and Strength Prediction of Lumber". Wood and Fiber Science 15(4):338-349.

Cramer, S.M., J.R. Goodman, J. Bodig, and F.W. Smith, 1984: "Failure Modeling of Wood Structural Members". Dept. of Civil Eng., Colorado State Univ., Fort Collins, Colorado. Structural Research Report No. 51.

Cramer, S.M., and J.R. Goodman, 1986: "Failure Modeling: A Basis for Strength Prediction of Lumber". Wood and Fiber Sci. 18(3):446-459.

Curry, W.T., and A.R. Fewell, 1977: "The Relationships between the Ultimate Tension and Ultimate Compression Strength of Timber and Its Modulus of Elasticity". BRE Current Paper CP 22/77.

Dabholkar, A., 1980: "Finite Element Analysis of Wood with Knots and Cross Grain". Ph.D. Dissertation, Dept. of Civil Eng., Colorado State Univ., Fort Collins, Colorado.

Dadswell, H.E., A.B. Wardrop, and A.J. Watson, 1958: "Fundamentals of Papermaking Fibers", pp.188-219, New York.

Dawe, P.S., 1964: "The Effect of Knot Size on the Tensile Strength of European Redwood". Wood 29.

DeBaise, G.R., A.W. Porter, and R.E. Pentoney, 1966: "Morphology and Mechanics of Wood Fracture". Mat. Res. Stand. 6:493-499.

Delorme, A., and S. Verhoff, 1975: "Zell wanddeformationen in Sturmgeschädigtem Fichtenholz unter dem Rasterelektronenmikroskop". Holz als Roh- und Werkstoff 33:456-460.

Dinwoodie, J.M., 1968: "Failure in Timber, Part 1: Microscopic Changes in Cell Wall Structure Associated with Compression Failure". J. Inst. Wood Sci. 21:37-53.

Dinwoodie, J.M., 1974: "Failure in Timber, Part 2: The Angle of Shear through the Cell Wall during Longitudinal Compression Stressing". Wood Science and Technology 8:56-67.

Dinwoodie, J.M., 1981: "Timber, Its Nature and Behavior". van Nostrand Reinhold Company.

Dugdale, D.S., 1960: "Yielding of Steel Sheets Containing Slits". J. Mechanics and Physics of Solids 8:100-104.

Echenique-Manrique, R., 1980: "Final Report to IDRC on Timber Grading in Mexico". LACITEMA-INIREB.

Ewart, A.C. J., and A.G. Mason-Jones, 1906: "The Formation of Redwood in Conifers". Ann. Bot. London, 20:201-3.

Fengel, D., and G. Wegener, 1984: "Wood, Chemistry, Ultrastructure, Reactions". de Gruyter.

Fewell, A.R., 1984: "The Determination of Softwood Strength Properties for Grades, Strength Classes, and Laminated Timber for BS 5268: Part 2". Building Research Establishment, England.

Fonselius, M., 1986: "Fracture Mechanics of Spruce and PLV" (in Swedish). Dept. Civ. Eng., Helsinki Univ. of Technology, Report No. 80.

Foschi, R.O., and J.D. Barrett, 1976: "Longitudinal Shear Strength of Douglas Fir". Can. J. Civ. Engineering 3(2):198-208.

Foschi, R.O., and Z.C. Yao, 1986: "Another Look at Three Duration of Load Models". Proc. IUFRO-Wood Engineering Meeting, Florence, Italy.

Foslie, M., and K. Moen, 1972: "Norsk granvirkes styrkeegenskaper, Del 2". The Norwegian Institute of Wood Working and Wood Technology, Report No. 45.

Frey-Wyssling, A., and F. Stüssi, 1948: "Festigkeit und Verformung von Nadelholz bei Druck quer zur Faser". Schweizerische Zeitschrift für Forstwesen, 99(3).

Frey-Wyssling, A., 1953: "Über den Feinbau der Stauchlinien in überbeanspruchtem Holz". Holz as Roh- und Werkstoff 11(7):283-288.

Gehri, E., and T. Steurer, 1979: "Holzfestigkeit bei Beanspruckung Schräg zur Faser". Schweizerische Arbeitsgemeinschaft für Holzforschung (SAH), Bulletin 7/2.

Goodman, J.R., and J. Bodig, 1970: "Orthotropic Elastic Properties of Wood". ASCE, J. Struct. Div., ST 11, pp. 2301-2319.

Goodman, J.R., and J. Bodig, 1971: "Orthotropic Strength of Wood in Compression". Wood Science 4(2):83-94.

Goodman, J.R., and J. Bodig, 1978: "Mathematical Model of the Tension Behavior of Wood with Knots and Cross Grain", Proc. First Int. Conf. on Wood Fracture, Banff, Alberta.

Goodman, J.R., and J. Bodig, 1980: "Tension Behavior of Wood - An Anisotropic, Inhomogeneous Material", Dept. Civ. Eng., Colorado State Univ., Fort Collins Structural Research Report No. 32.

Graf, O., 1938: "Trägfähigkeit der Bauhölzer und Holzverbindungen". Mitteilungen des Fachausschüsses für Holzfragen beim VDI und Deutschen Forstverein, Heft 20.

Green, A.E., and G.I. Taylor, 1939, 1940: "Stress Systems in Aeolotropic Plates". Proc. Roy. Soc. Pt.I-A173, 162; Pt.II-A173, 173; Pt.III-A184, 181.

Green, H.V., 1962: "Compression-Caused Transverse Discontinuities in Tracheids". Pulp and Paper Magazine of Canada, T155-T168.

Griffith, A.A., 1920: "The Phenomenon of Rupture and Flow in Solids". Philosophical Transactions of the Royal Society of London, Series A, 221:163-198.

Grossman, P.U.A., and M.B. Wold, 1971: "Compression Fracture of Wood Parallel to the Grain". Wood Science and Technology 5:147-156.

Hagen, G.H.L., 1842: "Über die Elasticität des Holzes". Bericht der königlichen Preussischen Akademie der Wissenschaften zu Berlin, Monat November: Sitzung der physikalisch-matematischen Kl.

Hankinson, R.L., 1921: "Investigation of Crushing Strength of Spruce at Varying Angles of Grain". Air Service Information Circular Vol. 3, No. 259, Washington, D.C.

Hansen, P. Freiesleben, 1967: "Ultra-Thin Polishing of Samples of Compression Failed Wood" (in Danish). B-Undervisning og Forskning 1967, Festskrift.

Hartler, N., 1969: "Misaligned Zones in Cellulosic Fibres, Part I, Survey". Norsk Skogindustri 4:114-120.

Hartler, N., and S. LéMon, 1969: "Misaligned Zones in Cellulosic Fibres". Norsk Skogindustri 5:151-158.

Haygreen, J.G., and J.L. Bowyer, 1982: "Forest Products and Wood Science". The Iowa State University Press.

Hearmon, R.F.W., 1948: "The Elasticity of Wood and Plywood". Dept. Sci. Ind. Res., For. Prod. Res.

Henningsson, B., 1967: "Changes in Impact Bending Strength, Weight and Alkali Solubility Following Fungal Attack on Birch Wood". Studie Forestalia Suecica, Nr. 41.

Hoadley, R.B., 1981: "Understanding Wood". The Taunton Press.

Hoffmeyer, P., 1969: "The Macroscopic Characteristics of Wood" (in Danish). In P. Hoffmeyer: Compendium on Wood Science and Technology, Paragraph 6:6.1-6.22.

Hoffmeyer, P., 1970: "Strength and Stiffness of Wood" (in Danish). In P. Hoffmeyer: Compendium on Wood Science and Technology, Paragraph 15:15.1-15.56.

Hoffmeyer, P., 1976: "Mechanical Properties of Soft Rot Decayed Scots Pine with Special Reference to Wooden Poles". In: Soft Rot in Utility Poles Salt Treated in the Years 1940-1954. Swedish Wood Preservation Institute, Report No. 117E.

Hoffmeyer, P., 1978: "The Pilodyn Instrument as a Non-Destructive Tester of the Shock Resistance of Wood". Proc. Non-Destructive Testing Meeting, Vancouver, Washington.

Hoffmeyer, P., 1981: "An Evaluation of the ECE and Nordic Stress Grading Rules". Proceedings of the IUFRO-Wood Engineering Meeting, Kyoto, Japan.

Hoffmeyer, P., 1984: "Strength and Grading of Dimension Lumber" (in Danish). In: Skovteknologi, Særtryk af Dansk Skovforenings Tidsskrift.

Hoffmeyer, P., 1987a: Pictures taken, small tests carried out, etc. to illustrate specific points of the present paper. May 1987.

Hoffmeyer, P., 1987b: "Duration of Load Effects for Spruce Timber with Special Reference to Moisture Influence". Proc. Seminar on Wood Technology. Commission of the European Communities, Munich, 14-15 April.

ISO-Draft International Standard for Timber Design, 1986. ISO/TC165.

Ifju, G., 1964: "Tensile Strength Behavior as a Function of Cellulose in Wood". For. Prod. J. 14(8):366-372.

Irwin, G.R., 1948: "Fracture Dynamics", in: Fracture of Metals, A.S.M. pp.147-166.

Isebrands, J.G., and R.A. Parham, 1974: "Tension Wood Anatomy of Short-Rotation *Populus* spp. before and after Kraft Pulping". Wood Science 6(3):256-265.

Jaccard, P., 1938: "Eccentric Increments and Anatomical-Histological Differentiation of Wood". Berl. Schweiz Bot. Ges. 48:491-537.

Jane, F.W., 1970: "The Structure of Wood". Adam and Charles Black Publ., London.

Jayne, B.A., and S.K. Suddarth, 1966: "Matrix-Tensor Mathematics in Orthotropic Elasticity". In Proceedings ASTM Symposium, 2 November 1965.

Jayne, B.A., 1972: "Orthotropic Elasticity". In: Theory and Design of Wood and Fiber Composite Materials, ed. B.A. Jayne. Syracuse University Press.

Jensen, E.K., 1980: "Compression Wood" (in Danish). Building Materials Lab., Tech. Univ. Denmark (internal report).

Jeronimidis, G., 1976: "The Fracture of Wood in Relation to Its Structure". Leiden Botanical Series 3:253-265.

Johns, K., and B. Madsen, 1982: "Duration of Load Effects in Lumber, Parts I-III". Proc. IUFRO-Wood Engineering Meeting, Borås, Sweden.

Jonasson, K., M. Faurschou, L. Eriksen, and N. Askov, 1984: "Size Effect" (in Danish), Internal Report, Building Materials Lab., Tech. Univ. Denmark.

Källsner, B., and B. Norén, 1978: "Influence of Stiffness Variations on the Load-Carrying Capacity of a Wooden Beam on Three Supports", Träteknik-Centrum. STFI-Meddelande serie A nr. 523.

Kärkäinen, M., and M. Raivonen, 1977: "Reaktiopuun mekaninen lujuus. Summary: Mechanical Strength of Reaction Wood". Silva Fennica Vol. 11(2):87-96.

Keith, C.T., and W.A. Côté, Jr., 1968: "Microscopic Characterization of Slip Lines and Compression Failures in Wood Cell Walls". For. Prod. J. 18:67-74.

Keith, C.T., 1970: "Microscopic Changes in the Structure of Wood Associated with Creep". Ph.D. Thesis, State University College of Forestry at Syracuse University.

Keith, C.T., 1971: "The Anatomy of Compression Failure in Relation to Creep-Inducing Stress". Wood Science 4(2):71-82.

Keith, C.T., 1972: "The Mechanical Behaviour of Wood in Longitudinal Compression". Wood Science 4(4):234-244.

Keylwerth, R., 1951: "Die anisotrope Elasticität des Holzes und der Lagenhölzen". VDI-Forschungsheft 430. Deutscher Ingenieur-Verlag.

Kim, K.Y., 1986: "A Note on the Hankinson Formula". Wood and Fiber Science 18(2):345-348.

Kisser, J., and A. Steininger, 1952: "Makroskopische und mikroskopische Strukturänderungen bei der Biegebeanspruchung von Holz". Holz als Roh- und Werkstoff 10:415-421.

Klauditz, W., and I. Stolley, 1955: "Über die biologisch-mechanischen und technischen Eigenschaften des Zugholzes". Holzforschung 9(1):5-10.

Kline, D.E., F.E. Woeste, and B.A. Bendtsen, 1986: "Stochastic Model for Modulus of Elasticity in Lumber". Wood and Fiber Science 18(2):228-238.

Knigge, W., 1958: "Das Phänomen der Reaktionsholzbildung und seine Bedeutung für die Holzverwendung". Forstarchiv 29(1):4-10.

Kollmann, F.F.P., 1934: "Die Abhängigkeit der Festigkeit und der Dehnungszahl der Hölzer vom Faserverlauf". Der Bauingenieur No. 19/20.

Kollmann, F.F.P., and W.A. Côté, 1984: "Principles of Wood Science and Technology, Volume I: Solid Wood". Springer-Verlag.

Kousholt, K.K., 1980: "On the Time Dependent Failure of Wood" (in Danish), Build. Mat. Lab., Tech. Univ. Denmark, Technical Report No. 85/80.

Kučera, B., 1970: "Einfluss einiger Fehler auf die Biegefestigkeit von Fichtenholz". Holztechnologie 11(4):219-224.

Kučera, B., 1973: "Holzfehler und ihr Einfluss auf die mechanischem Eigenschaften der Fichte und Kiefer". Holztechnologie 14(1):8-17.

Kučera, L.J., and M. Bariska, 1982: "On the Fracture Morphology in Wood. Part 1: A SEM-Study of Deformation in Wood of Spruce and Aspen upon Ultimate Axial Compression Load". Wood Science and Technology 16:241-259.

Kühne, H., 1955: "Über den Einfluss von Wassergehalt, Raumgewicht, Faserstellung und Jahrringstellung auf die Festigkeit und Verformbarkeit schweizerischen Fichten-, Tannen-, Lärchen-, Rotbuchen- und Eichenholzes". EMPA, Bericht No. 183.

Kunesh, R.H., and W. Johnson, 1972: "Effect of Single Knots on Tensile Strength of 2 by 8 Inch Douglas-Fir Dimension Lumber". For. Prod. J. 22.

Larsen, H.J., and H. Riberholt, 1983: "Trækonstruktioner, Beregning". SBI anvisning nr. 135.

Littleford, T.W., 1978: "Flexural Properties of Dimension Lumber from Western Canada". Western Forest Products Laboratory, Information Report VP-X-179.

Madsen, B., and A.H. Buchannan, 1985: "Size Effect in Timber Explained by a Modified Weakest Link Theory". Proc. CIB-W18 Meeting, Haifa, Israel.

Madsen, T. Lynge, 1980: "The Efficiency of Visual and Mechanical Stress Grading of Norway Spruce Timber and the Possibilities of Improving the Methods by Means of the Pilodyn Instrument or Additional Annual Ring Width Limits.

Maki, A.C., and E.W. Kuenzi, 1965: "Deflection and Stresses of Tapered Wood Beams". U.S. Forest Service, Research Paper FPL 34.

Mark, R.E., 1967: "Cell Wall Mechanics of Tracheids". Yale Univ. Press, New Haven.

Meylan, B.A., 1968: "Cause of High Longitudinal Shrinkage in Wood". For. Prod. J. 18(4):75-78.

Morell, J.J., and R.A. Zabel, 1985: "Wood Strength and Weight Losses Caused by Soft Rot Fungi Isolated from Treated Southern Pine Utility Poles". Wood and Fiber Sci. 17(1):132-143.

Murphy, J.F., 1979: "Using Fracture Mechanics to Predict Failure in Notched Wood Beams". Proc. of First International Conf. on Wood Fracture, Banff, Alberta.

Nielsen, L.F., 1978: "Crack Failure of Dead-, Ramp-, and Combined Loaded Viscoelastic Materials". Proc. of First International Conference on Wood Fracture, Banff, Alberta.

Nielsen, L.F., and K.K. Kousholt, 1980: "Stress-Strength-Lifetime Relationship for Wood". Wood Science 12(3):162-164.

Nielsen, L.F., 1985a: "Wood as a Cracked Viscoelastic Material, Theory and Applications". Proc. International Workshop on Duration of Load in Lumber and Wood Products. Forintek Canada Corp., Special Publication No. SP-27, issued 1986, pp. 67-78.

Nielsen, L.F., 1985b: "Wood as a Cracked Viscoelastic Material, Sensitivity and Justification of a Theory". Proc. International Workshop on Duration of Load in Lumber and Wood Products. Forintek Canada Corp., Special Publication No. SP-27, issued 1986, pp. 79-89.

Nix, L.E., and C.L. Brown, 1987: "Cellular Kinetics of Compression Wood Formation in Slash Pine". Wood and Fiber Science 19(2):126-134.

Norris, C.B., 1939: "Elastic Theory of Wood Failure". Trans. ASME 61(3): 259-61.

Norris, C.B., 1962: "Strength of Orthotropic Materials Subjected to Combined Stresses". U.S. For. Prod. Lab. Report No. 1816.

Ollinmaa, P.J., 1955: "Koivun vetopuun anatomisesta rakenteesta ja ominaisuuksista. Summary: On the Anatomical Structure and Properties of the Tension Wood in Birch". Acta Forestalia Fennica 64.3.

Ollinmaa, P.J., 1959: "Reaktiopuututkimuksia. Summary: Study on Reaction Wood", Acta For. Fenn. 72.1.

Orowan, E., 1955: "Energy Criteria of Fracture". Welding Research Supplement, pp. 157s-160s.

Osgood, W.R., 1928: "Compressive Stress on Wood Surfaces Inclined to the Grain". Eng. News Record 100(6):243-244.

Panshin, A.J., and C. de Zeeuw, 1970: "Textbook of Wood Technology, Vol. 1". McGraw-Hill.

Pearson, R.G., 1974: "Application of Fracture Mechanics to the Study of the Tensile Strength of Structural Lumber". Holzforschung 28(1):11-19.

von Peckmann, H., and O. Schaile, 1950: "Über die Anderung der dynamischen Festigkeit und der chemischen Zusammensetzung des Holzes durch den Angriff holzzerstörender Pilze". Forstwiss. Centralblatt 69:441-466.

von Peckmann, H., 1953: "Untersuchungen über die Bruchslagarbeit von Rotbuchenholz". Holz als Roh- und Werkstoff 11(9):361-367.

Perem, E., 1958: "The Effect of Compression Wood on the Mechanical Properties of White Spruce and Red Pine". For. Prod. J. 8(8):235-240.

Perkins, R.W., 1967: "Fundamental Concepts Concerning the Mechanics of Wood Deformation". For. Prod. J. 17(3):55-67, 17(4):57-68, 17(5):59-70.

Phillips, G.E., J. Bodig, and J.R. Goodman, 1981: "Flow-Grain Analogy". Wood Sci. 14(2):55-64.

Pillow, M.Y., and R.F. Luxford, 1937: "Structure, Occurrence, and Properties of Compression Wood". U.S. Dept. Agric. Tech. Bull. 546.

Pincus, G., 1967: "Nature of Compression Failure in Wood". J. ASCE, June.

Porter, A.W., 1964: "On the Mechanics of Fracture in Wood"., F.P.J. 8:325-331.

Riberholt, H., and P. Hauge Madsen, 1979: "Strength Distribution of Timber Structures", Structural Research Laboratory, Technical Univ. Denmark, Report No. R114.

Robertson, A., 1920: "Report on Materials of Construction Used in Aircraft and Aircraft Engines". Aeronautical Research Committee, London.

Robinson, W., 1920: "The Microscopical Features of Mechanical Strains in Timber and the Bearing of These on the Structure of the Cell Wall in Plants". Philos. Trans. Soc. London. Scr.B.210:49-82.

Rolfe, S.T., and R. Barson, 1977: "Fracture and Fatigue Control in Structures". Prentice Hall, Englewood Cliffs, N.J.

Schniewind, A.P., and J.D. Barrett, 1969: "Cell Wall Model with Complete Shear Restraint". Wood and Fiber 1(3):205-215.

Schniewind, A.P., and R.A. Pozniak, 1971: "On the Fracture Toughness of Douglas Fir Wood". Eng. Fract. Mech. 2:223-233.

Schniewind, A.P., and J.C. Centeno, 1973: "Fracture Toughness and Duration of Load Factor. I: Six Principal Systems of Crack Propagation and the Duration Factor for Cracks Propagating Parallel to the Grain". Wood and Fiber 5(2):152-159.

Schniewind, A.P., and D.E. Lyon, 1973: "A Fracture Mechanics Approach to the Tensile Strength Perpendicular to Grain of Dimension Lumber". Wood Science and Technology 7(1):45-59.

Schniewind, A.P., H.J. Bartels, and B.W. Gammon, 1978: "Effect of Pre-Loading on Fracture Toughness of Wood", Proc. First International Conf. on Wood Fracture, Banff, Alberta.

Schulz, H., B. Bellmann, and L. Wagner, 1984: "Druckholzanalyse in einem stark verkrümmten Fichtenbrett". Holz als Roh- und Werkstoff (3):109.

Schwendener, S., 1874: "Das mechanische Prinzip im anatomischen Bau der Monocotylen". Leipzig.

Schwerin, G., 1958: "The Chemistry of Reaction Wood II. The Polysaccharides of *Eucalyptus goniocalyx* and *Pinus radiata*". Holzforschung 12:43-48.

Smith, L., and S. Jacobsson, 1976: "Experiences of Soft Rot Damages in Salt-Treated Transmission Poles of Pine with Special Reference to the Residual Strength of Damaged Poles and Inspection Methods". In: Soft Rot in Utility Poles Salt-Treated in the Years 1940-1954, Swedish Wood Preservation Institute, No. 117E.

Stamm, A.J., 1964: "Wood and Cellulose Science". The Ronald Press Company, New York.

Stieda, C.K.A., 1966: "Stress Concentrations around Holes and Notches and Their Effect on the Strength of Wood Beams". J. Materials 1(3):560-581.

Stupnicki, J., 1968: "Analysis of the Behaviour of Wood under External Load Based on a Study of the Cell Structure". Acta Polytechnica Scandinavica, Civil Eng. and Build. Constr. Series No. 53.

Stupnicki, J., 1970: "Strukturmodell der Holzzelle zur Untersuchung von Bruchvorgängen". Holztechnologie 11:168-176.

Stüssi, F., 1945: "Zum Einfluss der Faserrichtung auf die Festigkeit und den Elasticitätsmodul von Holz". Schweizerische Bauzeitung 126(22).

Stüssi, F., 1946: "Holzfestigkeit bei Beanspruchung Schräg zur Faser". Schweizerische Bauzeitung 128(20):251-252.

Tang, R.C., 1970: "Note on a Paper by Schniewind and Barrett". Wood and Fiber 1(4):324-325.

Timell, T.E., 1982: "Recent Progress in the Chemistry and Topochemistry of Compression Wood". Wood Science and Technology 16:83-122.

Toole, E.R., 1971: "Reduction in Crushing Strength and Weight Associated with Decay by Rot Fungi". Wood Science 3(3):172-178.

Trendelenburg, R., 1932: Über die Eigenschaften des Rot- und Druckholzes der Nadelhölzer". Allg. Forst- und Jgd. Ztg. 108:1.

Trendelenburg, R., and H. Mayer-Wegelin, 1955: "Das Holz als Rohstoff". Carl Hauser Verlag, München.

Triboulot, P., P. Jodin, and G. Pluvinage, 1984: "Validity of Fracture Mechanics Concepts Applied to Wood by Finite Element Calculation". Wood Sci. and Technology 18:51-58.

Vinopal, G.W., 1980: "Determination of the Combined Influence of Density and Knots on the Mechanical Properties of Full-Size Structural Timber". Proceedings of IUFRO-Wood Engineering Meeting, Oxford, England.

Vitruvius, First Century B.C.: "On Architecture". In: F. Granger, "Vitruvius". Harvard University Press, 1955.

Voight, W., 1928: "Lehrbuch der Krystallphysik". Teubuer, Leipzig.

Walsh, P.F., 1974: "Linear Fracture Mechanics Solutions for Zero and Right Angle Notches". CSIRO Australia, Div. Build. Res., Technol. Pap. (Second Ser.) No. 2:1-16.

Wang, S.-C., O. Sachsland, and J.H. Hart, 1980: "Dynamic Test for Evaluating Decay in Wood". For. Prod. J. 30(7):35-37.

Wardrop, A.B., and H.E. Dadswell, 1947: "Contributions to the Study of the Cell Wall. 5. The Occurrence Structure and Properties of Certain Cell Wall Deformations. CSIRO Bulletin No. 221.

Wardrop, A.B., 1964a: "The Reaction Anatomy of Arborescent Angiosperms". In: The Formation of Wood in Forest Trees, ed. M.H. Zimmermann. Academic Press.

Wardrop, A.B., 1964b: "Formation and Function of Reaction Wood". In: Cellular Ultrastructure of Woody Plants, Ed. W.A. Côté, Syracuse University Press.

Westergaard, H.M., 1939: "Bearing Pressures and Cracks". J. Applied Mechanics 6(1):A49-A53.

Wilcox, W.W., 1973: "Degradation in Relation to Wood Structure". In: Wood Deterioration and Its Prevention by Preservative Treatment, Vol. I., ed. D.D. Nicolas, Syracuse University Press.

Wilkins, A.P., 1986: "The Nomenclature of Cell Wall Deformations". Wood Science and Technology 20:97-109.

Williams, J.G., and M.W. Birch, 1975: "Mixed Mode of Fracture in Anisotropic Media". N.A.T.O. Science Committee Conference, Working Papers, Les Arcs, France.

Wilson, J.B., R.P. McEvoy, Jr., and R.W. Perkins, 1978: "On Compression Failure in Wood Materials: A Mathematical and Experimental Simulation". Proc. First Int. Conf. on Wood Fracture, Banff, Alberta.

Wilson, T.R.C., 1921: "The Effect of Spiral Grain on the Strength of Wood". J. Forestry, Washington 19:747.

Winther, H., 1944: "Richtlinien für den Holzflugzeugbau". Beiträge BIIa2, BIIb, BIIc, BIId, BIIIb. Berlin (here after Kollmann and Côté, 1984).

Ylinen, A., 1953: "Über die mechanische Schaftformtheorie der Bäume". Holz als Roh- und Werkstoff 11:209.

A. ORTHOTROPIC ELASTICITY OF WOOD

A.1 Introduction

Hooke's law is the simple statement that the strain ε is proportional to the stress σ.

$$\varepsilon = \alpha\sigma \tag{A1}$$

where $\alpha = \varepsilon/\sigma$ is the compliance, i.e. the strain per unit stress. The reciprocal value $1/\alpha = E$ is known as Young's modulus or the modulus of elasticity.

Used on vanishingly small stresses and strains, Hooke's law applies for practically all materials. For finite values of stresses and strains, however, non-linear behavior will be seen, and the applicability of the law depends on the specific material, stress/strain level, temperature, moisture, duration of load, etc.

Although wood is not strictly a linear material, quite acceptable results can be obtained by using Hooke's law for those stresses usually relevant in wood construction. For long duration of the load, however, creep and relaxation is introduced which significantly complicate matters.

The application of Hooke's law for wood has been treated by numerous researchers (e.g. Hearmon, 1948; Keylwerth, 1951; Jayne and Suddarth, 1966; Perkins, 1967; Goodman and Bodig, 1970; Jayne, 1972; Dinwoodie, 1981; Bodig and Jayne, 1982). Below is presented a brief introduction to linear elastic theory for wood based on a slightly altered and translated version of Hoffmeyer (1970). The notation used is based on Hearmon (1948) and Keylwerth (1951).

A.2 Generalized Hooke's Law

Hooke's law in rectangular coordinates is written as

$$\bar{t} = \bar{\bar{S}}\,\bar{s} \quad \text{or} \tag{A2}$$

$$\bar{s} = \bar{\bar{C}}\,\bar{t} \tag{A3}$$

where

$$\bar{t} = \text{strain matrix} = \begin{bmatrix} \varepsilon_x \\ \varepsilon_y \\ \varepsilon_z \\ \gamma_{yz} \\ \gamma_{xz} \\ \gamma_{xy} \end{bmatrix} \tag{A4}$$

$$\bar{s} = \text{stress matrix} = \begin{bmatrix} \sigma_x \\ \sigma_y \\ \sigma_z \\ \tau_{yz} \\ \tau_{zx} \\ \tau_{xy} \end{bmatrix} \tag{A5}$$

$$\bar{\bar{S}} = \begin{bmatrix} S_{11} & S_{12} & S_{13} & S_{14} & S_{15} & S_{16} \\ S_{21} & S_{22} & S_{23} & S_{24} & S_{25} & S_{26} \\ S_{31} & S_{32} & S_{33} & S_{34} & S_{35} & S_{36} \\ S_{41} & S_{42} & S_{43} & S_{44} & S_{45} & S_{46} \\ S_{51} & S_{52} & S_{53} & S_{54} & S_{55} & S_{56} \\ S_{61} & S_{62} & S_{63} & S_{64} & S_{65} & S_{66} \end{bmatrix} \tag{A6}$$

$$\bar{\bar{C}} = \begin{bmatrix} C_{11} & C_{12} & C_{13} & C_{14} & C_{15} & C_{16} \\ C_{21} & C_{22} & C_{23} & C_{24} & C_{25} & C_{26} \\ C_{31} & C_{32} & C_{33} & C_{34} & C_{35} & C_{36} \\ C_{41} & C_{42} & C_{43} & C_{44} & C_{45} & C_{46} \\ C_{51} & C_{52} & C_{53} & C_{54} & C_{55} & C_{56} \\ C_{61} & C_{62} & C_{63} & C_{64} & C_{65} & C_{66} \end{bmatrix} \tag{A7}$$

ε_x, ε_y, ε_z are normal strains,

σ_x, σ_y, σ_z are normal stresses in the direction of the axis x, y, z, while

$\gamma_{yz}, \gamma_{zx}, \gamma_{xy}$ are shear strains, and

τ_{yz}, τ_{zx}, τ_{xy} are shear stresses in the planes indicated by indices.

$\bar{\bar{S}}$ is termed compliance matrix, and S_{ij} are termed compliance parameters.

$\bar{\bar{C}}$ is termed stiffness matrix, and C_{ij} are termed stiffness parameters.

From Equations A2 and A3 it appears that

$$\bar{\bar{S}} = \bar{\bar{C}}^{-1} \tag{A8}$$

and

$$\bar{\bar{C}} = \bar{\bar{S}}^{-1}$$

Equations A6 and A7 imply that 36 elastic parameters are necessary to describe the elastic behavior of a material. However, not all parameters are independent, and often materials will have a structural symmetry which further reduces the number of necessary elastic parameters.

Thermodynamic considerations (e.g. Alfrey, 1948, p. 12) proves the matrices to be symmetric, and thus

$$S_{ij} = S_{ji} \quad \text{and} \quad C_{ij} = C_{ji} \tag{A10}$$

which reduces the number of independent elastic parameters to 21 for the generalized Hooke's law.

A.3 Orthotropic Behavior

A further reduction of the number of independent parameters is obtained by considering wood as an orthotropic material, i.e. a material with three rectangular planes of elastic symmetry. The principal axes L, T, and R are each perpendicular to a principal plane.

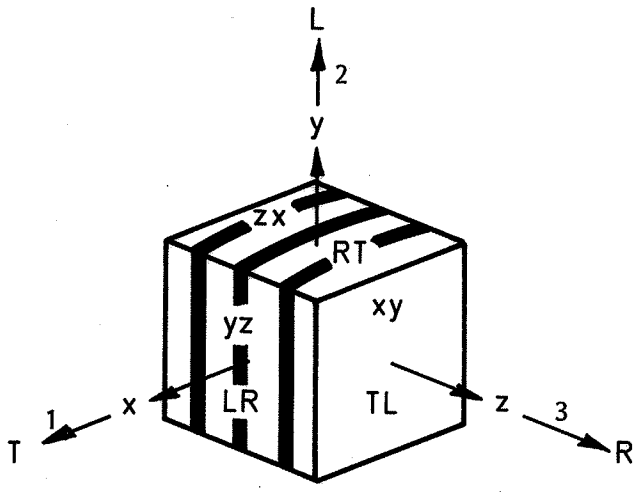

Figure A.1. Principal axes and principal planes in wood.

For the T, L, and R axes identical to the x, y, and z axes, respectively, a further reduction of parameters is possible. The compliance matrix is now written:

$$\bar{\bar{S}} = \begin{bmatrix} S_{11} & S_{12} & S_{13} & 0 & 0 & 0 \\ S_{21} & S_{22} & S_{23} & 0 & 0 & 0 \\ S_{31} & S_{32} & S_{33} & 0 & 0 & 0 \\ 0 & 0 & 0 & S_{44} & 0 & 0 \\ 0 & 0 & 0 & 0 & S_{55} & 0 \\ 0 & 0 & 0 & 0 & 0 & S_{66} \end{bmatrix} \qquad \text{(A11)}$$

or using A2 and A3:

$$\begin{aligned} \varepsilon_x &= S_{11}\,\sigma_x + S_{12}\,\sigma_y + S_{13}\,\sigma_z \\ \varepsilon_y &= S_{21}\,\sigma_x + S_{22}\,\sigma_y + S_{23}\,\sigma_z \\ \varepsilon_z &= S_{31}\,\sigma_x + S_{32}\,\sigma_y + S_{33}\,\sigma_z \\ \gamma_{yz} &= S_{44}\,\tau_{yz} \\ \gamma_{zx} &= S_{55}\,\tau_{zx} \\ \gamma_{xy} &= S_{66}\,\tau_{xy} \end{aligned} \qquad \text{(A12)}$$

where $S_{ij} = S_{ji}$, and

$$
\begin{aligned}
\sigma_x &= C_{11}\,\varepsilon_x + C_{12}\,\varepsilon_y + C_{13}\,\varepsilon_z \\
\sigma_y &= C_{21}\,\varepsilon_x + C_{22}\,\varepsilon_y + C_{23}\,\varepsilon_z \\
\sigma_z &= C_{31}\,\varepsilon_x + C_{32}\,\varepsilon_y + C_{33}\,\varepsilon_z \\
\tau_{yz} &= C_{44}\,\gamma_{yz} \\
\tau_{zx} &= C_{55}\,\gamma_{zx} \\
\tau_{xy} &= C_{66}\,\gamma_{xy} \qquad \text{where } C_{ij} = C_{ji}
\end{aligned}
\tag{A13}
$$

The physical meaning of the elastic parameters can be illustrated by assuming uniaxial stresses. Equation A12 gives

$$
\begin{aligned}
&\varepsilon_x = S_{11}\,\sigma_x \;,\; \varepsilon_y = S_{21}\,\sigma_x \;,\; \varepsilon_z = S_{31}\,\sigma_x \\
&\tau_{yz} = S_{44}\,\tau_{yz} \;,\; \gamma_{zx} = S_{55}\,\tau_{zx} \;,\; \gamma_{xy} = S_{66}\,\tau_{xy}
\end{aligned}
\tag{A14}
$$

The first equation gives

$$
\frac{\sigma_x}{\varepsilon_x} = \frac{1}{S_{11}} = E_x \tag{A15}
$$

where E_x is Young's modulus in the direction of the x-axis. The first and second equations of A15 give

$$
\frac{\varepsilon_y}{\varepsilon_x} = \frac{S_{21}}{S_{11}} = -\,\nu_{yx} \quad \text{or} \quad S_{21} = \frac{\nu_{yx}}{E_x} \tag{A16}
$$

where ν_{yx} is Poisson's ratio.

Through similar considerations Equation A12 can be rewritten as

$$
\begin{aligned}
\varepsilon_x &= \frac{1}{E_x}\,\sigma_x - \frac{\nu_{xy}}{E_y}\,\sigma_y - \frac{\nu_{xz}}{E_z}\,\sigma_z \\
\varepsilon_y &= -\,\frac{\nu_{yx}}{E_x}\,\sigma_x + \frac{1}{E_y}\,\sigma_y - \frac{\nu_{yz}}{E_z}\,\sigma_z \\
\varepsilon_z &= -\,\frac{\nu_{zx}}{E_x}\,\sigma_x - \frac{\nu_{zy}}{E_y}\,\sigma_y + \frac{1}{E_z}\,\sigma_z \\
\gamma_{yz} &= \frac{1}{2G_{yz}}\,\tau_{yz} \\
\gamma_{zx} &= \frac{1}{2G_{xy}}\,\tau_{xy} \\
\gamma_{xy} &= \frac{1}{2G_{xy}}\,\tau_{xy}
\end{aligned}
\tag{A17}
$$

Because of symmetry:

$$\frac{\nu_{xy}}{E_y} = \frac{\nu_{yx}}{E_x} \quad , \quad \frac{\nu_{xz}}{E_z} = \frac{\nu_{zx}}{E_x} \quad \text{and} \quad \frac{\nu_{yz}}{E_z} = \frac{\nu_{zy}}{E_y} \tag{A18}$$

As the $\bar{\bar{C}}$ matrix is calculated by inversion of the $\bar{\bar{S}}$ matrix, it is possible to calculate the stiffness parameters of A13 from A12 and A17:

$$C_{11} = \frac{E_x\,(1 - \nu_{zy}\,\nu_{yz})}{1-2\,\nu_{xy}\,\nu_{yz}\,\nu_{zx} - \nu_{xz}\,\nu_{zx} - \nu_{xy}\,\nu_{yx} - \nu_{yz}\,\nu_{zy}}$$

$$C_{12} = C_{21} = \frac{E_x\,(\nu_{xy} + \nu_{zy}\,\nu_{xz})}{1-2\,\nu_{xy}\,\nu_{yz}\,\nu_{zx} - \nu_{xz}\,\nu_{zx} - \nu_{xy}\,\nu_{yx} - \nu_{yz}\,\nu_{zy}}$$

$$C_{13} = C_{31} = \frac{E_x\,(1 - \nu_{xz}\,\nu_{zx})}{1-2\,\nu_{xy}\,\nu_{yz}\,\nu_{zx} - \nu_{xz}\,\nu_{zx} - \nu_{xy}\,\nu_{yx} - \nu_{yz}\,\nu_{zy}}$$

$$C_{22} = \frac{E_y\,(1 - \nu_{xz}\,\nu_{zx})}{1-2\,\nu_{xy}\,\nu_{yz}\,\nu_{zx} - \nu_{xz}\,\nu_{zx} - \nu_{xy}\,\nu_{yx} - \nu_{yz}\,\nu_{zy}}$$

$$C_{23} = C_{32} = \frac{E_y\,(\nu_{yz} + \nu_{xz}\,\nu_{yx})}{1-2\,\nu_{xy}\,\nu_{yz}\,\nu_{zx} - \nu_{xz}\,\nu_{zx} - \nu_{xy}\,\nu_{yx} - \nu_{zy}\,\nu_{yz}} \tag{A19}$$

$$C_{33} = \frac{E_z\,(1 - \nu_{xy}\,\nu_{yx})}{1-2\,\nu_{xy}\,\nu_{yz}\,\nu_{zx} - \nu_{xz}\,\nu_{zx} - \nu_{xy}\,\nu_{yx} - \nu_{yz}\,\nu_{zy}}$$

$$C_{44} = 2G_{yz}$$

$$C_{55} = 2G_{xz}$$

$$C_{66} = 2G_{xy}$$

Table A.1 lists elastic parameters for some common wood species as given in Kollmann and Côté (1984) after Keylwerth (1955).

Table A.1. Elastic constant for different species (condensed from Keylwerth, 1955)

Species	Density ρ_u kg/m³	Moisture Content u %	S_{11} S_{22} S_{33} mm²/N	S_{44} S_{55} S_{66} mm²/N	$-S_{12}$ $-S_{13}$ $-S_{23}$ mm²/N	$E_x = \frac{1}{S_{11}}$ $E_y = \frac{1}{S_{22}}$ $E_z = S_{33}$ MPa	$G_{yz} = \frac{1}{S_{44}}$ $G_{zx} = \frac{1}{S_{55}}$ $G_{xy} = S_{66}$ MPa	$\frac{E_y}{G_{yz}}$	$\frac{E_y}{G_{xy}}$
SOFTWOOD									
Oregon pine	450-510	11-13	0.00126 0.0000625 0.000994	0.00111 0.0111 0.00111	0.0000279 0.000427 0.0000190	8.00 160.00 10.10	9.00 90 9.00	17.8	17.8
Spruce	430	12	0.00204 0.0000727 0.00110	0.00136 0.0307 0.00196	0.0000390 0.000615 0.0000329	4.90 137.60 9.10	7.30 30 5.10	18.8	27.0
Spruce	500	12	0.00155 0.0000587 0.00121	0.00157 0.0279 0.00115	0.000033 0.000517 0.000022	6.50 170.40 8.30	6.40 40 8.70	26.6	19.6
Pine	540	9	0.00172 0.0000602 0.000890	0.000563 0.0148 0.00146	0.000027 0.00054 0.000028	5.80 166.10 11.20	17.80 70 6.80	9.3	24.4
HARDWOOD									
Beech	740	10-11	0.000862 0.0000714 0.000438	0.000610 0.00215 0.000929	0.000037 0.00031 0.000032	11.60 140.10 22.80	16.40 4.10 10.80	8.5	13.0
Ash	680	9	0.00122 0.0000621 0.000651	0.000730 0.00363 0.00110	0.000032 0.00045 0.000029	8.20 161.00 15.40	13.70 2.80 9.10	11.8	17.7

A.4 Rotation of Orthotropic Axes

The general equations linking for example the compliance matrix $\bar{\bar{S}}$ of the x, y, z system with the compliance matrix $\bar{\bar{S}}'$ of a differently oriented coordinate system x', y', z' are rather complex and will not be presented here. A complete set of equations is found in Voigt (1928).

As an example, let us look at the rotation as depicted in Figure A.2. The material when referenced to the new x', y', z' system is no longer orthotropic. A plane problem in the y', z' plane is transformed into an anisotropic problem, while problems in both the x', y' plane and the x', z' plane are still orthotropic.

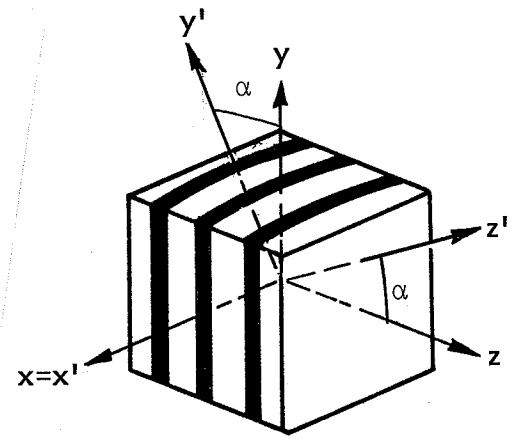

Figure A.2 Special plane anisotropy resulting from the rotation of orthotropic axes in the y,z plane.

Accordingly, the $\bar{\bar{S}}'$ matrix will not only have compliance parameters different from $\bar{\bar{S}}$, but four new compliance parameters are introduced: S'_{14}, S'_{24}, S'_{34}, and S'_{56}. The first three of these link a shear stress in the y',z' plane with the three normal strains. S'_{56} links together a shear stress in the x',y' plane and a shear strain in the x',z' plane:

$$\bar{\bar{S}}' = \begin{bmatrix} S'_{11} & S'_{12} & S'_{13} & S'_{14} & 0 & 0 \\ S'_{21} & S'_{22} & S'_{23} & S'_{24} & 0 & 0 \\ S'_{31} & S'_{32} & S'_{33} & S'_{34} & 0 & 0 \\ S'_{41} & S'_{42} & S'_{43} & S'_{44} & 0 & 0 \\ 0 & 0 & 0 & 0 & S'_{55} & S'_{56} \\ 0 & 0 & 0 & 0 & S'_{65} & S'_{66} \end{bmatrix} \qquad \text{(A20)}$$

The new compliance parameters are expressed as:

$$S'_{11} = S_{11} = 1/E_x$$

$$S'_{22} = S_{22}\cos^4\alpha + (2S_{23} + S_{44})\sin^2\alpha\cos^2\alpha + S_{33}\sin^4\alpha = 1/E_{y'} \qquad (A21)$$

$$S'_{33} = S_{22}\sin^4\alpha + (2S_{23} + S_{44})\sin^2\alpha\cos^2\alpha + S_{33}\cos^4\alpha = 1/E_{z'}$$

$$S'_{21} = S_{21}\cos^2\alpha + S_{31}\sin^2\alpha = -\nu_{y'x'}/E_{x'}$$

$$S'_{31} = S_{21}\sin^2\alpha + S_{31}\cos^2\alpha = -\nu_{z'x'}/E_{x'} \qquad (A22)$$

$$S'_{23} = (S_{22} + S_{33})\sin^2\alpha\cos^2\alpha + S_{23}(\sin^4\alpha + \cos^4\alpha) - S_{44}\sin^2\alpha\cos^2\alpha$$

$$= -\nu_{y'z'}/E_{y'}$$

$$S'_{44} = 4(S_{22} + S_{33} + 2S_{23})\sin^2\alpha\cos^2\alpha + S_{44}(\cos^2\alpha - \sin^2\alpha)^2$$

$$= 1/G_{y'z'} \qquad (A23)$$

$$S'_{55} = S_{55}\cos^2\alpha + S_{66}\sin^2\alpha = 1/G_{z'x'}$$

$$S'_{66} = S_{55}\sin^2\alpha + S_{66}\cos^2\alpha = 1/G_{x'y'}$$

$$S'_{14} = 2(S_{12} - S_{13})\cos\alpha\sin\alpha$$

$$S'_{24} = 2(S_{22}\cos^2\alpha - S_{33}\sin^2\alpha)\cos\alpha\sin\alpha$$

$$- (2S_{23} + S_{66})\cos\alpha\sin\alpha(\cos^2\alpha - \sin^2\alpha) \qquad (A24)$$

$$S'_{34} = 2(S_{22}\sin^2\alpha - S_{33}\cos^2\alpha)\cos\alpha\sin\alpha$$

$$+ (2S_{23} + S_{66})\cos\alpha\sin\alpha(\cos^2\alpha - \sin^2\alpha)$$

$$S'_{56} = (S_{66} - S_{55})\cos\alpha\sin\alpha$$

Equations A21 and A17 combined for instance express Young's moduli in the x',y',z' system by Young's moduli, shear moduli, and Poisson's ratios of the x,y,z system:

$$E_{x'} = E_x$$

$$\frac{1}{E_{y'}} = \frac{1}{E_y}\cos^4\alpha - \left(2\frac{\nu_{zy}}{E_y} - \frac{1}{G_{yz}}\right)\sin^2\alpha\cos^2\alpha + \frac{1}{E_z}\sin^4\alpha \qquad \text{(A25)}$$

$$\frac{1}{E_{z'}} = \frac{1}{E_y}\sin^4\alpha - \left(2\frac{\nu_{zy}}{E_y} - \frac{1}{G_{yz}}\right)\sin^2\alpha\cos^2\alpha + \frac{1}{E_z}\cos^4\alpha$$

A.5 The Simplified Hooke's Law

For many engineering purposes it is not only unrealistic, but even wrong to distinguish between the radial and tangential directions. For big timber dimensions the orientation of these two principal axes may change dramatically within a cross section.

For such purposes it is sufficient to distinguish between the longitudinal direction ($_0$) and the transverse direction ($_{90}$). The number of elastic parameters to describe such a state is 7:

$$E_{90} = E_x = E_T = E_z = E_R$$

$$E_0 = E_y = E_L$$

$$G_{90} = G_{xz} = G_{TR}$$

$$G_0 = G_{yx} = G_{LT} = G_{yz} = G_{LR} \qquad \text{(A26)}$$

$$\nu_{90} = \nu_{xz} = \nu_{TR} = \nu_{zx} = \nu_{RT}$$

$$\nu_0 = \nu_{yx} = \nu_{LT} = \nu_{yz} = \nu_{LR}$$

$$\nu_{xy} = \nu_{TL} = \nu_{zy} = \nu_{RL}$$

Five of these parameters are independent, while two may be calculated from these through the equations:

$$\frac{\nu_{xy}}{E_0} = \frac{\nu_0}{E_{90}} \quad \text{og} \quad G_{90} = \frac{E_{90}}{2(1 + \nu_{90})} \tag{A27}$$

A17 is now written:

$$\varepsilon_0 = \frac{1}{E_0}\sigma_0 - 2\frac{\nu_0}{E_{90}}\sigma_{90}$$

$$\varepsilon_{90} = \frac{1}{E_{90}}(1 - \nu_{90})\sigma_{90} - \frac{\nu_0}{E_{90}}\sigma_0 \tag{A28}$$

$$\gamma_0 = \frac{1}{2G_0}\tau_0$$

$$\gamma_{90} = \frac{1}{2G_{90}}\tau_{90}$$

Average values of the elastic constants for some species are given in Table A.2.

Table A.2. Typical average elastic constant for some softwoods and hardwoods.

	Pine/Spruce	Oak/Beech
E_0 (MPa)	12000	13000
E_{90} (MPa)	600	1200
G_0 (MPa)	700	1000
G_{90} (MPa)	100	300
ν_0	0.02	0.05
ν_{90}	0.35	0.45

The numbers in the table are all mean values of test results, and the condition of Equation A27 therefore cannot be expected to be quite fullfilled.

B. FRACTURE MECHANICS

B.1 Elastic Fracture Mechanics

Consider a semi-infinite plate of material loaded in tension and containing a crack of length 2a (Figure B.1). The strain energy for the uncracked material is

$$W = \tfrac{1}{2} \frac{\sigma^2}{E} \qquad \text{(B1)}$$

where

σ = external tensile stress
E = modulus of elasticity

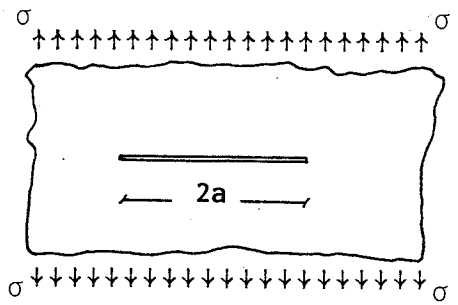

Figure B.1. Semi-infinite plate of material loaded in tension and containing a crack of length 2a.

Creation of a crack results in the gain of energy (W_s) of the fracture surfaces and the loss of energy (W_e) due to the release of strain particularly in the immediate vicinity of the crack.

$$W_e = \tfrac{1}{2} \frac{\sigma^2}{E} (\pi \cdot a \cdot 2a) = \frac{\pi a^2 \sigma^2}{E} \qquad \text{(B2)}$$

$$W_s = 4\, a\, \gamma_s \qquad \text{(B3)}$$

where

γ_s = specific surface free energy

Griffith (1920) formulated a failure criterion for unstable crack propagation

$$\frac{\partial W_e}{\partial a} \geq \frac{\partial W_s}{\partial a} \tag{B4}$$

which expresses that in brittle solids which behave elastically up to failure cracks will grow if the loss of strain energy is larger than the gain of surface free energy. Equations B2, B3, and B4 give

$$\sigma_c = \sqrt{\frac{2\,\gamma_s\,E}{\pi a}} \tag{B5}$$

which establishes a relationship between fracture stress (σ_c), crack length, and surface free energy. The expression is valid for plane stress conditions.

In order to extend Equation B5 to also cover non-brittle materials, Irwin (1948) and Orowan (1955) introduced a term γ_f, the work of fracture, which includes all the energy absorbed by mechanisms other than the creation of crack faces:

$$\sigma_c = \sqrt{\frac{E(2\gamma_s + \gamma_f)}{\pi a}} \tag{B6}$$

Irwin introduced the strain energy release rate, G, also termed the crack extension force

$$G = 2\gamma_s + \gamma_f \tag{B7}$$

and Equation B6 is now written

$$\sigma_c = \sqrt{\frac{E \cdot G}{\pi a}} \tag{B8}$$

The two materials property parameters E and G are conveniently combined into one parameter K_I, termed the stress intensity factor

$$K_I = \sqrt{G \cdot E} \tag{B9}$$

and Equation B8 becomes:

$$K_{Ic} = \sigma_c \sqrt{\pi a} \tag{B10}$$

where K_{Ic} is the critical stress intensity factor at failure.

Real specimens always have a finite width, b, and a correction factor, C, therefore must be introduced which takes different geometries into account.

$$K_{Ic} = \sigma_c \sqrt{\pi a}\ C \tag{B11}$$

The factor C is found in handbooks (e.g. Rolfe and Barson, 1977).

Griffith's failure criterion produces the critical ultimate stress σ_c, but gives no information about stresses at the crack tip. Irwin (1957) solved the problem using a technique from Westergaard (1939) (Figure B.2):

$$\begin{bmatrix} \sigma_x \\ \sigma_y \\ \tau_{xy} \end{bmatrix} = \frac{K_I}{\sqrt{2\pi r}} \begin{bmatrix} 1 - \sin\frac{\theta}{2}\sin\frac{3\theta}{2} \\ 1 + \sin\frac{\theta}{2}\sin\frac{3\theta}{2} \\ \sin\frac{\theta}{2}\cos\frac{3\theta}{2} \end{bmatrix} \cos\frac{\theta}{2} \tag{B12}$$

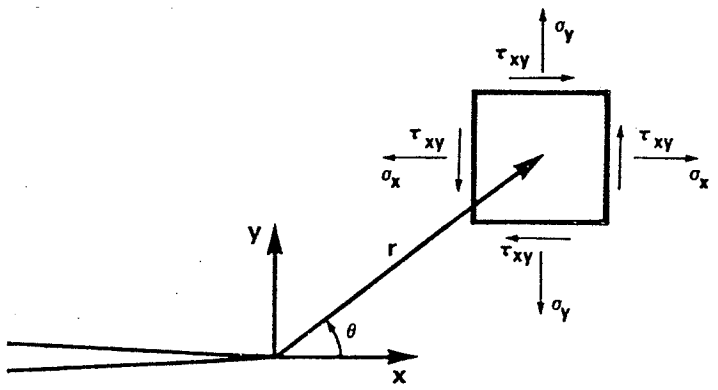

Figure B.2. Coordinate system and stress notation at crack tip.

Note that 1) the stresses are completely determined by the stress intensity factor K_I and that 2) $\sigma_{ij} \to \infty$ for $r \to 0$.

To overcome this inconsistency of infinite stresses, Barenblatt (1959a, 1959b, 1962) assumed varying molecular cohesion forces acting in a zone of the length, s, at the crack tip. Dugdale (1960) simplified the model by assuming a constant stress acting over the whole length s (Figure B.3). This stress is supposed to assume a maximum value equal to the "yield stress" σ_Y.

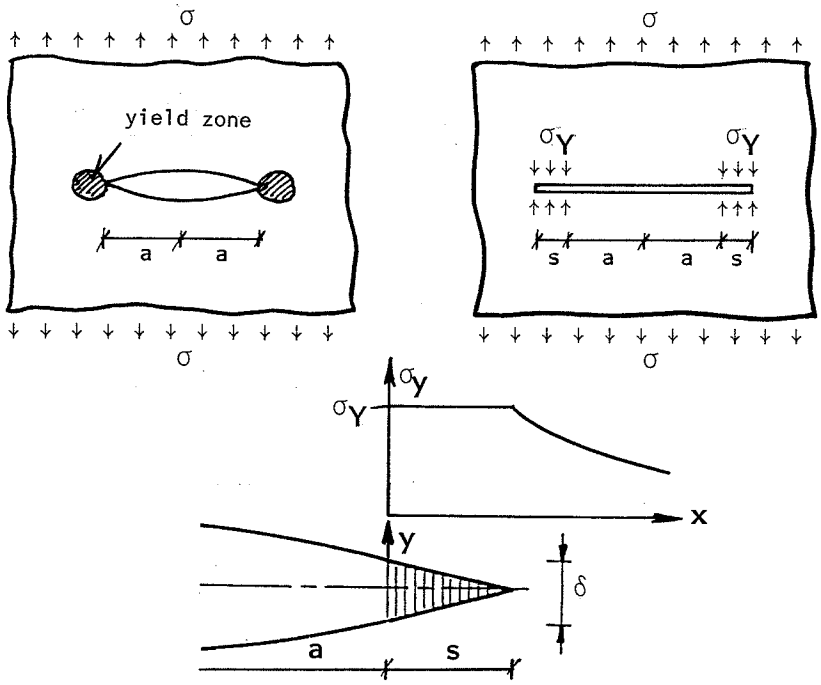

Figure B.3. The Dugdale-Barenblatt model.

The Dugdale-Barenblatt model now superimposes on the K_I factor from the external stresses, σ, the K_I^* factor from the yield stress σ_Y. K_I^* is dependent on the length of the yield zone, $K_I^* = K_I^*(s)$, and s is now adjusted so that

$$K_I + K_I^*(s) = 0 \qquad \text{(B13)}$$

As a result, finite stresses are defined at the crack tip.

Equation B13 results in

$$s = a\,\frac{\pi^2}{8}\left(\frac{\sigma}{\sigma_Y}\right)^2 = \frac{\pi}{8}\left(\frac{K_I}{\sigma_Y}\right)^2 \qquad \text{(B14)}$$

The elongation, δ, of a "fiber" in the crack-front zone is given by

$$\delta = \frac{\sigma^2 \pi a}{E \sigma_Y} = \frac{K_I^2}{E \sigma_Y} \tag{B15}$$

As the resulting stress intensity factor is now zero in the Dugdale-Barenblatt model, a new criterion for crack propagation is needed. It is now assumed that there is a critical value, δ_c, of the "fiber elongation" which causes crack growth:

$$\delta = \delta_c \tag{B16}$$

δ_c is often termed the critical crack opening displacement.

Equations B14 and B15 are valid only for $s \ll a$. For $s/a \to 0$ (large cracks) it can be shown that Equations B9 and B16, B15 are identical.

The critical crack length is derived from

$$a_c = \frac{E \, \delta_c \, \sigma_Y}{\pi \sigma^2} \tag{B17}$$

Defining the critical energy

$$G = \sigma_Y \, \delta_c \tag{B18}$$

and combining Equations B8 and B18 gives

$$\sigma_c = \sqrt{\frac{E \, \sigma_Y \, \delta_c}{\pi a}} = \sqrt{\frac{EG}{\pi a}} \tag{B19}$$

B.2 Viscoelastic Fracture Mechanics

The concept of Dugdale-Barenblatt may be used to assess the time to failure for wood (Nielsen, 1978, 1985a, 1985b; Nielsen and Kousholt, 1980; Kousholt, 1980). A time dependent modulus of elasticity $E = E(t)$ is introduced, and time (t_s) to the start of crack growth and the additional time ($t_{cat} - t_s$) to ultimate failure is expressed as:

$$t_s = F(SL^{-2}) \tag{B20}$$

$$t_{cat} - t_s = \frac{8(\alpha \cdot Q + 1)}{\pi^2} \cdot FL^{-2} \cdot SL^{-2} \int_1^{SL^{-2}} \frac{F(\theta)}{\theta} \, d\theta \qquad \text{(B21)}$$

where

SL = stress level = $\frac{\sigma}{\sigma_c}$

FL = strength level = $\frac{\sigma_c}{\sigma_n}$ (σ_n = strength of non-cracked material)

θ = time variable

Q = constant (related to shape of crack profile)

α = constant (related to creep function)

Note that time to failure (t_{cat}) is dependent only on stress level, strength level (quality of wood), and a creep function.

Nielsen (1985a and b) introduced into Equation B20 and B21 a simple power creep law (Clouser, 1959) and showed good agreement between test results and theoretical time to failure.

Johns and Madsen (1982) extended Equation B20 to take into account the grain angle deviation around knots. They showed good agreement between theory and results of the very large duration of load program at U.B.C., Vancouver.

Foschi and Yao (1986) tested three duration of load models and found that the fracture mechanics model above along with the Foschi damage accumulation model "were suitable to represent accurately the experimental trends in Western hemlock lumber in bending".

A simplified, conservative estimate of time to failure is possible by assuming that catastrophic failure occurs soon after cracks start growing:

$$t_{cat} \cong t_s = F(SL^{-2}) \qquad \text{(B22)}$$

Introducing the power creep law

$$J(t) = \frac{1}{E} \left(1 + \left(\frac{t}{\tau}\right)^b\right) \qquad \text{(B23)}$$

where

τ = constant (doubling time)
b = constant

gives

$$t_{cat} \cong t_s = \tau(SL^{-2} - 1)^{1/b} \qquad \text{(B24)}$$

Hoffmeyer (1987b) - assuming that failure of lumber containing knots is caused by tension perpendicular to grain - used τ and b values typical of this failure mode. Good agreement between time to failure of spruce dimension lumber subjected to bending was found.

Bending failures in *Picea abies*. Arrow points to tension side.

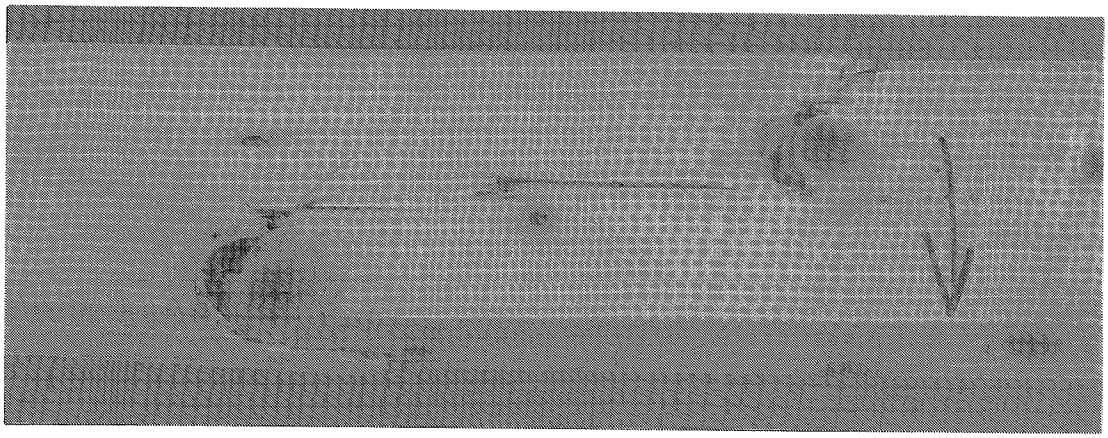

Figure C.1. Tension perpendicular to grain failure at knot. Note the short fibered failure revealed in the compression side.

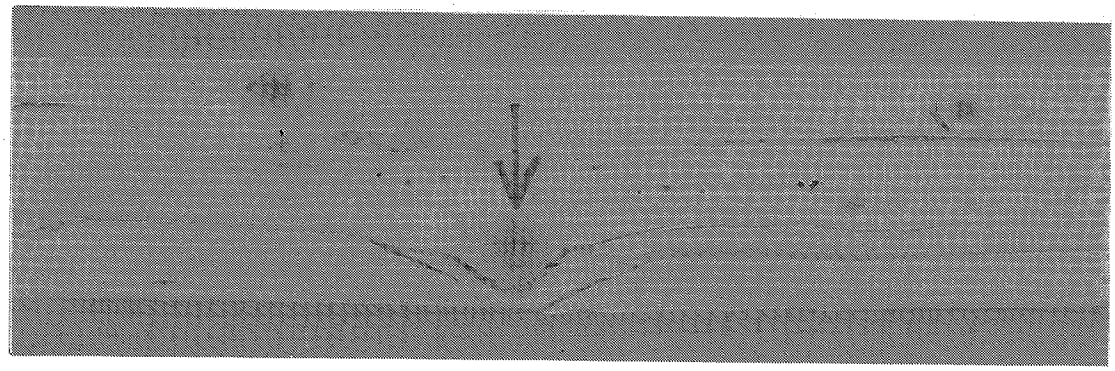

Figure C.2. Typical failure for face knot in tension side. The failure is always caused by shear or tension perpendicular to grain stresses at the outermost fibers due to the inclined grain.

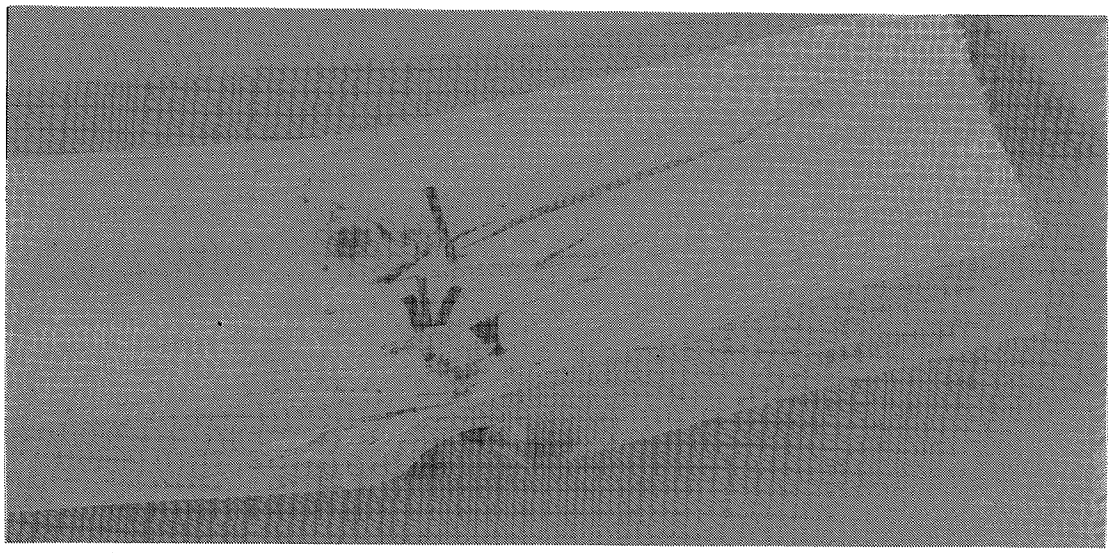

Figure C.3. Tension parallel to grain failure in clear wood and tension perpendicular to grain failure in knot.

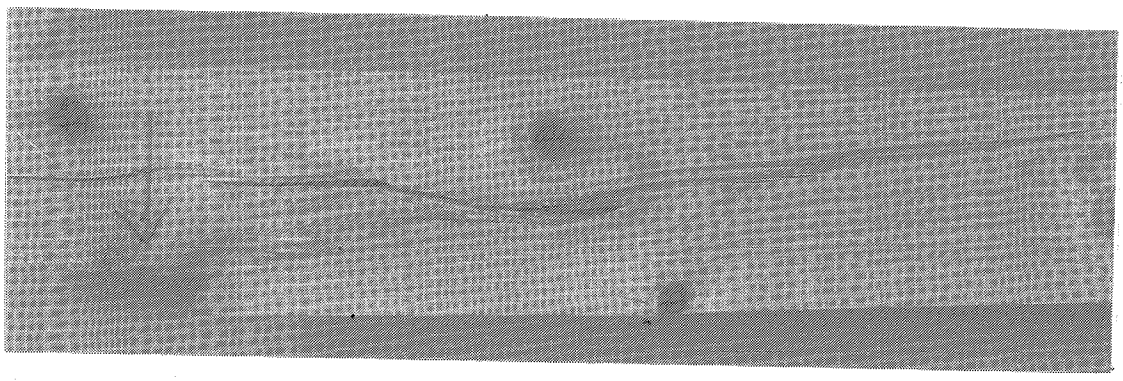

Figure C.4. Combined tension perpendicular to grain and shear failure at knot.

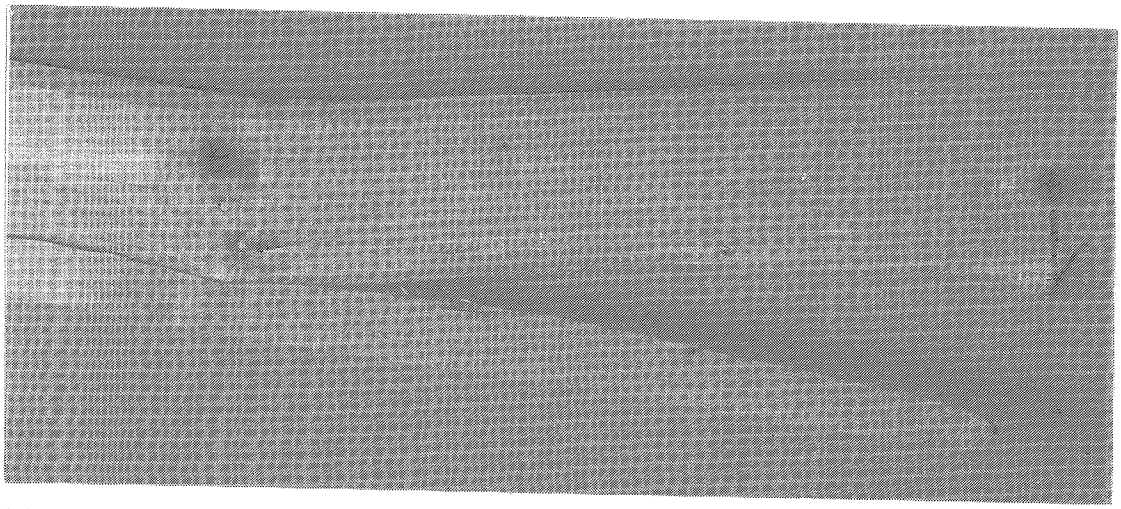

Figure C.5. Combined tension perpendicular to grain and shear failure at knot.

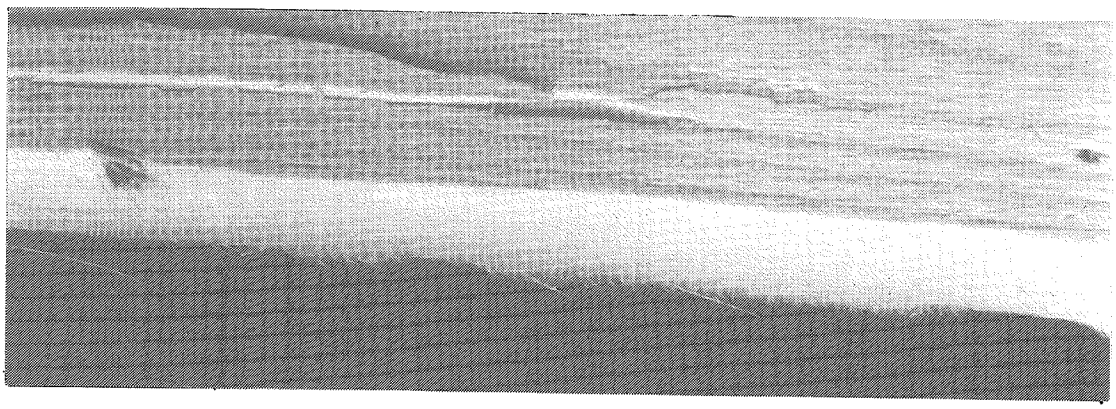

Figure C.6. Enlargement of Figure C.5 showing how tracheids have been pulled loose.